Design of Silent, Miniature, High Torque Actuators

by

John Henry Heyer III

Bachelor of Science in Mechanical Engineering
University of Rochester, 1995

SUBMITTED TO THE DEPARTMENT OF MECHANICAL ENGINEERING IN PARTIAL FULFILLMENT OF THE REQUIREMENTS FOR THE DEGREE OF

MASTER OF SCIENCE IN MECHANICAL ENGINEERING
AT THE
MASSACHUSETTS INSTITUTE OF TECHNOLOGY

MAY 1999
[June 1999]

Author .....
Department of Mechanical Engineering
May 7, 1999

Certified by .....
Woodie C. Flowers
Pappalardo Professor of Mechanical Engineering
Thesis Supervisor

Certified by .....
David R. Wallace
Ester and Harold Edgerton Assistant Professor of Mechanical Engineering
Thesis Supervisor

Accepted by .....
Ain A. Sonin
Professor of Mechanical Engineering
Chairman, Department Committee for Graduate Students

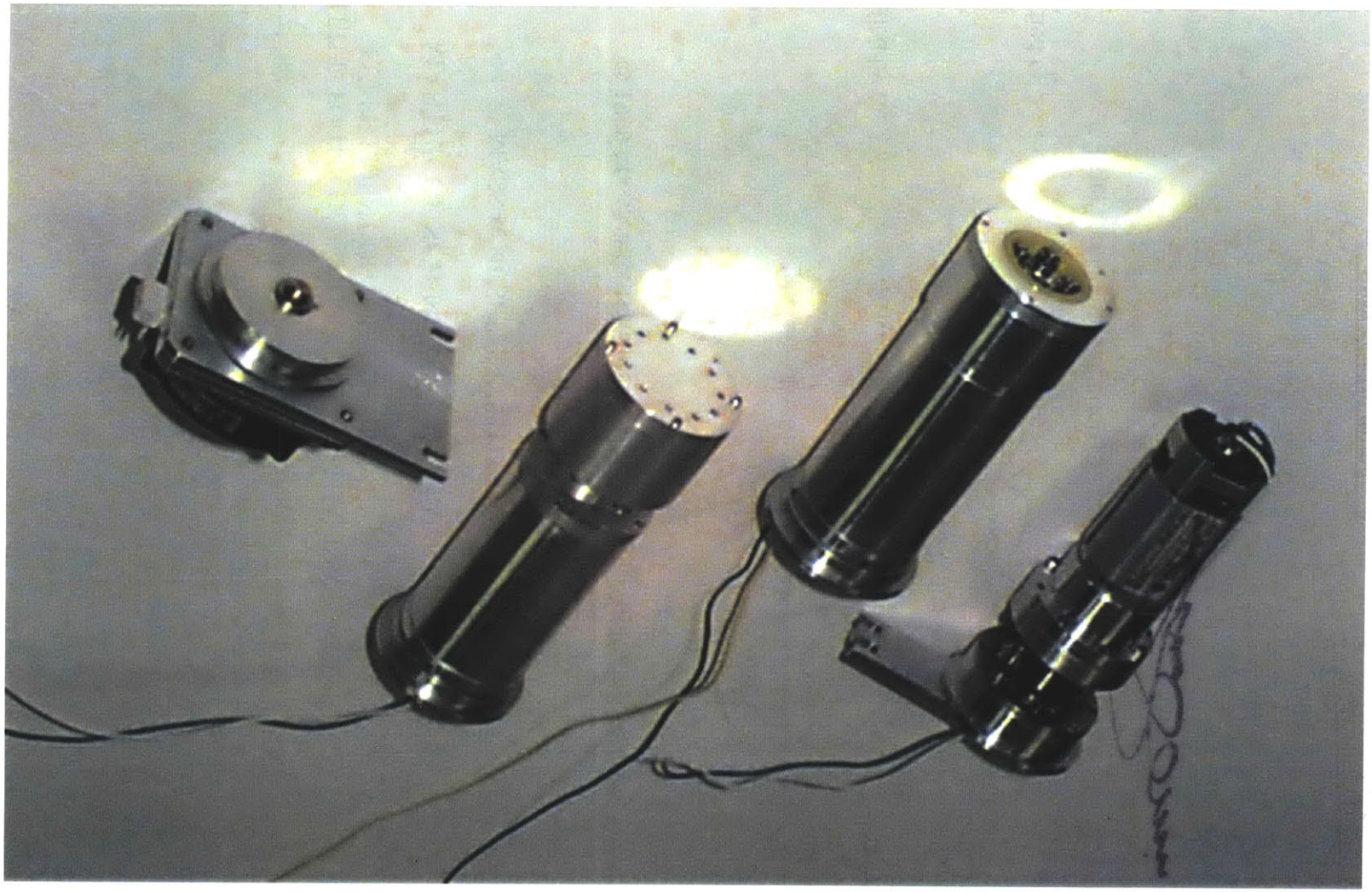

Design of Silent, Miniature, High Torque Actuators

by

John Henry Heyer III

Submitted to the Department of Mechanical Engineering on May 7, 1999
in partial fulfillment of the requirements for the degree of
Master of Science in Mechanical Engineering

Abstract

Specifications are given for an actuator for tubular home and office products. A survey of silent, miniature, low cost, low-speed-high-torque actuators and transmissions is performed. Three prototype actuators, including an in-line spur gear actuator, a differential cycloidal cam actuator, and a novel actuator concept, all driven by direct current motors, are designed, built, and tested. A fourth actuator, an ultrasonic motor, is purchased off-the-shelf and tested. The prototypes are ranked according to noise, torque, efficiency, and estimated cost, among other criteria.

Thesis Supervisor: Woodie C. Flowers
Title: Pappalardo Professor of Mechanical Engineering

Thesis Supervisor: David R. Wallace
Title: Ester and Harold Edgerton Assistant Professor of Mechanical Engineering

Acknowledgements

Mr. Joel Spira, Chairman and Director of Research, Lutron Electronics Co., is gratefully acknowledged for sponsoring this work, and providing an excellent educational opportunity.

Professors Woodie Flowers and David Wallace are gratefully acknowledged for their advice, patience, and clever ideas.

In addition, the following people are respectfully acknowledged:

- Tony Caloggero of the MIT Edgerton Center for use of the high-speed photography equipment.
- Roman of the MIT Machine Shop for machining services.
- Nathan, John, Jeff, and Greg of Technique Applied Science for machining and assembly services.
- Tim Glenn of the MIT Department of Aeronautics and Astronautics for ultrasonic motor information.
- K. Tuchiya of Shinsei Corporation for the ultrasonic motor and information.
- Robert Pighetti of Igarashi Motor for the DC motors and information.
- Ken Heiting of Heiting Tool and Die for rapid machining services.
- William Rouverol of Axicon Gear for differential crowning information.
- Donald Houser, Lynn Faulkner, and Rod Kleiss for gear noise information.
- Scott Hoffman of Accu-Prompt for manufacturing information.
- Gary Rawding of G&D Enterprises for rubber and urethane molding information.
- Lawrence Van Epps of Meridian Laboratory for prompt provision of molded parts.
- John Carver of the Gleason Works for information on nutating gears.
- Tom Mifflin of Arrow Gear for gear information.
- Jim Lombara and Jason Killo of Lutron for helpful correspondence.
- Matt, Ben, John, and Julie for use of the computer and room.
- Joel Spira for the candy bars.
- All others who contributed information and services.

Table of Contents

List of Figures

List of Tables

Chapter 1

Introduction

1.1 Purpose

The purpose of this work is to evaluate, design, and build quiet, low-speed-high-torque, compact actuators for tubular automated home and office products, such as window roller shades and projection screens.

1.2 Assumptions

The reader is assumed to be familiar with machine design and the operation of gears, direct-current (DC) motors, and other standard design components. For more detailed background information, consult the references.

Chapter 2

Design Specifications and Approach

2.1 Specifications

Actuator performance is specified according to the following criteria. The target for each specification is described, followed by its measurement procedure.

2.1.1 Power Source

The actuators operate on a 12-Volt DC power supply converted from 110-Volt, 60 Hz, AC power from a typical wall outlet. The AC to DC conversion is not addressed in this thesis.

2.1.2 Noise

Target: As quiet as possible. The goal is to minimize the noise perceived by a human user. This specification is difficult to quantify (see section 2.4.3 below). A maximum decibel (dB) level is not specified, nor are other characteristics of the power spectrum.

Measurement: A-weighted dB level from a CEL 231 sound level meter and subjective listening. The noise and operation of the final prototypes are captured on videotape for subjective and quantitative noise analysis.

2.1.3 Size

Target: As compact as possible, with two guiding parameters:

- Minimum gap width: Gap width is defined as the distance between the end of the tube and the end of the actuator furthest away or protruding from the tube. For the window shade application, the gap width is the distance between the tube end and the inside of the window frame. For an actuator fitting inside the tube, the gap width can be very small (see Figure 2.1).

- Minimum diameter: For an actuator placed outside the tube, this is crucial to appearance and mounting flexibility. For an actuator placed inside the tube, this minimizes the amount of necessary tube material. A maximum outer diameter (outer diameter) of 2" – 2 1/2" is specified based on the minimum tube diameter to meet operating bending deflection requirements (tube wall thickness = 1/8"). 2" is therefore used as the maximum diameter for the space envelope.

Measurement: Calipers.

2.1.4 Torque and Speed

Target: The load on the actuator is a linearly increasing and then decreasing torque profile, from 0 to a maximum of 14 to 0 in.-lbs. The torque is always applied in the same direction. This corresponds to unwrapping and wrapping a 2" diameter, 10' long tube with a 10' x 10' shade fabric of density 20 oz./yard^2. The output speed for a 2" diameter tube is calculated as 30-35 RPM from a full cycle time specification of 1 min. For high-speed actuators, a speed reducing transmission is necessary. A review of DC motors fitting inside the space envelope reveals that the lowest reasonable operating speed is around 3500 RPM. This demands a transmission ratio of at least 100:1 (input to output). In practice, speed will be given a non-

linear profile by the actuator controller, but here it is taken to be constant, ignoring initial and final accelerations.

Measurement: Torque is measured with a force gauge attached to the output of the actuator with the actuator held rigidly. Speed is measured with a stopwatch by counting the number of output turns in a time interval.

2.1.5 Back-Driving and Shock Overload

Target: The driven tube must be able to sustain a 200% shock overload. If an actuator cannot meet this requirement, provision must be made for a torque-limiting coupling. Back-driven rotation of the output at loads between 100% and 200% is considered acceptable.

Measurement: Manual application of back-driving torque with the force gauge.

2.1.6 Efficiency

Target: 50%. This compares with existing efficient actuators (taking the transmission into account). For example, a high-end DC motor (ε_{max} = 75%) with a precision spur gear head (ε_{max} = 98%), fitting within the space envelope and meeting the power requirement, operates at a maximum efficiency of about 73%. A more typical low cost production gear motor operates at approximately 60%.

Measurement: Actuator efficiency is given by the ratio of output to input power. The power input to the actuator from a variable current and voltage DC power supply is calculated from input current and voltage. The power output of the actuator is obtained by multiplying measured torque and angular velocity.

2.1.7 Life

Target: The actuator must perform 10,000 intermittent load cycles, with minimal change in noise output. Each cycle consists of about 19 turns of the output shaft in one direction followed by 19 turns in the opposite direction.

Measurement: Cycle testing is the only way to prove the actuators for this specification. This is reserved for future work.

2.1.8 Positioning Accuracy

Target: The output position is to be accurate to within 1/8" arc length at the outer diameter of the driven tube. This corresponds to accuracy to within 0.125 radians (3.581°) for the maximum diameter of the space constraint given above.

Measurement: Estimated. No sensor or position-velocity controller is applied. Sensor selection is not performed, in part because the type of sensor selected depends on the type of actuator chosen. It will be seen that two of the chosen actuator concepts are based on friction drive and two on toothed wheel drive. The friction drives require sensing at the output (possibly using an optical sensor), while toothed wheel drive position can be measured at the DC motor shaft (possibly using a Hall effect sensor), provided the sensor is accurate to 0.125 radians divided by the transmission ratio. Control response testing is reserved for future work. Schempf provides a modeling and control approach that can be used for the actuators discussed in this thesis [1].

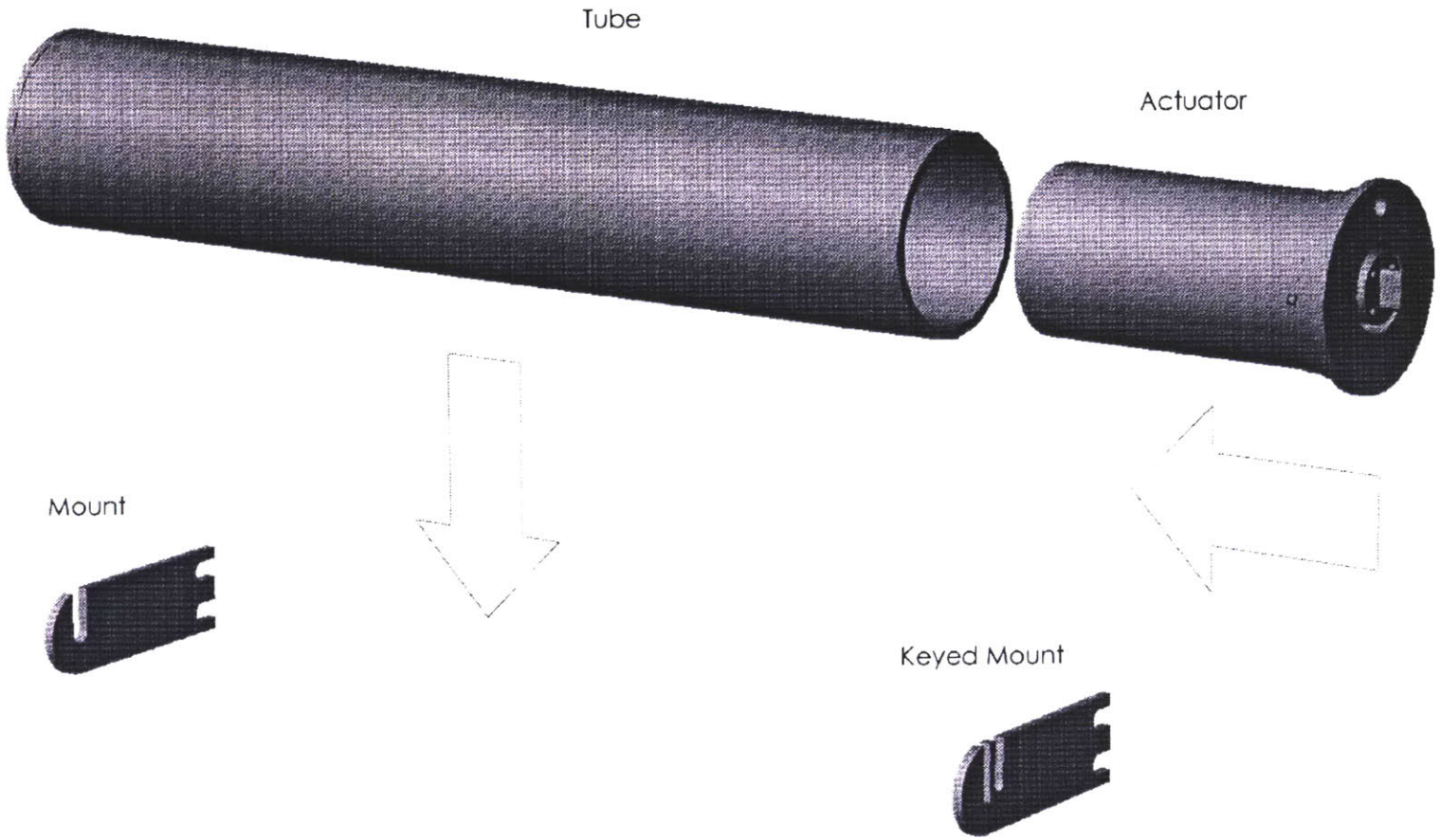

Figure 2.1 Power Pack Concept and Simple Mount Configuration

2.1.9 Installation

Target: Easy and fast installation, with the guiding concepts:

- Power pack concept: Provision is to be made for quick, easy replacement of the tube or actuator. Ideally there are two components, the tube and the power pack, which are easily coupled and mounted (Figure 2.1). The suggested tube is extruded aluminum, which can be keyed for the actuator.

- One size power pack is to be manufactured to actuate the tube, invariant to tube length.

- The design should allow for alternate mounting locations and hardware.

Measurement: Actuators are coupled to polycarbonate tubes, installed with minimal hardware, and tested.

2.1.10 Cost

Target: Minimum, with a $50/each suggested cost to manufacture in production quantities of 10,000/year.

Measurement: Estimated based on quotes from suppliers and shops and prices of existing actuators.

2.1.11 Summary

A summary of specifications is given in Table 2.1.

Table 2.1 Actuator Specifications

Variable	Specification
Size	Minimum Gap Width, ≤ 2" OD
Noise	Minimum
Torque	≥ 14 in-lbs. Continuous at 35 RPM
Overload	200% Rated
Efficiency	≥ 50%
Life	380,000 Output Revolutions
Positioning	1/8" Arc Length Resolution at 2" OD
Cost	$50/Each for 10,000/Year

2.2 Design Approach

2.2.1 Actuator Level

The approach is to focus on the actuator. Alternative actuator concepts are surveyed and selected, based on evidence, including results of preliminary calculations, that the specifications can be met. Emphasis is placed on design for low noise. The ideal actuator inherently makes no audible noise and has only to be designed to meet the remaining specifications. An exhaustive search of concepts is performed so that no inherently silent drive concept is overlooked. However, few actuators are truly silent, and it is difficult to predict an actuator's noise potential. For this reason, several competing concepts are selected

and designed and built in parallel to minimize the risk of an unforeseen noise source halting the project. For actuators chosen from the survey which are known to produce vibrations and noise, the approach is to minimize noise at the source. Generally, the source of noise is a cyclic displacement of a machine component subject to cyclic loading or instability, or of a fluid subject to cyclic pressure fluctuations. By cyclic is meant some manner of time dependence, technically the value of the parameter changes sign at least twice over a given time interval and remains within certain bounds. Specific causes of noise are treated in Chapter 3.

2.2.2 Systems Level

At a systems level (actuator plus coupling, tube, and mounts), a general vibration minimization treatment is provided, and several aspects of this treatment are implemented on the hardware. An important consideration in concept selection is the potential of a concept for isolation, having quantified the noise source. In the long term, this can lead to a less costly design with an acceptable noise level. An actuator with complex or quantitatively evasive noise sources can be difficult to isolate. Note that this is most likely the reason why it is suggested that isolation be a last resort in machine design [2] [3].

2.2.3 Design Architecture and Relation to Noise

Only concepts fitting inside the tube are considered. This choice of architecture allows the designer to design for effectively zero gap width, leaving room for a variety of mounts designed for specific applications, and to use the tube and surrounding material as a barrier to noise emitted from the actuator. This approach is made reasonable by the need for a fairly large diameter tube to meet other product specifications. There are two choices of mounting architecture:

- Supported in five degrees of freedom by the tube and held from rotation by the mount with the actuator subject to a bending moment and the mount subject to a vertical load. In this case, the vibrations of the actuator are directly transmitted to the tube through the coupling.

- Supported rigidly in all degrees of freedom by the mount and subject to a vertical load and displacement due to mount bending. In this case, there is the potential to design a rigid mount such that the actuator vibrations are of such high frequency and small amplitude as to be negligible, but the nature of the architecture is for the mount to be loaded in bending. If the load, including the weight of the actuator mass, is located a significant distance away from the mount, the vibration frequency will decrease and the amplitude increase.

Both architectures are used for the actuators, as will be seen in Chapter 4. The goals are to minimize the effects of actuator mounting and loading on performance and to give a high degree of freedom in coupling and mount design.

2.3 Discussion on Simulation

Simulations are used as design tools when possible and beneficial to avoid multiple design changes and prototypes. Ideally, the system characteristics could be predicted through the following steps:

- Several alternative concepts for the system are selected.
- Time- and space-dependent forces are determined.
- The relation between these forces and the resulting sound pressure or power level distribution in the room is determined numerically through design parameters, physical laws governing the system, and experimental correlations.
- This relation is used with an optimization and accurate measurement procedure to optimize the sound power or pressure overall or at specific points in the room (i.e. the bed

and doorway), or with an audio player and auditioning room for more subjective noise analysis.

Such simulations have been performed. Sabot and Kato estimate exciting forces at the bearings of a simple one-stage spur gearbox by computing spur gear transmission error, use numerical analysis to predict the forced vibration of the housing, and finally implement the finite element method to simulate the sound field in a room [4, 5]. Oswald describes a similar boundary element approach [6]. Nurhadi also simulates the noise radiated from a simplified gear mesh and gearbox structure using finite element models with direct time integration [7]. Zhang describes an optimization procedure using the same analytical framework [8]. Rook and Singh focus on noise transmission through bearings [9]. General Motors has developed an optimization program for gear pairs, no doubt based on their extensive research, and most likely incorporate noise as a parameter [10]. Steyer and Lim discuss two methods, coarse and fine, to simulate noise of general complex mechanical systems based on finite element models [11]. This work summarizes what has been done with noise dynamic simulation techniques. Simulation of the effect of any important actuator or transmission parameter on room sound is the goal, but too much basic physics of actuator component interactions needs to be quantified by theory and/or designed experiment to enable creation of a complete simulation and optimization for an arbitrary actuator. For example, there exists no experimentally verified theoretical relation between worm gear parameters and sound level for a miniature worm and worm gear pair. Concluding, simulation can only be performed at certain stages, where experimental or proven theoretical relations are known.

2.4 Background and Discussion on Noise

This discussion is intended to cover more thoroughly the topic of noise, illustrate the need for and difficulty in defining specifications, and provide insights for future work.

2.4.1 Design Goals

Consider the general problem of noise in consumer products to be used and/or installed in quiet home or work environments. Many products use some form of actuator, usually an electric motor and mechanical transmission (e.g., a gear reducer), to perform their tasks (i.e., a dishwasher, can opener, or blender). These devices all produce sound, but it is a more subjective matter as to whether or not they make noise. Noise is defined as unwanted or unpleasant sound [3]. In an engineering sense, noise can be thought of as obscuring silence or making it difficult to discern some signal such as speech. For design purposes, the goals are to:

- Set and measure the product noise target; that is, determine if the sound emitted by the product is noise, and decide when the level is too high.

- Relate product design parameters to sound.

2.4.2 Noise Standards and Measurement

Recall that sound is a spherical pressure wave, consisting of compressions and rarefactions of air caused by a vibrating source. Sound pressure is the most widely used measure of sound, and is expressed relative to a base level in decibels (dB):

$$Sound\ Pressure\ Level = L_p = 20Log\left[\frac{p_{RMS}}{p_{base}}\right] \text{ dB} \qquad (2.1)$$

where $p_{base} = 2 \times 10^{-5}$ Pa. Figure 2.2 presents typical sound levels throughout the hearing range.

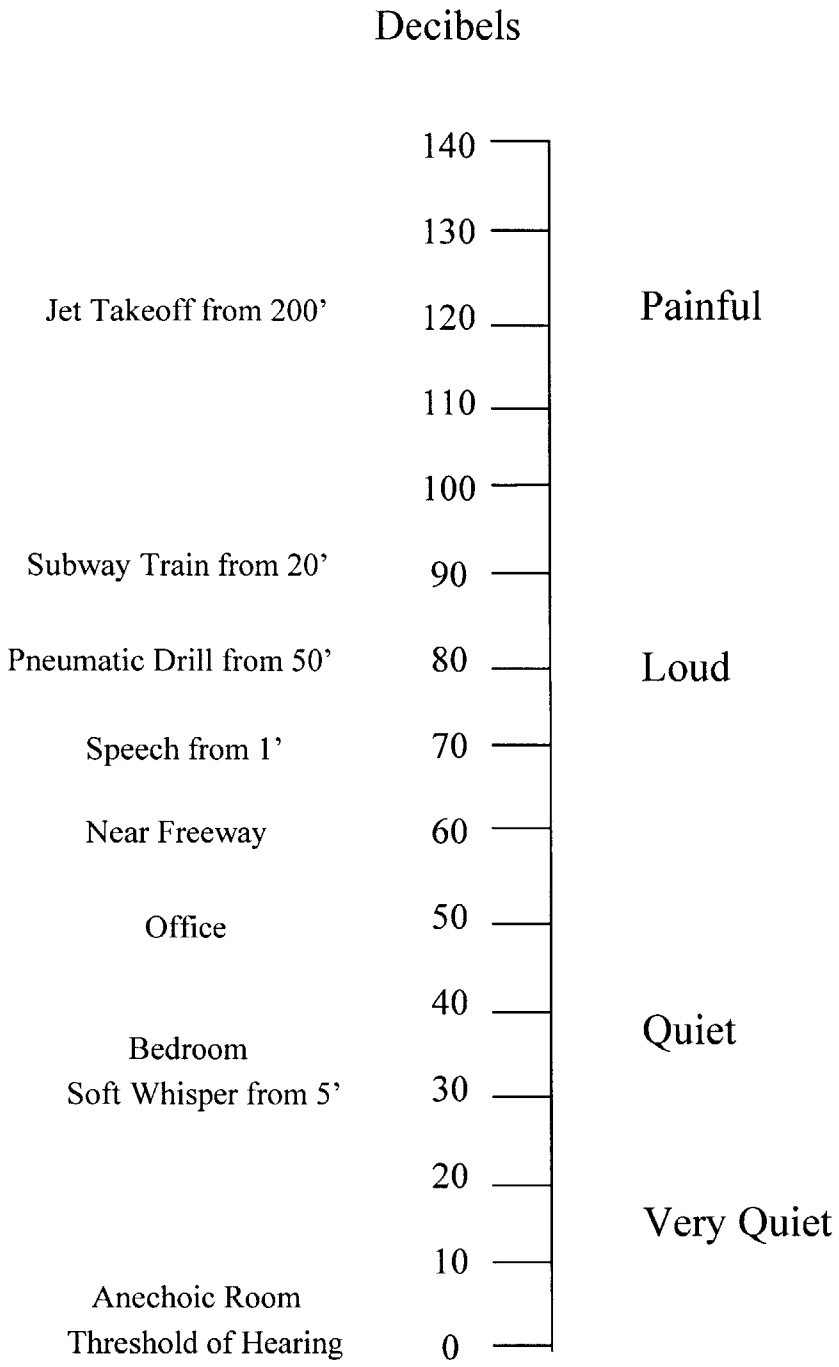

Figure 2.2 Typical A-Weighted Sound Pressure Levels

The federal government, through OSHA, has set standards for industry, using the onset of hearing damage as the noise criterion. This standard specifies how much time a person can be exposed to a certain level of noise. Certainly a product should hit this target, but it is not particularly useful in design. For machines driven by gears, AGMA has set standards on noise measurement. The standard used in this thesis, AGMA 495.04, is for gear actuators with center distances of 4" or below. Sound pressure level is measured with a sound level meter positioned 3 ft. away (perpendicularly) from the radiating surface and more than 1 ft. above the floor (level with the actuator in this thesis). ISO has also set standards for some home products [12].

2.4.3 Further Noise Considerations

Two relations are desired: sound characteristics vs. displeasure and design parameters vs. emitted sound. For example, certain sound characteristics are annoying, and therefore considered noise (whining, grinding, whistling, rattling, etc.). Also, large magnitude, short duration sound at any frequency (such as from an impact) is usually considered noise. These represent different waveforms that must be compared if used to select one product over another. Supposing noisy sound is quantified and different noises are compared, the design relation is then influenced by factors such as listener identity and characteristics (i.e. sound sensing ability and mood) and conditions of use. For example:

- The human ear is sensitive to a certain range of frequencies (Figure 2.3). Sensitivity to magnitude varies with frequency. This is the reason for weighting decibel levels according to sensitivity. The A-weighting matches the human ear's response at levels below 55 dB. This frequency sensitivity relation is an average, and actually varies considerably between people.

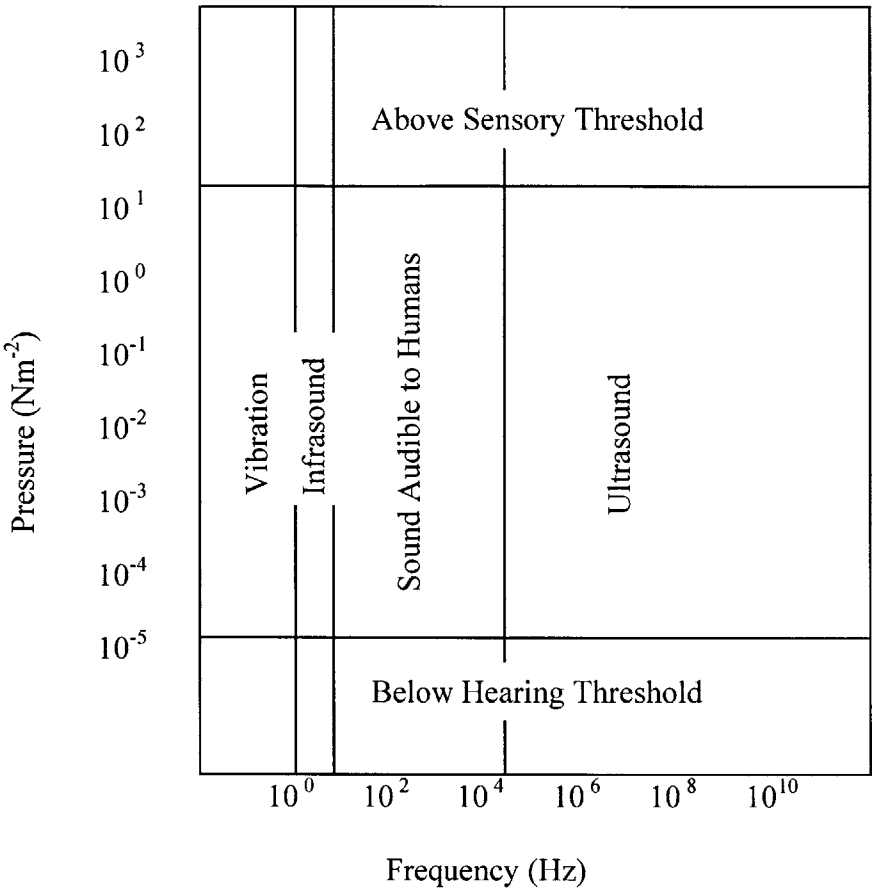

Figure 2.3 Frequency Range of Human Hearing

- An actuator operating in a bedroom while the consumer sleeps may be considered noisy, despite emitting less sound power than an actuator operating in the kitchen while the dishwasher is running (unless the bedroom is directly over a six-lane freeway). An actuator operating at the back of a refrigerator intermittently may be considered less noisy than one on the counter operating all day.

Design for low noise should ideally take these factors into account.

Chapter 3

Survey and Selection of Concepts

This chapter presents most actuator concepts reviewed. Each concept is pictured or referred to a picture in the literature, and is accompanied by a description of how it works, known applications, and the merits and faults leading to its selection or rejection.

3.1 Electromagnetic Motors with Speed Reducing Transmissions

These represent the dominant choice of actuators in product design. Components common to many of these actuators are discussed first, mainly with respect to noise generation.

3.1.1 Common Components

3.1.1.1 Electromagnetic Motors

Electromagnetic motors contain several noise sources. The angular variation in magnetic flux density in the air gap between the stator and rotor gives rise to a radial force wave [13]. This wave distorts the rotor and stator, giving rise to vibrations that can be transmitted though the bearings and coupling to excite a resonant frequency in the housing or transmission. This type of noise can be minimized at the design stage by reducing the flux density by reducing the supply voltage or increasing the number of turns in the winding, but this is accompanied by a reduction in output power. Stator and rotor slot numbers and mechanical design also influence the noise. Extensive rules have been developed to choose the proper rotor slot numbers. Design changes, such as skewing the rotor slots, can bring about a decrease in the

radial bending amplitude of the rotor and thus reduce the radial force effect. Eccentricity of the rotor with respect to the stator creates a once per revolution vibration. Aerodynamic sources such as cooling fans give rise to noise at blade pass frequency.

The prominent noise sources in DC motors are rotating unbalance of the rotor and brush noise, so the quietest motor will have a balanced rotor and carefully chosen brush material and mounting configuration. A properly pre-stressed brush-slip ring system is much quieter than a brush-commutator system. For a brush-commutator system, the brush noise depends heavily on the operating conditions. When operating at rated current, a layer of patina forms on the surface of the commutator, reducing friction and bringing brush noise to a minimum. Low or high current operation leads to, respectively, a very thin layer or a thick layer that breaks down at different places. Both conditions result in noisier sliding contact between the brush and commutator surface. Sliding noise varies with motor size and operating speed. Increase of brush pressure and decrease of brush contact area both increase noise. Increased magnetization of the permanent magnet also increases noise [14].

Finally, the effect of other machine forces must be considered. The motor represents a structure that can be excited to resonate at frequencies generated by the transmission, and care must be taken that the motor housing, for example, does not resonate due to gear meshing forces.

3.1.1.2 Shafts

Eccentric or unbalanced shafts vibrate at shaft rotation frequency. The vibration may be transmitted through the support bearings and force a structural member, possibly exciting resonance. Also, every shaft has a critical speed that depends on its size and loading and support conditions. At the design stage, precision shafts are specified, shaft length is kept to a minimum, and critical speeds are avoided.

3.1.1.3 Bearings

The types of bearings considered are plain and frictionless (ball and roller). Plain bearings generally are made of bronze or plastic and have less accurate tolerances, a higher rate of friction and wear, and lower strength than frictionless bearings, and depending on size and speed, they can be quieter or noisier. Plain bearing noise is due mainly to oil film whirl and a high frequency vibration due to sliding and intermittent contact of poorly finished or lubricated surfaces. Quiet plain bearings are designed by selecting the proper lubricant viscosity, specifying the proper clearances and materials, and maintaining the proper bearing pressure. In addition to possible sliding and skidding, frictionless bearing noise is due to manufacturing errors in the rolling elements, race, and separator.

Quiet ball bearings are designed by selecting the proper surface finish and race geometry, minimizing eccentricity and maximizing parallelism of the inner race with respect to the outer race, and maximizing ball spheriatry. For radial ball bearings, the dominant vibration frequencies (in Hz) can be calculated from the following formulas [3]:

- Unbalance vibration frequency:

$$f = \omega \qquad (3.1)$$

  where ω is the shaft frequency.

- Frequency due to ball or separator defect:

$$f_r = \frac{f}{2}\left(1 \pm \frac{d}{E}\cos\beta\right) \quad \text{(- outer race stationary, + inner race stationary)} \qquad (3.2)$$

  where β is contact angle, E is pitch diameter, and d is rolling element diameter.

- Frequency due to spin of ball defect:

$$f_{spin} = \frac{E}{d} f\left(1 - \left(\frac{d}{E}\right)^2 \cos^2 \beta\right) \qquad (3.3)$$

- Frequency due to race defect (rotating race):

$$f_{race\_defect} = \omega(f - f_r) \qquad (3.4)$$

- Frequency due to race defect (stationary race):

$$f_{race\_defect} = \omega f_r \qquad (3.5)$$

Maintenance of a minimum load on the bearing and accurate bearing fit into the housing are critical to ensure operation at design conditions [15]. In practice, bearing fits are specified by the manufacturer and adjusted for each bearing when necessary.

3.1.1.4 Gears

The gears discussed are of involute tooth profile, which has been proven geometrically to produce a constant speed ratio. The reader unfamiliar with gears is referred to references [16-18].

The literature provides a wealth of information on intermediate size involute spur and helical gear noise, but little on other sizes and types of gears and tooth form. In general, noise increases with size and power, so there is an inherent advantage to miniaturization. However, the applicability of any design procedure or analytical method may change with scale.

Transmission Error:

There are many causes of noise in gears. A unified way of treating gear noise is to quantify it in terms of static and dynamic transmission error. Transmission error is defined as the error in angular position of the output shaft from what the theoretical position should be. This error

causes deviation from ideal operation and leads to vibration and noise. Transmission error can be thought of as the result of an imperfect involute mesh, leading to a non-constant velocity transmission, leading to acceleration, vibration, and noise.

Static transmission error is the error in a statically loaded gear pair and is caused by:

- Backlash: A real gear pair cannot operate without some backlash. Center distance increase is the only way to theoretically impart backlash with no transmission error, but any backlash allows for loss of tooth contact and rattle. Backlash can be imparted by tooth thinning or profile modification, but the result can be static transmission error for gears that must operate in forward and reverse directions.

- Geometric inaccuracy (e.g., profile deviations) and assembly errors (e.g., misalignment caused by non-concentric bearing housings and looseness of installation of shafts, bearings, or gears) leading to an imperfect mesh: Staab and Henning show the importance of manufacturing and measurement accuracy to quiet gear operation [19]. Aitchison correlates manufacturing errors with gear noise for helical gears [20]. Greeves investigates the effects of geometric errors and material property variations on gear noise for cast iron gears [21].

- Gear material elasticity, which causes a change in the theoretical tooth profile and a relative tooth position error: the deflection of the engaged teeth causes the next pair of teeth to contact sooner than desired. At moderate to high speeds, this leads to impacts at tooth mesh frequency, given by:

$$f_{tooth\_mesh} = N\omega \qquad (3.6)$$

  where N is the number of gear teeth and ω is the gear angular velocity. WenBeen uses finite element analysis to model the influence of impacts on gear noise [22].

Dynamic transmission error is the angular position error due to forces that vary in position, direction, or magnitude with time acting at the mesh. These dynamic effects give rise to angular accelerations and vibration. Specific causes of dynamic transmission error include:

- Variations in mesh stiffness through the line of action of a gear pair: as the driving gear (pinion) tooth first contacts the driven gear (gear) tooth, both teeth deflect under the applied torque, resulting in static transmission error. The deflection vs. load characteristic is nonlinear throughout the mesh, leading to a dynamic excitation force. Rouverol has plotted mesh stiffness vs. roll angle through the mesh for spur gears and found two points of extreme low stiffness and one point of extreme high stiffness, and suggests that this is the cause of gear noise at the second harmonic (multiple) of mesh frequency [23].

- Variation in tooth contact force throughout the mesh causes cyclic compressive stresses and strains propagating as waves in the gear teeth. The rapid deformations can be heard as a whine. Mesh stiffness and contact force variations give rise to vibrations and whine at tooth mesh frequency and its harmonics.

- Geometric inaccuracy, such as periodic errors in tooth spacing, eccentricity of the gear wheel on its shaft, and assembly errors such as shaft misalignment: eccentricity can excite natural frequencies of shafts and leads to unbalance vibration at shaft rotation frequency. Misalignment can be heard at first, second, and third harmonics of shaft rotation frequency. If both pinion and gear have once per revolution errors, the excitation frequency is given by:

$$f_{error} = \frac{\omega_{gear}}{N_{pinion}} \qquad (3.7)$$

  If the gear cutter has geometric errors or if significant positioning error is present between the gear and cutter what is known as gear ghost noise results. Geometric error is considered unavoidable, and the degree of error is directly proportional to the cost of the gear.

- Non-constant input torque: any fluctuation in input torque will force a vibration, which may be amplified at a component or system resonance.

- Gear blanks have natural frequencies with the predominant mode generally in the rotational direction. This mode can be excited in operation, and the frequency will depend on the gear geometry. The frequency and sound power can be calculated from static transmission error and the dynamic increment [24]. For compound gears, the common shaft is loaded in torsion and the gears and shaft can vibrate, possibly at a resonance, about the shaft axis.

Other Causes of Noise:

- As a tooth leaves the mesh, a high frequency plucking vibration may be produced.

- Sliding friction as the teeth roll in and out of mesh produces noise. The noise is proportional to sliding velocity and affected by stick-slip.

- Windage noise is caused by the rapid fluctuation of air pressure in and near the mesh as well as by a fan-like effect of very high-speed gears.

Any of the above excitations can be transmitted through machine elements and give rise to element, housing, or system resonance.

Methods of Noise Minimization at the Design Stage:

Note that a constant velocity ratio is necessary for zero acceleration, and any method that does not aim to bring the gears into perfect involute mesh may not be reasonable.

- Selection of the best tooth form: the ranking from quietest to noisiest is given as: worm, helical, spur, bevel [3].

- Profile modification and crowning: the effect of transmission error can be eliminated at a given load with the use of an appropriate profile modification [25] [26]. Tip relief, for example, is a common modification to allow the teeth to come together smoothly in spite of elastic deflections. Yoon shows that cubic splines can be used as modified profiles to reduce noise [27]. Dynamic effects due to mesh stiffness variation can also be treated with the proper modifications. Tooth crowning is commonly used to control mesh stiffness and compensate for misalignment, and has been proven to reduce noise [28]. Hardy uses a differential tip relief in an attempt to reduce noise [29]. Differential crowning, which essentially varies the width if the line of contact of spur gears through the mesh roll angle, is claimed to completely eliminate the variation in gear mesh stiffness [23, 30-34]. For mass-produced gears, it is suggested that the optimal tooth shape depends on ability to control quality [35].

- Precise manufacturing held to very tight tolerances and a robust assembly to minimize geometric and assembly errors: for single and compound gears, one way to do this is to use monolithic gear-shaft structures with the gear(s) cut on the shaft instead of assembled to the shaft [36]. Mori presents a compact differential gear with a rigid carrier design to create a robust assembly [37]. Hambric uses the planets of a planetary gearbox to support a floating sun to tighten tolerances [38]. Yamamori presents a stable bearing arrangement for differential gears [39]. Mochizuki uses spring-loaded partial (split) gears to cancel backlash [40]. Similar gears are widely available in drive component catalogs. An interesting approach is taken by Maier, who uses a special cutter to impart inaccuracies on gears to control noise characteristics [41].

- Damping can be accomplished by selection of a damped gear, bearing, or housing material. For example, Tsuda uses flexible supports for the motor and bearings of a gearbox [42]. Tsunoda mounts his gearbox to a rigid plate with a layer of damping material [43]. Hansen uses damping material between the motor and motor mounting plates and as bearing supports [44]. Tsukamoto places damping material in gaps in the gear body [45]. Rivin forms composite teeth by bonding contact plates to the gear teeth

with damping material [46]. Bowers places damping material in the gear tooth roots [47]. Mizuno sticks magnetic rings on the sides of the gear body, and suggests that microslip between the gear body and rings damps resonant vibrations of the gear body [48]. Nilsson "meshes" two friction wheels mounted to the same shafts as the gears to create a parallel damper [49]. Igaku uses a similar approach, but "meshes" rigid disks of larger diameter than the gears in an attempt to control deviation from perfect rotation [50]. Finally, Yi studies the noise of bimetallic gears. These are gears of a strong metal with slits cut in teeth, filled in with soft metal. The resulting gear looks like several gears stacked axially, alternating hard and soft materials. An extensive analysis is given [51].

- Matching a hard gear with a compliant, damped gear can result in a quiet gear set. Seragnoli presents an embodiment of this concept [52]. Imazaike imparts compliance in a gear by using axially staggered teeth to allow a greater deflection [53].

- Gear blank mass can be varied (i.e. by changing face width) to tune the natural frequency of the system.

- Designing the gear mesh to operate at a low pitch-line velocity has been shown to produce a quieter gear set [54]. The effect of other parameters on noise has been investigated experimentally and used to produce formulas for noise based on gear parameters such as velocity, helix angle, etc., but the results do not correlate well with measurement [55]. This demonstrates why complete simulations are difficult to perform.

- Increasing the contact ratio apparently decreases the magnitude of the variation in mesh stiffness and tooth contact force by distributing the load over more teeth [15]. The easiest way to do this is to use a fine pitch, which has the disadvantage of reducing load capacity. Hirt creates a discrete, three-part "helical" gear by placing spur gears on a shaft at different angles about the shaft axis, thereby increasing contact ratio [56]. Hayduk designs a gear pair operating at high temperature to increase contact ratio as the gears heat up in operation [57]. Experiment shows that a high contact ratio or any integer contact ratio may be used with optimal noise results [58, 59].

- Gears can be designed to operate at low pressure angle, essentially reducing the normal force at the mesh and therefore the magnitude of excitation.

- Smooth, accurate surface finishes can be obtained by a precision mold or by grinding.

- Enclosures can be used to muffle noise [60, 61].

- Flexible couplings can be used to reduce the effect of driving torque fluctuations. Kurre and Faulkner substantially reduce noise in a gear drive this way [62].

- Vibration mounts can be very effective in preventing noise transmission to supports. A variety of mounts are commercially available and design is simple. Mount stiffness is determined from the weight of the machine, the dominant excitation frequencies, and the desired degree of isolation. Bouthors implements a flexible mount, as well as a flexible coupling between the motor and gearbox [63].

3.1.2 Transmission Concepts

3.1.2.1 In-Line Involute Spur or Helical Gear

How it works: This is the simplest of gear drives (Figure 3.1). Gears are mounted on parallel shafts fixed in space, with the transmission ratio dependent on the ratios of mating gear pitch diameters.

Applications: Widely used in commercial and industrial actuators.

Plus:

- Simple to design with standard components.
- Configurations can be created to fit almost any application.

- Can be made and assembled with high precision.
- Much is known about the general design and design for low noise.
- Highest efficiency of all gear drives.

Minus:

- High ratios require several stages, giving a range of potential excitation frequencies.

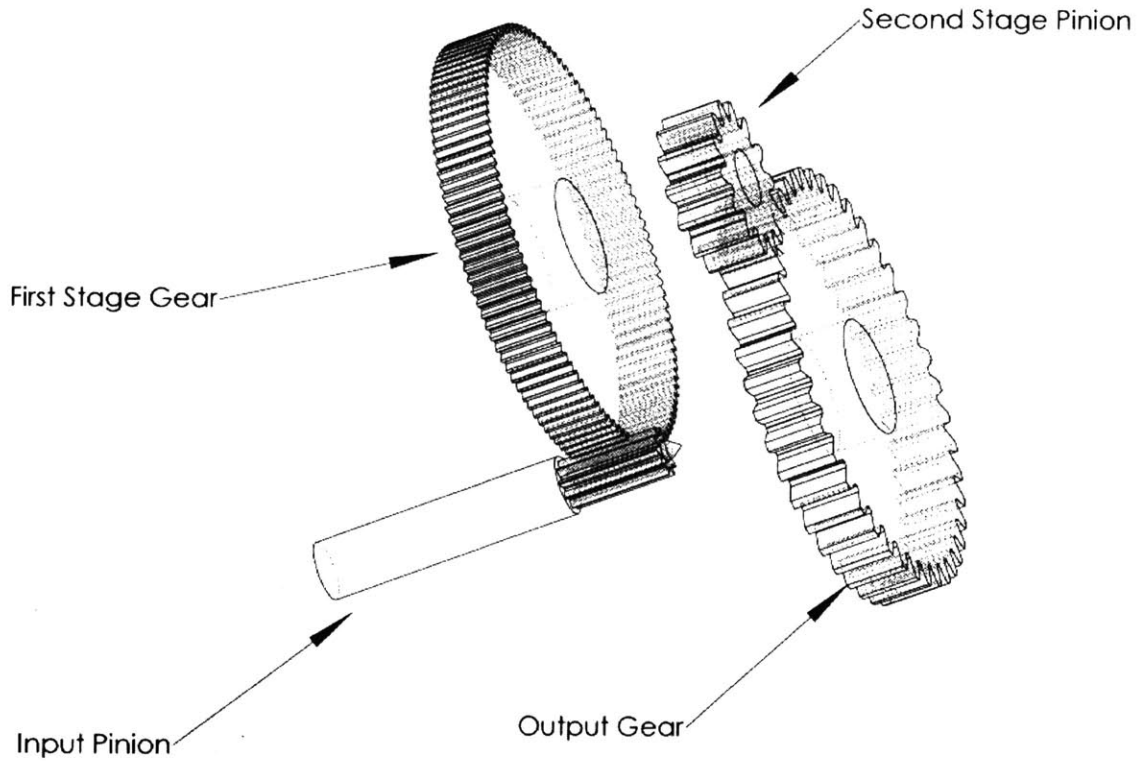

Figure 3.1 In-Line Involute Spur Gear Transmission

3.1.2.2 Planetary Involute Spur or Helical Gear

How it works: The planetary arrangement is shown in Figure 3.2. The sun gear is typically the input member, turning the planets. The internal (ring) gear is fixed and the planet carrier rotates slowly. Theoretically, load is shared between the planets and among several teeth of the sun and ring gear. The ratio of one stage of this arrangement can be as high as 25:1.

Applications: Widely used in commercial and industrial actuators.

Plus:

- High torque.
- Compact arrangement.

Minus:

- The Bayside Controls Whisper Quiet helical planetary gearheads, which represent the highest quality, are advertised as producing 68 dB, presumably for the AGMA noise test [64].
- Many gears are required for one stage: using more than one stage multiplies the part count rapidly.
- A poor planet-carrier assembly can lead to loose, rattling gears and a high noise level.
- Design of tight gear meshes results in quieter operation, but precision must be increased with tightness, and therefore cost.
- In reality, there exists an uneven balance of load, leading to increased wear of one of the planets and early gear failure at rated load.

Lagarde proposes floating the planets radially, and designing tooth parameters such that the resultant load points toward the pinion on the input stage, to reduce clearance and noise at the high speed meshes. At the last stage the resultant is directed toward output gear to balance load [65]. A compromise is made at each stage, and the free-floating gears may still vibrate.

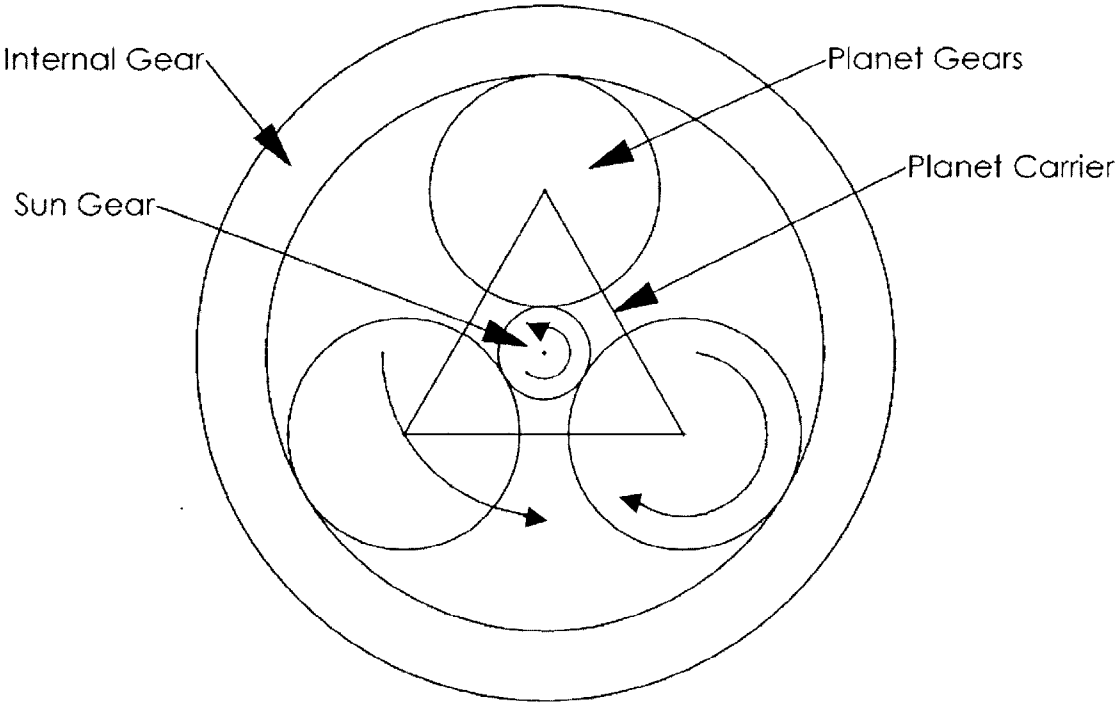

Figure 3.2 Planetary Gear Transmission

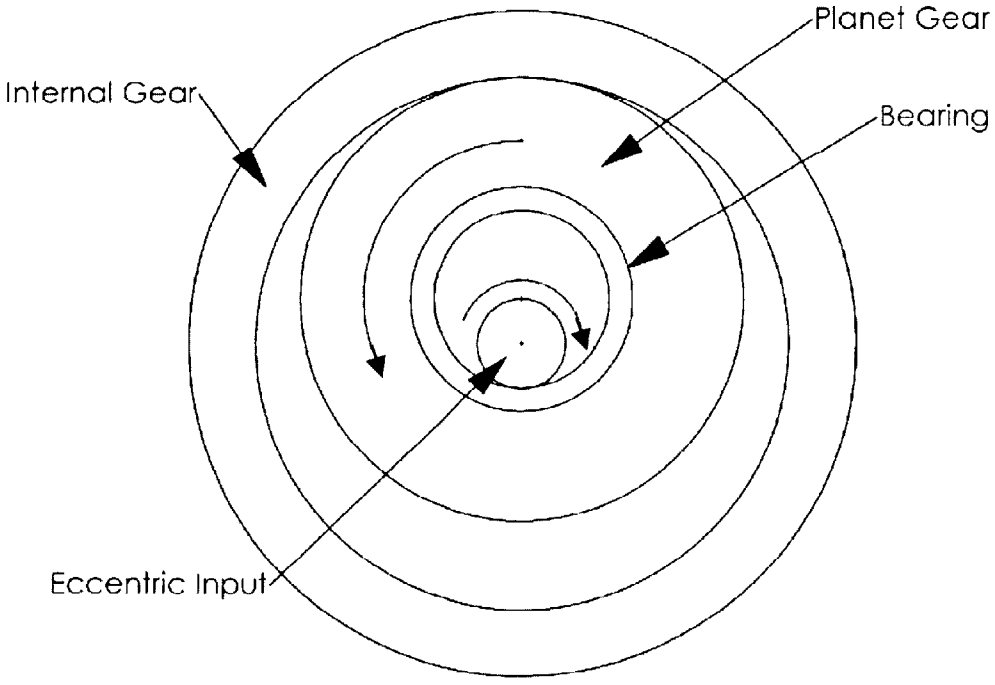

Figure 3.3 Planocentric Transmission

3.1.2.3 Planetary Ball Bearing

How it works: This concept uses ball bearings as friction planetary transmissions [66].

3.1.2.4 Planocentric

How it works: This concept is similar to the planetary arrangement, with the exception that the carrier takes the form of an eccentric shaft or bearing (Figure 3.3). The output is taken from the slow rotation of the planet as it orbits the fixed ring gear. The planet has large holes in its body coupled to pins attached to an output member, which is held concentric to the fixed ring gear. The tooth form may be involute [67] or any form producing a constant velocity ratio. A successful form used in industry is the cycloidal profile [68]. This form is used with cylindrical rollers to obtain a nearly frictionless drive with no sliding contact. Another tooth form is the circulute [69]. A kinematic analysis of a friction planocentric drive is given by Romiti [70].

Applications: Industrial speed reducers.

Plus:

- High overload torque with cycloidal profile.
- No sliding contact occurs with cycloidal profile.

Minus:

- The reduction ratio for the cycloidal drive is given by:

$$Ratio = \frac{N_1}{N_2 - N_1} \qquad (3.8)$$

where N_1 is the number of teeth on the planet gear and N_2 is the number of teeth on the ring gear. For available cam followers to serve as rollers, two stages are needed to get a suitable reduction.

- To balance forces, two cycloidal gears are used 180° out of phase. The arrangement becomes complex.

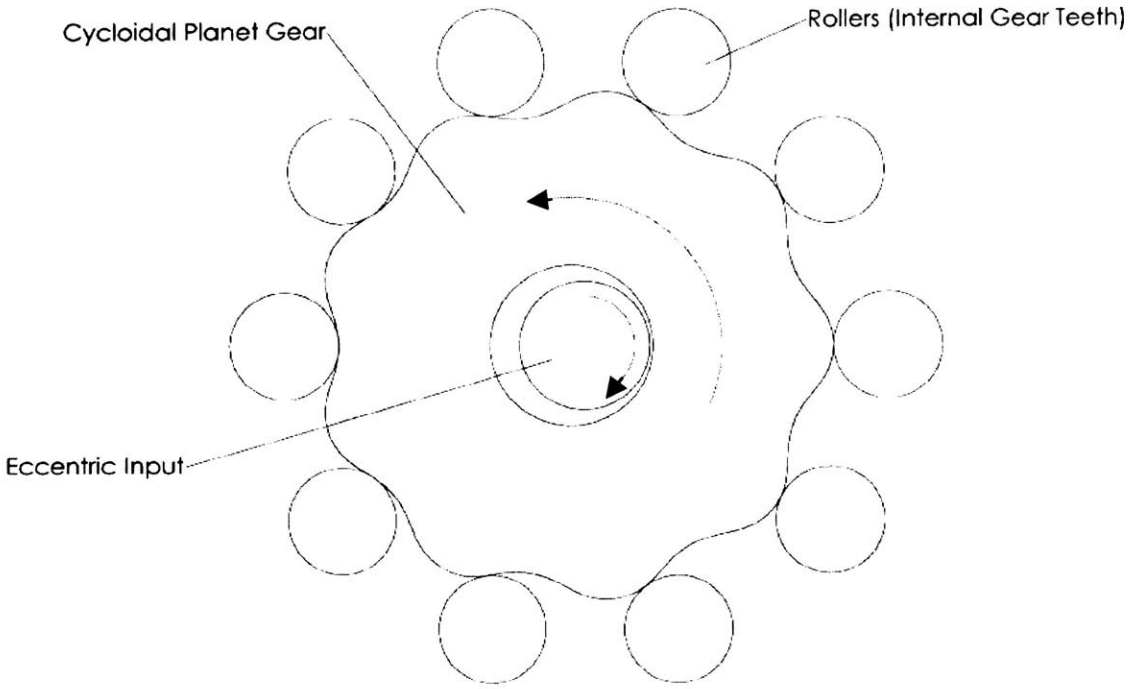

Figure 3.4 Cycloidal Planocentric Transmission

3.1.2.5 Differential Involute Spur or Helical Gear

How it works: This is a type of planetary arrangement that uses compound planets and two ring gears to obtain a very high ratio. The ratio is based on the difference between the diameters of the planet gears and the difference between the diameters of the ring gears. The carrier drives the planets around the inside of the ring gears. One ring gear is fixed and the

other is free to rotate. It can be seen that if the difference between planet gear diameters is very small, the free ring gear will move very slowly (Figure 3.5).

Applications: Widely used in commercial and industrial actuators.

Plus:

- Very high ratio in one stage.

Minus:

- If the input speed is high, the planet-ring gear mesh rate will be extremely high as the planets orbit the sun gear.
- Same problems as with the planetary arrangement.
- Custom gears are needed.

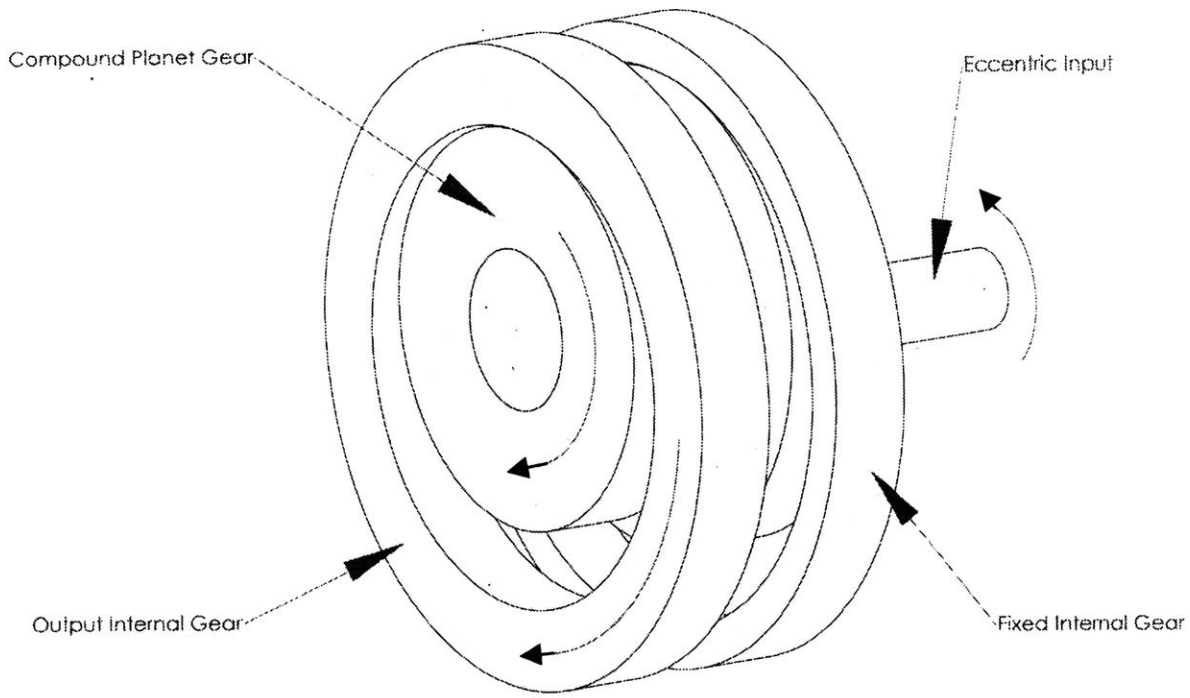

Figure 3.5 Differential Gear Transmission

3.1.2.6 Differential Cycloidal Cam

How it works: This is a differential arrangement that works like the gear differential described above, except using planet gears of cycloidal profile and ring gears consisting of cylindrical rollers, like the cycloidal planocentric described above. All teeth or lobes are in contact with all rollers at the same time, resulting in load sharing.

Applications: Industrial speed reducers.

Plus:

- High torque and shock overload due to load sharing between the teeth.
- High ratio given by:

$$Ratio = \frac{N_1(N_2 + 1)}{N_1 - N_2} \qquad (3.9)$$

  N_1 and N_2 are the numbers of teeth or lobes on the first and second planet gears. This can be derived based on the fact that for every time the cam orbits, the output member moves the difference between the arc lengths of the larger and smaller lobes [71].
- Low noise for the smallest commercially available Mectrol unit (40 dB using the AGMA standard) [72]. This is much quieter than other gear drives of comparable power.
- The stiffer cycloidal teeth allow less theoretical transmission error than involute teeth.

Minus:

- Commercial size is large and price is high (4" OD, $1600 for the Mectrol vs. 2.2" OD, $700 for the planetary helical mentioned above).
- Many bearings are needed (one for each ring gear roller "tooth").

3.1.2.7 Three-Gear Differential

How it works: In this arrangement, one planet gear is driven around the inside of a fixed ring gear by an eccentric input [73]. The planet is axially thicker than the ring gear, and also engages a free ring gear, concentric with the fixed ring gear and with one or two fewer teeth than the fixed gear. The free ring gear is forced to rotate by the wedging action of the planet teeth as it orbits.

Plus:

- Uses fewer parts than a typical differential arrangement.

Minus:

- Wedging action may be associated with sliding noise and wear.

3.1.2.8 Worm and Bevel Gear

How it works: A worm drives a worm gear mounted to the same shaft as a bevel pinion. The bevel pinion drives the output bevel gear. This concept attempts to take advantage of the low noise of worm gears.

Applications: Worm and bevel gears are standard design components. Single stage worm gear actuators are used extensively in automobiles.

Plus:

- Worm gears are relatively quiet and widely used commercially for high ratio single stage reductions.

Minus:

- Little literature on worm or bevel gear noise.
- Standard bevel sets with high enough load capacity don't fit in the space envelope. Custom gears are needed.

- The worm must be offset from the center of the bevel gear. Standard motors with the required power to drive the worm do not fit into the space envelope.
- The ratio for the standard components shown in Fig. 3.6 is 40:1. A significant improvement is needed.

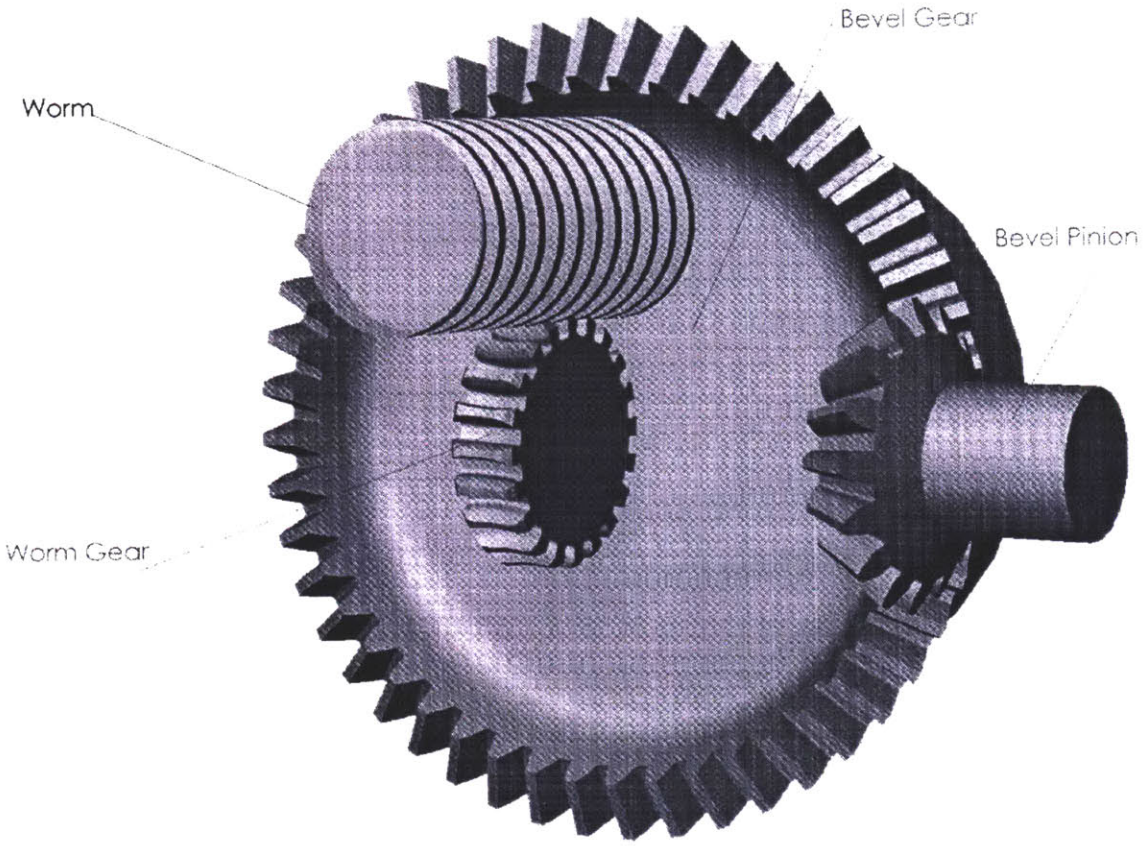

Figure 3.6 Worm and Bevel Gear Transmission

3.1.2.9 Nutating Bevel or Spiral Bevel Gear

How it works: Imagine a coin dropped on a table. The coin will wobble as its perimeter traverses the tabletop. If the coin is held concentric about a vertical axis from the table, it will rotate as it wobbles (nutate) due to the difference between the perimeter of the coin and that of the circle it projects onto the table (provided no slippage occurs). Now make the table a fixed

bevel, spiral bevel, or face gear. Turn the coin into a gear with one or two more teeth than the table gear and engaging the table gear at an angle. The coin gear can now be used to rotate a shaft as in the planocentric configuration with a bent input shaft used to force the coin gear nutation (2 in Figure 3.7). Conversely, if the coin gear is held from rotation but allowed to wobble, the table gear will rotate (1). A differential is created by cutting teeth on both sides of the coin gear and introducing a free gear, concentric about the table gear axis, to engage the other side of the coin gear. The free gear will rotate in the same manner as the free ring gear in the differential drive (3). The ratio for the differential configuration is very high [74].

Applications: Winches, automotive A/C compressors [75], cordless screwdrivers.

Plus:

- High ratio.

Minus:

- Uncertain dynamic effects of wobbling.
- The noise of bevel and face gears is higher than for spur gears.

3.1.2.10 Nutating Ball

How it works: Similar to the differential nutating gear design, this friction drive uses the difference between the diameters of two sets of balls to obtain the speed ratio. One set is retained by one face of the coin gear and the other set by the other face. Since both balls are in continuous contact with the plates as the coin gear nutates, one set rolls at a slightly different velocity than the other, imparting a rotation to the free plate [76].

Plus:

- High ratio.

Minus:

- Complicated mechanism.

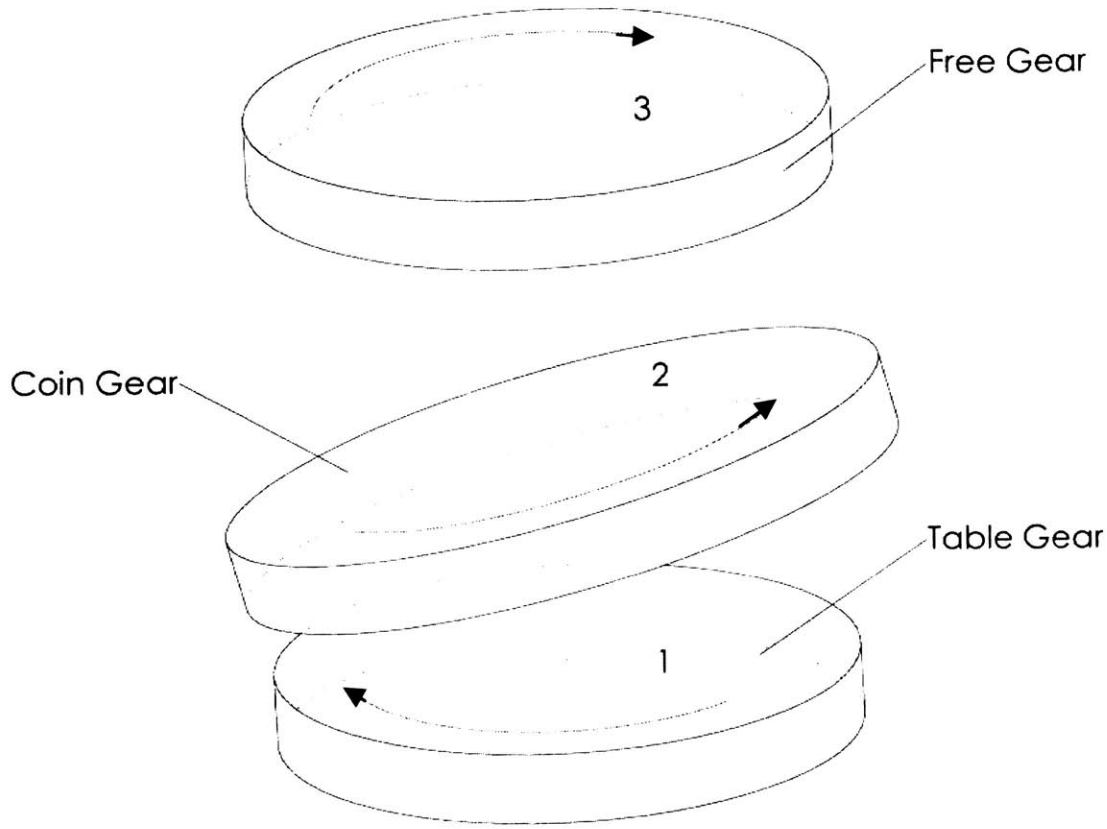

Figure 3.7 Nutating Gear Transmission

3.1.2.11 Cycloidal Ball

How it works: The ball reducer transmission is a friction drive. To understand how it works, consider two disks, one fixed and the other eccentric to the first disk. If the eccentric disk is revolved, without rotating, on an eccentric carrier or bearing about the fixed disk axis, and a sphere is sandwiched between the disks, the sphere will trace out cycloids on both disks (a hypotrochoid on the fixed and an epitrochoid on the eccentric). In practice, the disks can be machined with trochoidal races to carry several balls. If the hypocycloidal disk has two more lobes than the epicycloidal disk, a slow rotation is imparted to the eccentric disk.

Applications: Industrial speed reducers.

Minus:

- The trochoidal races are expensive to machine precisely.
- The speed ratio is given by [77]:

$$Ratio = \frac{2}{N-2} \qquad (3.10)$$

where N is the number of hypocycloidal lobes. Two stages are needed to achieve the desired ratio.

3.1.2.12 Harmonic Drive

How it works: A flexible planet is forced into mesh at two or more points on a rigid ring gear by an input shaft, called a wave generator, having the appropriate shape (Figure 3.8). The input rotates, forcing the flexible planet to deform while remaining in mesh with the rigid gear. If the flexible and rigid gear teeth are the same size, and the rigid gear is held fixed, the progressive meshing will force the flexible gear to rotate in the opposite direction to the input, similar to the planet in the Three-gear differential described above. The ratio is controlled by the difference in flexible and rigid gear tooth numbers [78]:

$$Ratio = \frac{N_{Flexible} - N_{Rigid}}{N_{Flexible}} \qquad (3.11)$$

or alternatively on the undeformed pitch diameters (simply replace N by pitch diameter in the above equation).

Applications: Robot joints.

Plus:

- High ratio with few parts, lightweight and compact.
- Gear tooth profile is straight sided or modified for low stress and noise [79].

Minus:

- A high ratio means small teeth, low overload capacity.
- Although an actuator of the appropriate size and torque is commercially available, it is not recommended for use in quiet product design.

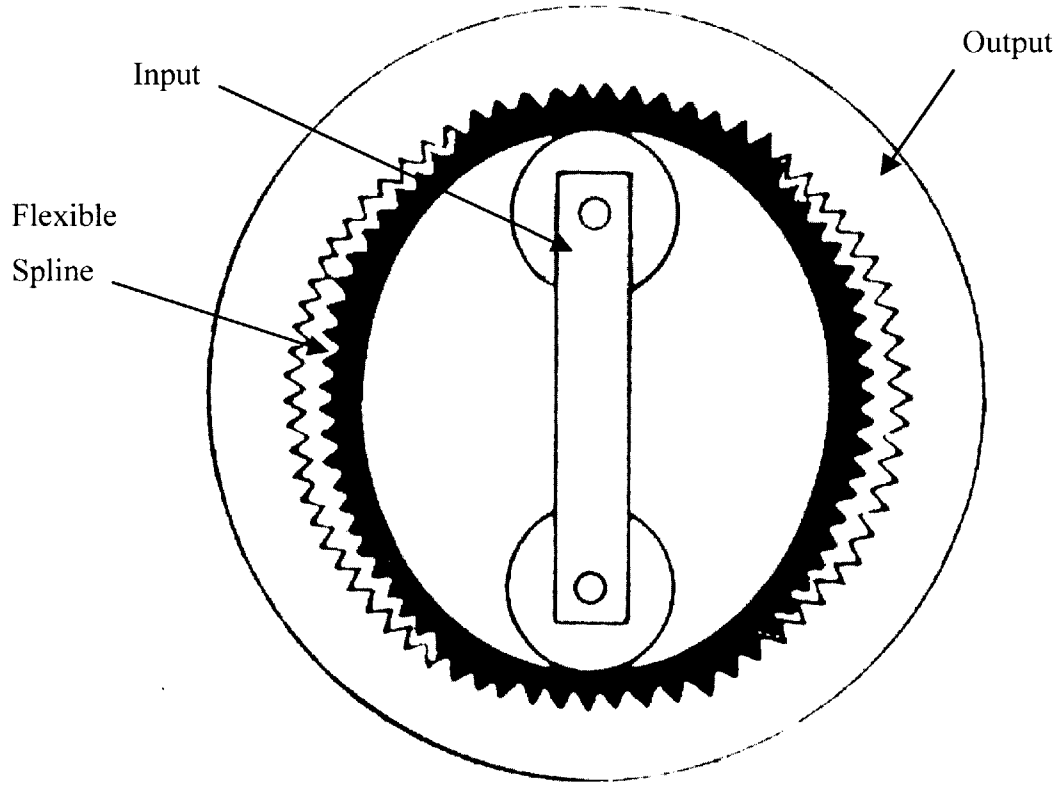

Figure 3.8 Harmonic Drive Transmission

3.1.2.13 Harmonic Face Gear

How it works: This concept uses flexible and rigid face gears with a wave generator to achieve the same effect as the harmonic drive [78].

3.1.2.14 Differential Screw

How it works: This is essentially a screw inside a screw (Fig. 3.9). One fine pitch screw drives a nut along rails, which take up the load torque. The nut is threaded coarsely on its outer diameter. The nut acts as a coarse pitch screw used to drive a very long nut (the tube threaded coarsely on the inside), held from translating along the axis of rotation [80]. This architecture is evaluated for lead, ball, and roller screws. The Rholix, essentially a friction lead screw, is also reviewed, but is for low torque applications [81].

Plus:

- Lead screws can be quiet due to the continuous contact.
- There is axial space inside tube to fit this architecture.
- The nuts can be made by injecting epoxy into a mold [82].

Minus:

- Roller screws are very efficient but very expensive.
- Ball screws are less expensive but noisier.
- Very coarse pitch is not feasible for ball or roller screws.
- Lead screws are known to chatter due to backlash and noise moments [83].
- There is a trade-off between efficiency, load capacity, and critical speed that makes the lead screw architecture undesirable. The analysis follows:

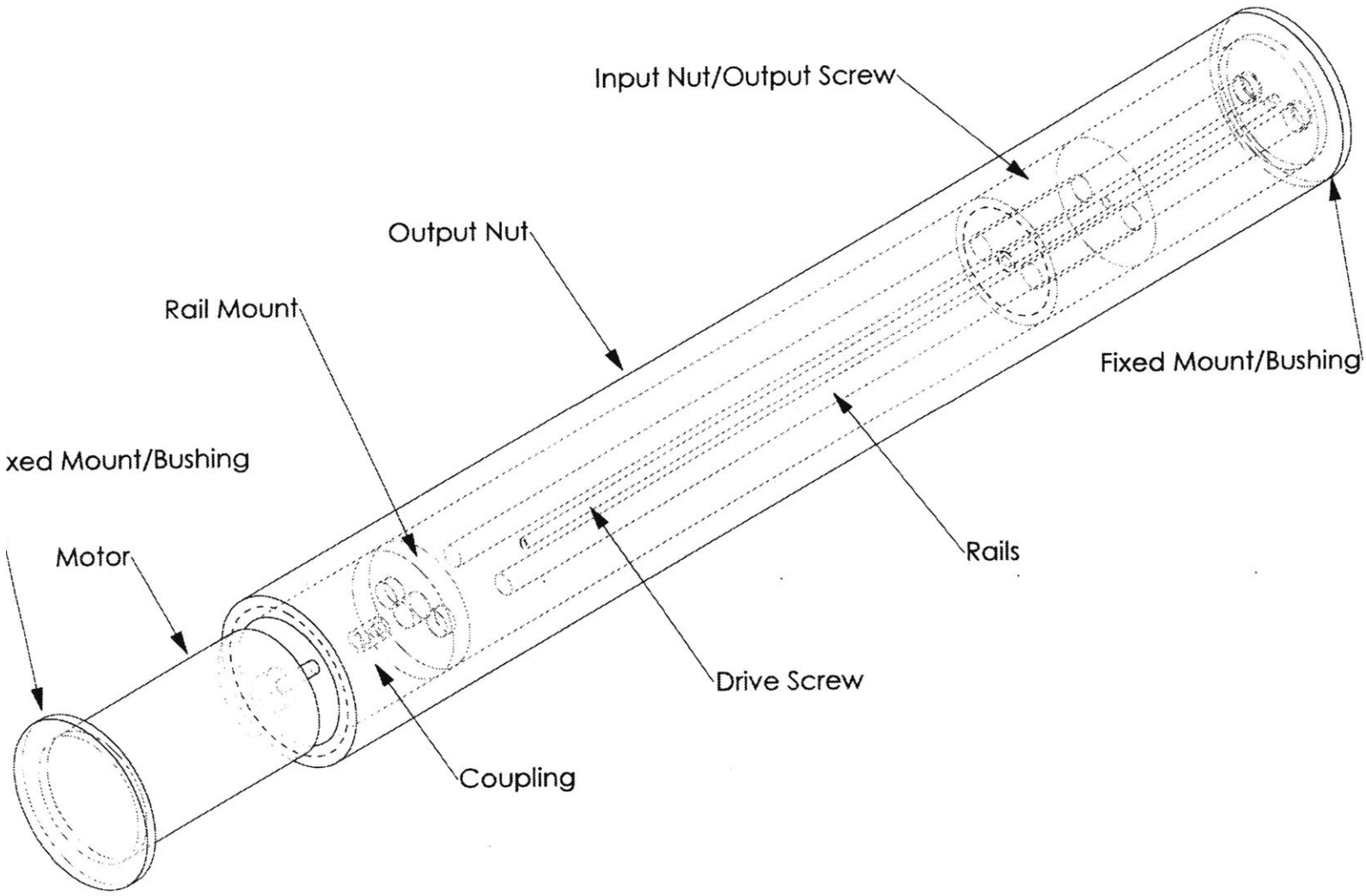

Figure 3.9 Differential Screw

Ratio:

The axial velocity of the nut is given by:

$$v_{Nut} = L_{DriveScrew}\omega_{DriveScrew} \qquad (3.12)$$

where L denotes lead (reciprocal of pitch). From this equation it is clear that the transmission ratio is the ratio of the screw leads:

$$Ratio = \frac{L_{InputScrew}}{L_{OutputScrew}} \qquad (3.13)$$

Using a coarse pitch screw (L=2.5", r_{Pitch}=1.5") along with a #4-48 steel drive screw, the ratio is 120:1.

Buckling Load and Critical Speed:

The differential screw can be arranged to put the drive screw in continuous tension, due to the one-directional nature of the loading, so buckling is not a consideration.

The critical speed in RPM of a steel lead screw is given by:

$$\omega_{cr} = F \times 4.76 \times 10^6 \times \frac{d}{Length^2} \qquad (3.14)$$

where d is the root diameter and the end support factor F is given a maximum value of 2.23, for a lead screw doubly supported at each end by ball bearings [84]. Since the lead of the output screw is 2.5", the length of the input screw must be at least 19 turns x 2.5"/turn, or 48". A 48" long #4-48 lead screw has a critical speed of 400 RPM. Reducing the number of turns required and therefore the screw length (using a 4' x 4' shade) raises the critical speed to 2500 RPM, still low for the desired output speed and calculated ratio.

Screw Tensile Failure and Thread Stripping:

The torque (τ) to axial load (Q) conversion is given by:

$$\tau_{Resist} = Qr_{Pitch}\left(\frac{L + 2\pi\mu r_{Pitch}}{2\pi r_{Pitch} - \mu L}\right) \qquad (3.15)$$

for input torque acting against the applied load, and by:

$$\tau_{Assist} = Qr_{Pitch}\left(\frac{2\pi\mu r_{Pitch} - L}{2\pi r_{Pitch} + \mu L}\right) \qquad (3.16)$$

for input torque acting to assist the load [85]. L is lead, r_{pitch} is the pitch radius, and μ is the coefficient of friction. For the #4-48 drive screw, tensile failure does not occur based on the axial load divided by the tensile area, which is given by:

$$A_t = 0.7854\left(D - \frac{0.9743}{p}\right)^2 \qquad (3.17)$$

for steel screws, where D is the basic major diameter of the screw and p is the pitch. The length of engagement necessary for thread stripping not to occur is given by:

$$L_e = \frac{2A_t}{\pi K_{n\max}\left[0.5 + .57735p\left(E_{s\min} - K_{n\max}\right)\right]} \qquad (3.18)$$

where L_e must be multiplied by J, a factor depending on the screw and nut material yield stresses σ_{screw} and σ_{nut}:

$$J = \frac{A_s\sigma_{screw}}{A_n\sigma_{nut}} \qquad (3.19)$$

where A_s and A_n, the shear areas of the external and internal threads are given by

$$A_s = \pi p L_e K_{n\max}\left[\frac{1}{2p} + .57735\left(E_{s\min} - K_{n\max}\right)\right] \qquad (3.20)$$

$$A_n = \pi p L_e D_{s\min}\left[\frac{1}{2p} + .57735\left(D_{s\min} - E_{n\max}\right)\right] \qquad (3.21)$$

p is the pitch, K_{nmax} is the maximum minor diameter of the internal thread, E_{smin} is the minimum pitch diameter of the external thread, D_{smin} is the minimum major diameter of the external thread, and E_{nmax} is the maximum pitch diameter of the internal thread. The total length of engagement for the calculated axial load is just over 1/4", well under a reasonable length nut.

Efficiency:

The formula for the forward driving efficiency of a screw-nut combination is:

$$\varepsilon_{Forward} = (\tan\lambda)\left[\frac{(\cos\Phi_n - \mu\tan\lambda)}{(\cos\Phi_n \tan\lambda + \mu)}\right] \qquad (3.22)$$

and:

$$\varepsilon_{Backdrive} = (\tan\lambda)^{-1}\left[\frac{(\cos\Phi_n \tan\lambda - \mu)}{(\cos\Phi_n + \mu\tan\lambda)}\right] \qquad (3.23)$$

for the backward driving efficiency [84]. Φ_n is the thread angle in the normal plane, and λ is the thread lead angle. The friction coefficient μ is given an optimistic value of 0.1. Note these equations can be used for both inner and outer screws of the differential screw with

proper rearrangement of terms. The efficiency of the differential screw with the #4-48 input screw is 30%.

Returning to the critical speed issue, if the drive screw is changed to 1/4"-40 (ratio now = 100:1), the critical speed is over 10,000 RPM for the reduced turn criteria (4" x 4" shade). The efficiency is now reduced to less than 1%. Using the 10' x 10' shade with these parameters now results in thread stripping. Note that in every case the differential screw is not driven back by the maximum load based on the back-driving condition for the outer screw. It is clear that this concept is a compromise between critical speed, efficiency, and yielding.

An alternative architecture consists in driving a typical high lead nut along its lead screw with a fine pitch screw offset parallel to the high lead screw. The high lead screw is rotated as the nut travels along it, and is coupled to the tube. The same compromise is made with this concept, with the added disadvantage that the motor must now be offset from the center.

Another alternative is to drive a high lead screw though its nut by means of a linear motor. HSI linear actuators seem ideal for this purpose [86]. These are rotary stepper motors that drive lead screws through their center by rotating an axially constrained nut. Calculating the axial force for the largest actuator results in thread stripping for 60% of the full load.

3.1.2.15 Chain or Belt Drive

How it works: Chain and belt drives use a sprocket or pulley to drive a chain or belt, which in turn drives a larger sprocket at a lower speed. The ratio is the ratio of pitch diameters of the sprockets or pulleys.

Applications: Widely used in commercial and industrial actuators.

Plus:

- Standard design components.

Minus:

- Noisy.
- The belt and pulley configuration fitting the space envelope and providing the required ratio is difficult to arrange in less than four stages with standard components [87].

3.1.2.16 Capstan Drive

How it works: A wire is wrapped in a figure-8 around two pulleys [88]. The smaller pulley, driven by a motor, drives the wire by friction. The wire drives the larger pulley by friction at a lower speed. The reduction ratio is the ratio of the pulley diameters.

Applications: Instruments, appliances.

Plus:

- Quiet.

Minus:

- Calculations show that the wire yields on the input stage of a two-stage drive.
- The friction contact at the output stage cannot drive the load.

3.1.2.17 Friction Wheel Drive

How it works: This concept is the same as the in-line gear drive architecturally, but uses friction wheels instead of gears.

Applications: Instruments, appliances.

Plus:

- Inexpensive.

Minus:

- Low torque. The power rating of a friction drive is given by:

$$Power = cDNPWf \qquad (3.24)$$

D is the wheel diameter, N the number of revolutions per minute, P the compression force, W the face width of the wheel, and f the coefficient of friction between the wheels [85]. c is a constant depending on units. A rough calculation gives a horsepower a fraction of that possible with a gear drive of the same size.

3.2 Active Materials with Friction Drive

The disadvantage of using a high-speed motor with a reducer is clearly that some vibration will always be present due to the imperfect nature of real mechanisms, e.g. rotating shafts and bearings. Following is a review of actuators that operate at much different frequencies than traditional machines, and therefore are promising for low noise power transmission.

3.2.1 Piezoelectric Ultrasonic Actuators

A review of piezoelectric actuators is given by Uchino [89], and Sashida and Ueha cover all aspects of piezoelectric ultrasonic motors extensively [90, 91].

Piezoelectric ceramics deform when a voltage is applied across them. Several types of deformation can be exploited for use in actuators, including compression-expansion and shear. Most rotary actuators use the compression-expansion strain of the ceramic to create out-of-phase vibratory displacements in two directions at the surface of a stator. This gives rise to an elliptical motion at the stator surface. A rotor placed against the stator surface is driven by friction contact. The elliptical motion can be amplified by operating the stator at

the resonance frequencies of the displacement modes. The excitation voltage and resonance frequencies are usually above 20 kHz, the reason the actuators are called ultrasonic. Provided there are no other vibrating machine components, this type of actuator is completely silent.

A wide variety of rotary piezoelectric ultrasonic motors, employing many different ways to create the elliptical motion, have been proposed [91]. The concepts are reviewed below. Non-rotating resonance mode motors, single resonance combination motors, flex-flex double mode motors, and rectangular plate motors are not considered because of low efficiency, improper shape, or low torque.

3.2.1.1 Wedge Type Mode Conversion Ultrasonic Motor

How it works: This motor uses a Langevin vibrator, consisting of layers of piezoceramic sandwiched between two short cylinders. One cylinder is held fixed. A mechanical horn or vibrator piece is attached to the other cylinder. A voltage is applied to the ceramic and it expands and contracts, causing the horn to vibrate in the axial direction (the horn amplifies the displacement of the actuator). The end of the horn is cut off at an angle. If a rotor is placed near it as in Figure 3.10, it will deflect in one direction, imparting a rotation to the rotor.

Plus:

- Cylindrical construction.
- High efficiency.

Minus:

- Low torque – a version of the motor was built using an array of vibrators around a rotor, but synchronization proved difficult.

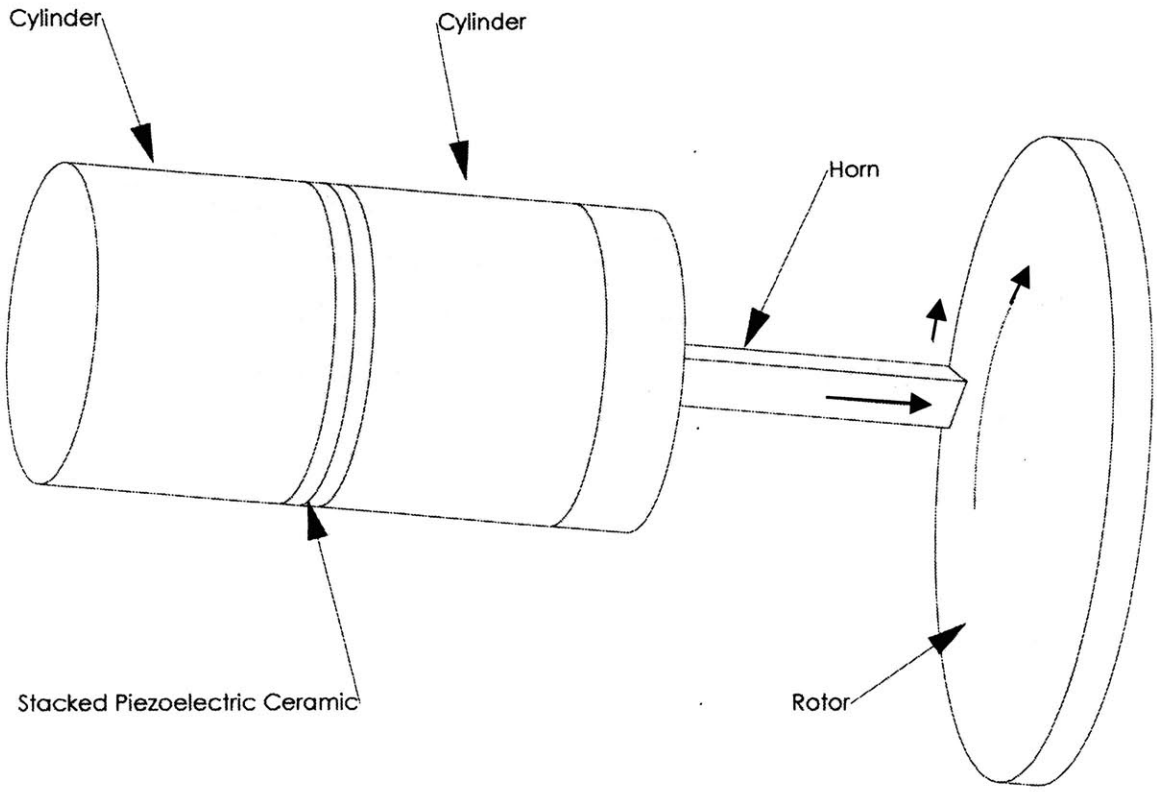

Figure 3.10 Wedge Type Ultrasonic Motor

3.2.1.2 Longitudinal-Torsional Mode Ultrasonic Motor

How it works: Several versions of this motor exist, that invented by Kumada the most promising [90] [91]. This motor uses bending, torsional, and longitudinal distortions of the stator to move the rotor (Figure 3.11). The rotor is held a tiny distance from the stator such that the stator contacts the rotor while moving to rotate the rotor in one direction.

Plus:

- Cylindrical construction.

Minus:

- No holding torque – some type of catch-release mechanism is needed to hold the load.

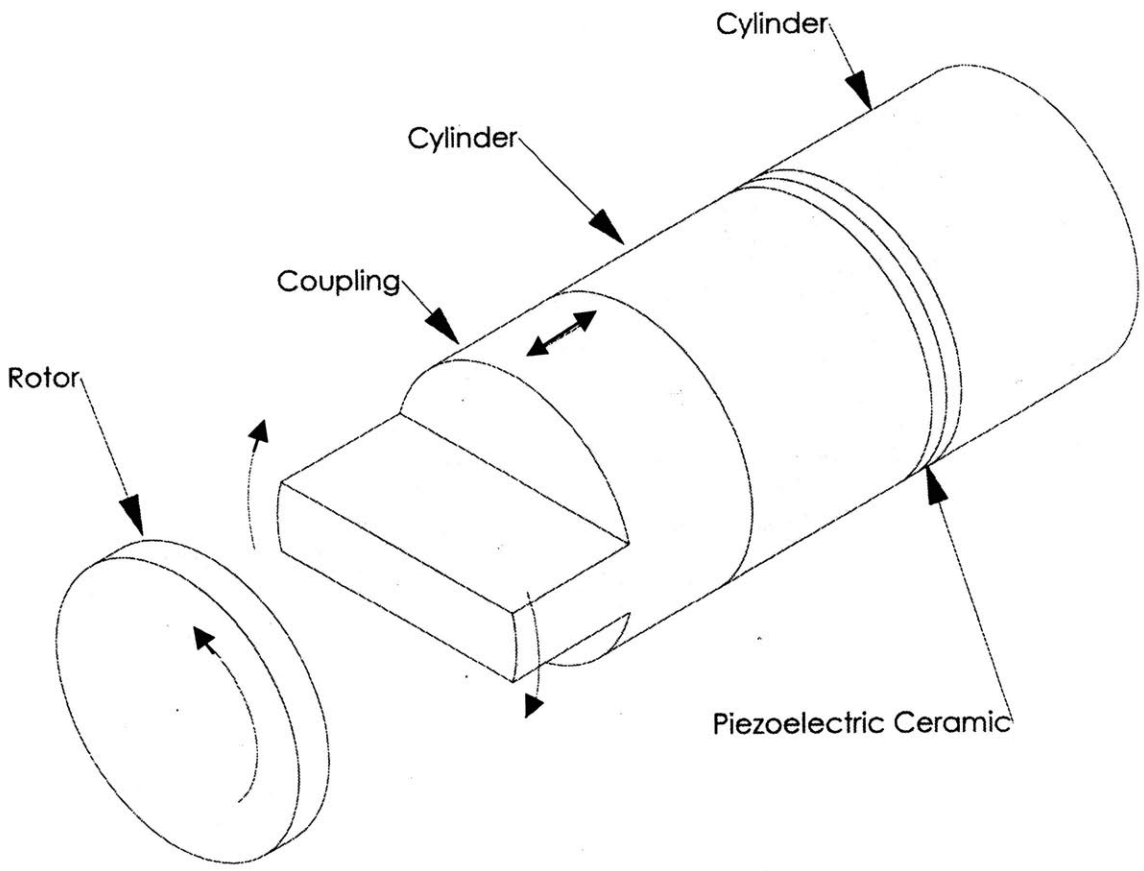

Figure 3.11 Longitudinal-Torsional Mode Ultrasonic Motor

3.2.1.3 Shear Mode Ultrasonic Motor

How it works: Uses shear strain of curved piezoelectric ceramic plates to rotate the end of a cylinder in one direction as it extends, with the recovery stroke a rotation in the opposite direction as it retracts. This motor has the same practical advantages and disadvantages as the Longitudinal-Torsional motor.

3.2.1.4 Travelling Wave Ring or Disk Ultrasonic Motor

How it works: One method of construction of this type of motor is shown in Figure 4.21. A composite stator disk (or ring) shaped beam is formed by bonding a ceramic disk (or ring) to a

metal disk (or ring). The ceramic ring is poled in segments around the circumference, in alternating directions. In any given segment, an applied voltage will cause the ceramic to expand or contract, causing the beam to bend with a curvature depending on the stiffness of the metal. With the alternate poling scheme, an applied voltage produces a wave shape in the beam. Notice each half of the ceramic ring is one-half wavelength out of phase with the other half. One half receives a sinusoidal voltage at a frequency above 20 kHz and the other receives a co-sinusoidal voltage at the same frequency. Thus, the ring is forced to vibrate in two modes at once, corresponding to two induced standing waves out of phase by 90°, or 1/4 wavelength, in position and time. Addition of these modes results in a progressive flexural wave that travels circumferentially around the ring, with amplitude in the axial direction (Figure 3.12). The composite ring is designed to resonate at the driving frequency for the modes created by the ceramic, amplifying the displacement. The particular resonant mode induced in the ring, determined by the number and size of segments, affects the displacement. Analysis reveals that the B_{14} mode gives the theoretically largest displacement (and also the greatest power) for the disk motor [91].

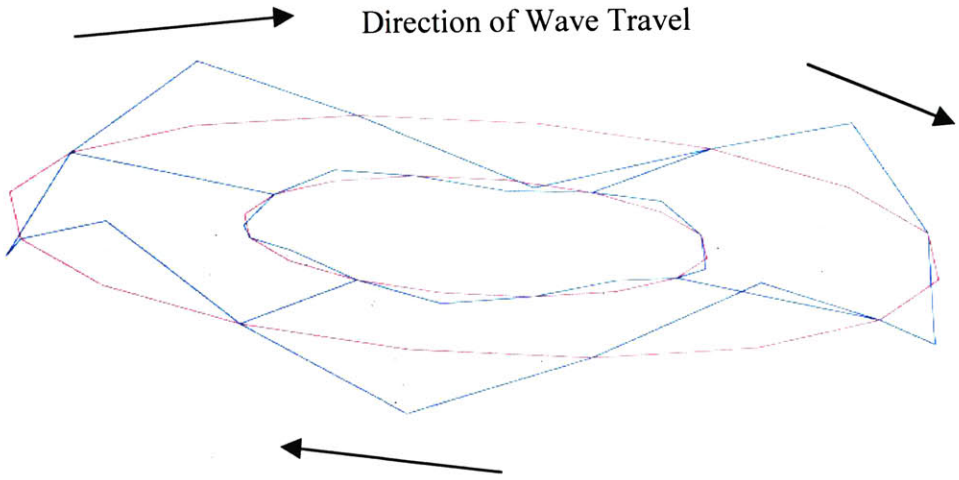

Figure 3.12 Stator Ring Vibration Mode and Travelling Wave (Deformed in Blue)

A flexural progressive wave travelling through a beam (or ring or disk in this case) results in a motion perpendicular to the neutral axis at the neutral axis, but in an elliptical motion at points

away from the axis and at the surface of the beam or ring. This elliptical motion can be amplified by cutting radial slits in a thicker metal ring, giving the appearance of teeth. If a rotor disk is placed against the surface of the composite beam stator, it will rotate in the opposite direction to the wave. The total displacement is on the order of micrometers, which means that the surfaces must be precise. Design of the motor is given in section 4.2.

Glenn provides a great aid in understanding the operation of this type of motor [92]. He describes the operation of a similar motor developed at the MIT Active Materials and Structures Laboratory, and shows a movie of the wave travelling through the composite ring and a schematic of the drive mechanism. This motor uses ceramic bonded to two sides of a metal disk to excite the modes. The operation is inverted: the composite disk serves as the rotor, contacting stators on both sides, doubling the torque of the motor. The electrical contact is made with brushes.

Applications: 10,000 motors were installed in 1993 in Tokyo City Hall to actuate window blinds and are still working [90]. The 1999 Lexus LS400 steering column is positioned by disk motors [93]. Honda produces low torque actuators for other automotive applications. Canon Ultrasonic autofocus lenses are actuated by low-torque ring motors. Shinsei Corporation produces a line of commercially available high torque motors.

Plus:

- No noise.

Minus:

- Ring design is not the right shape to go inside a tube.
- Torque does not meet the specification with off-the-shelf motors.

3.2.2 Magnetostrictive Actuator

How it works: A magnetostrictive material, such as Terfenol-D and some metallic glasses, changes its shape in response to an applied magnetic field. This effect can be used to create a linear motor. A rod of this material is placed in tube. The tube is wrapped with induction coils. Progressively activating the coils down the length of the tube causes the rod to expand progressively. A progressive wave is created in the rod, which causes it to crawl down the tube [94]. Wrapping this configuration into a ring creates a rotary motor.

Applications: Wing trailing edge actuators (linear actuators).

Plus:

- Development of the linear actuator proves high torque density.

Minus:

- Expensive material.
- Rotary concept not proven.

3.2.3 ICPF Actuator

How it works: ICPF's (ionic conducting polymer film gels) can change shape with an applied voltage. A friction drive element is demonstrated by Tadokoro [95]. The ends of a polymer film gel rod are plated with platinum at the ends to imbue them with voltage sensitivity. The rod is bent into an arch, and the ends connected to voltage sources. Applying voltages out of phase excites an interesting mode of vibration in the arch, resulting in an elliptical motion at the top. This can be used as a friction drive.

Applications: Microcatheters.

Minus:

- Low torque – ICPF as well as polymer gel and piezoelectric high polymer actuators are all rejected for low torque.

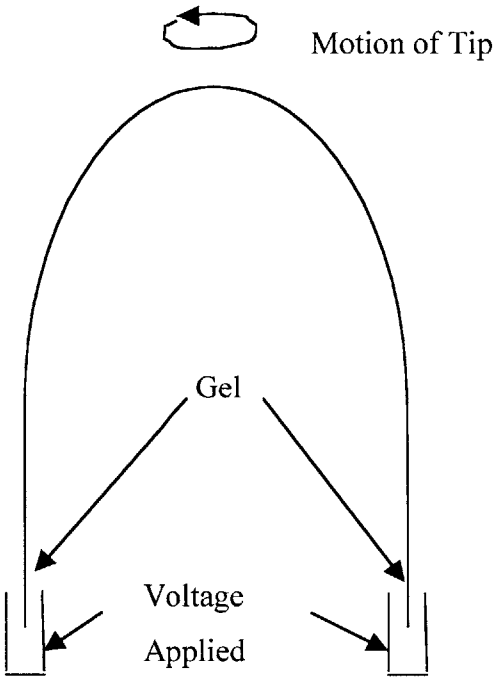

Figure 3.13 ICPF Actuator

3.2.4 Shape Memory Alloy Actuator

How it works: Shape memory alloys change shape with temperature. An applied voltage can be used to induce the temperature change. The shape change can be exploited in the same way as for piezoelectric and magnetostrictive actuators.

Minus:

- Temperature dependence.
- Slow performance.

3.3 Other Actuators

3.3.1 ELVIRA

How it works: ELVIRA (Electronically-Operated, Linear, Variable-Reluctance, Integrating, Reversible Actuator) can be described as an electromagnetic ratcheting system. An electromagnet is mounted to a bracket ("blocker") which can slide along a rod, as in Figure 3.14. A voltage is applied to the coil. The coil attracts a spring-loaded "mover" which moves toward the coil, ratcheting the whole mount/coil/spring/blocker assembly along the rod. The blocker prevents backdrive. Two assemblies can be mounted to a rod for reversibility [96].

Plus:

- Operation is possible at high frequency.
- It could be used to drive a lead screw through a long nut in place of the HSI actuator mentioned in section 3.1.2.14.

Minus:

- Development is needed.

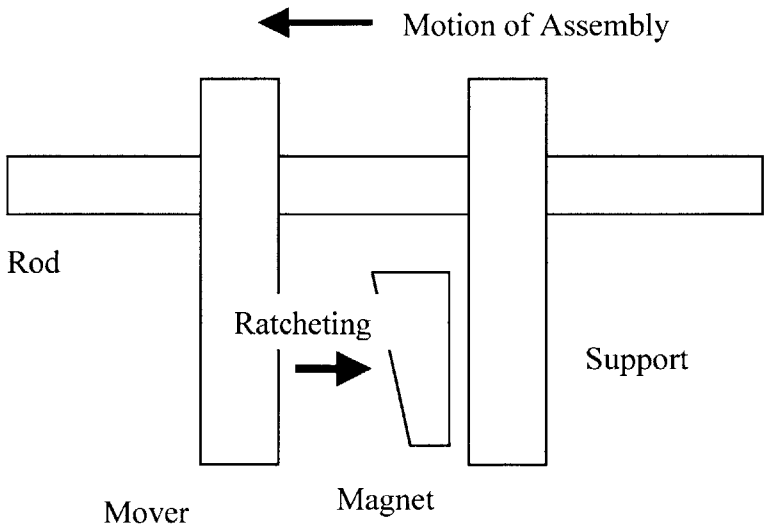

Figure 3.14 ELVIRA

3.3.2 Perturbation of Elastic Field

How it works: Multiple actuators, for example piezoelectric, are put in series with springs and distributed about an eccentric bearing. When the actuators perturb the springs in a progressive manner, a resonance is excited and the bearing is rotated [97].

Plus:

- Proposed as a way to reduce the amount of piezoelectric or other actuator material needed to drive a rotor.

Minus:

- Development is needed.

3.4 State of the Art in Motorized Window Shade Design

Following are the results of a search for actuators currently used in window roller shades:

- Somfy actuators, sold by Rollease, use a planetary gear reducer with a DC motor. They fit into a 2.25" diameter tube, and provide very high torque [98].

- Elero actuators, sold by BTX, use both DC and AC motors with planetary gearboxes for transmission. The sizes and corresponding torques follow: DC Motor, 1" Tube, 8 in.-lbs., 21-48 RPM; AC Motor, 1.5" Tube, 26 in.-lbs. [99].

- Vimco, DFB, and Mechoshade Systems produce similar actuators [100] [101].

3.5 Final Concepts

3.5.1 Existing Concepts Selected

The concepts selected are:

- In-Line Involute Gear Transmission with Electromagnetic Motor
- Differential Cycloidal Cam Transmission with Electromagnetic Motor
- Travelling Wave Ring Ultrasonic Motor

In addition, a fourth, novel concept is selected. A fifth, novel concept is also discussed. Time does not permit construction of the fifth concept. Descriptions of novel concepts follow.

3.5.2 Novel Concepts

3.5.2.1 Flexural Wave Actuator

How it works: Consider the harmonic drive. The operation is explained through the progressive meshing of gear teeth [102]. Toothless harmonic drives are proposed in several patents [103] [104] [105] [106]. The patents describe the ratio as that of the harmonic drive, or that of the harmonic drive modified for a planetary input arrangement. The ratio of the harmonic drive, using pitch diameters, is explained as follows:

Continuous Contact Explanation: Suppose the flexible tube is held fixed and the rigid output member is free to rotate. In Figure 3.15, as the top input roller (assumed rigid) rotates clockwise, each point on the flexible annular member or tube is urged into contact with each point on the rigid output member. If contact is continuous with no sliding, and the arc lengths from the top point of roller/tube/output contact to points 1 and 2 are equal, then point 2 on the rigid output member will be in contact with the flexible tube at point 1 when the top roller

reaches point 1. The output member will rotate an arc length at the pitch diameter equal to the difference between the arc lengths (or half circumferences in this case) of the flexible tube and output member between the initial top and bottom roller contact points. The rigid output member must rotate in the same direction as the input for this to happen.

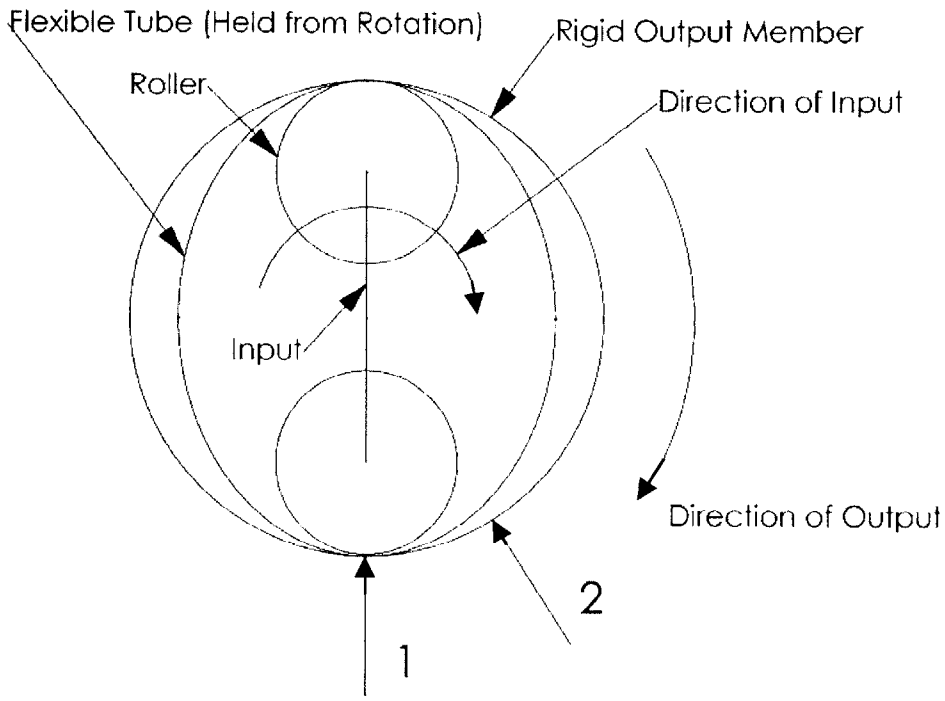

Figure 3.15 Toothless Harmonic Drive Continuous Contact Explanation

The patents claim this operation for a harmonic drive with no teeth. They fail to account for the bending of the finite-thickness flexible member (regarded as a curved beam) or possible slippage between the rotor and stator resulting in non-continuous contact, and provide no physical explanation for the tangential force required to rotate the output. Use of a zero thickness beam results in purely radial motion for a point on the flexible member. There is no reason for point-to-point contact to occur if any slippage is allowed. Assuming point-to-point contact can be enforced by wedging of teeth, the output motion, with the flexible member fixed, is in the same direction as the input. The real operation is very different when a tube of

finite thickness is used in place of the flexible spline of the harmonic drive and there is no enforcement of continuous contact:

Wave Theory of Operation: Consider one segment of the flexible tube, which is essentially a curved beam (Figure 3.16). Assume no rigid output member is present. As the rollers traverse the ID (inner diameter) of the flexible tube beam, a beam section is drawn inward and forced outward radially, and rotates clockwise and counter-clockwise out of phase with the radial movement. The motion of points on the outer surface of the tube beam is therefore elliptical. As the points move radially, they also move tangentially due to the rotation of the beam section about the beam neutral axis. This is similar to the motion induced in the composite beam of the travelling wave ultrasonic motor described above. The analogy is straightforward: a travelling, flexural wave is induced in the flexible tube by the roller(s), and the points on the outer surface of the beam trace elliptical trajectories.

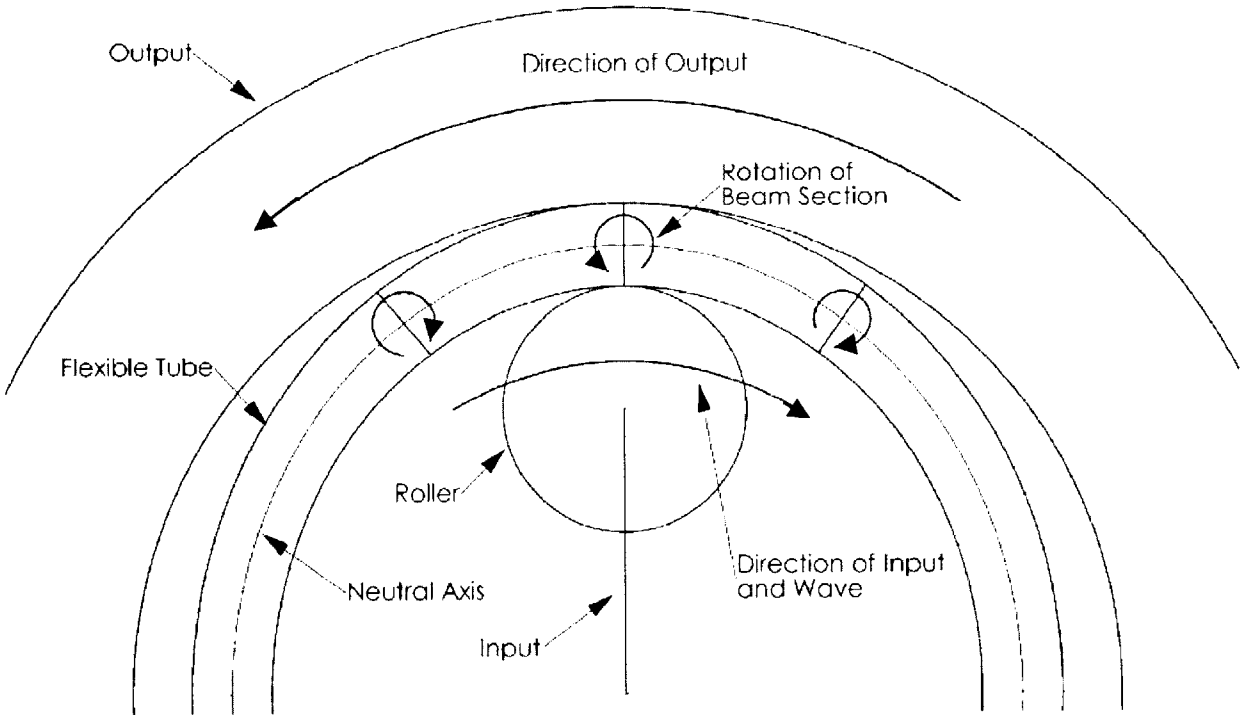

Figure 3.16 Toothless Harmonic Drive Flexural Wave Explanation

If the rigid output member (rotor) is introduced then the motion becomes more complicated (assume the tube wall thickness is slightly larger than the roller OD-rotor ID clearance). As the input roller travels along the ID of the flexible tube, a compression deformation is superimposed on the travelling wave motion. A shear deformation is superimposed due to the inertia of the output member and any applied load. Constraints are imposed by the other locations of roller-flexible tube-rotor contact around the circumference of the flexible tube. The overall effect is the transmission of power to the rotor by frictional contact between the inner surface of the rotor and the outer surface of the flexible tube, whose points describe elliptical trajectories induced by the travelling wave cyclic deformation of the flexible tube induced by the rollers. Slippage is allowed if the tangential velocity of the flexible tube outer surface is higher than that of the rotor inner surface and will be dependent on parameters such as coefficient of friction and compression. The motion of the output member is in the opposite direction from the travelling wave and is therefore in the opposite direction from the input.

Plus:

- Quiet.
- Built-in torque limit.
- Inexpensive.

Minus:

- Low efficiency for large deformations of the flexible tube.

3.5.2.2 Travelling Wave Tube Ultrasonic Motor

How it works: This concept is a hybrid of the travelling wave ring ultrasonic motor and flexural wave actuator described above. A composite cylindrical tube is used in place of a disk or ring. The ceramic tube is poled and bonded to the metal tube as shown in Figures 4.22 and 4.23. The travelling wave in this case is created by addition of modes with amplitudes in the radial instead of the axial direction. The wave thus travels around the circumference of the stator tube (Figure 3.17). A rigid, tubular rotor, clamped around the stator, is driven by

frictional contact between the rotor inner surface and stator outer surface by the elliptical motion of points on the stator outer surface. A mode search similar to that done for the disk motor can be performed to obtain optimal output torque and power for the cylindrical motor. One possible mode, for the stator tube constrained as in Figure 4.22, is shown in Figure 3.17.

Plus:

- The tubular shape fits the design envelope.
- The axial length of the contact surface is arbitrary, giving the potential to design for very high torque.
- The stator outer diameter can be finished by lapping.

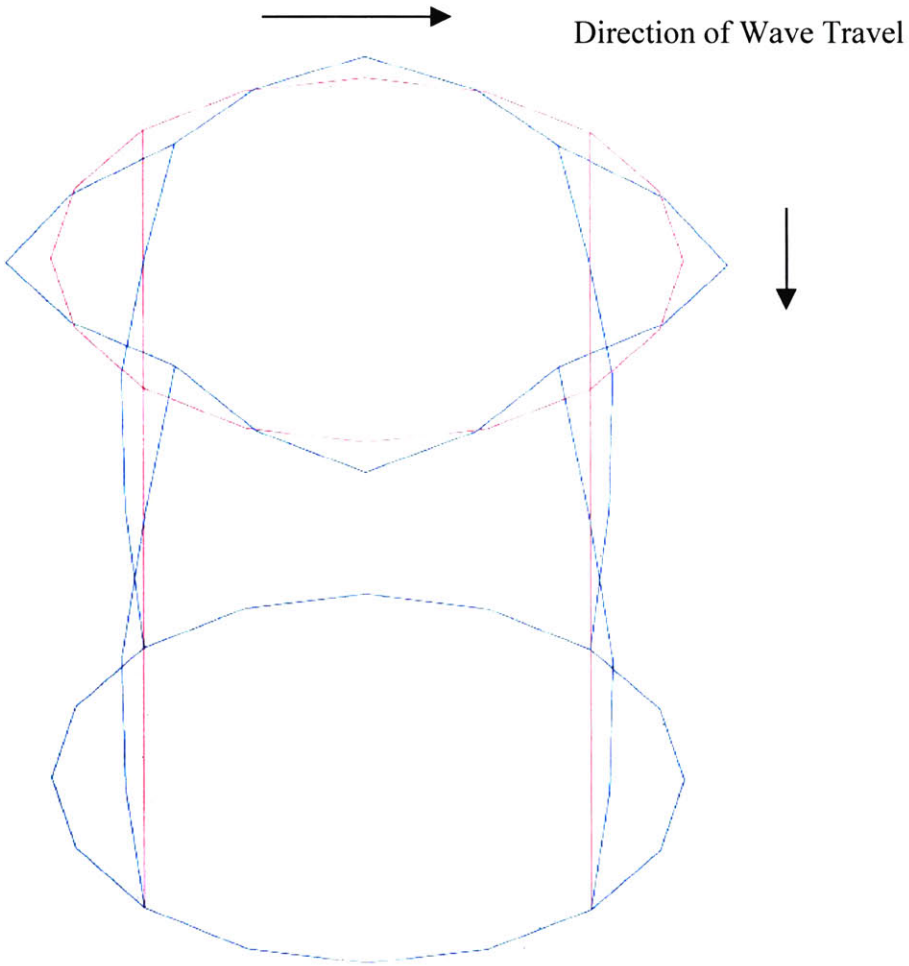

Figure 3.17 Stator Tube Vibration Mode and Travelling Wave (Deformed in Blue)

Note on Friction Drive: A friction drive can provide a torque proportional to the normal force and friction coefficient between the contacting surfaces. The friction force can be very high, as in the ultrasonic motor, but at some point the material will yield or slippage will occur. This is advantageous in the sense that a torque limit is built in to the design. To increase torque, surface area and normal force can be increased. The effect of increasing surface area is uncertain. For rubber, increasing contact area increases friction force, but is associated with yielding and wear. For the ultrasonic motor and drive, increasing contact area may reduce the normal force and may increase the required input power to create a travelling wave in a greater volume of material. A normal force increase may have to accompany an area increase to increase the torque.

Chapter 4

Design and Fabrication

4.1 Electromagnetic Motors with Speed Reducing Transmissions

4.1.1 Motor Selection

Four major factors affect the choice of motor: Noise, cost, torque-speed characteristic, and size. AC and DC motors are similar with respect to noise emission at a given load. However, DC motors are a better choice due to the variable speed requirement [15]. Brushed DC motors can be found at competitive prices in large quantities. Brushless DC motors are quieter but expensive.

It remains to design or select a brushed DC motor from many alternatives. The approach taken is to test available motors meeting power, torque-speed, and efficiency specifications to find a quiet commercial motor at low cost. Several high- and low-end motors are evaluated. A high-end but low-cost and very silent motor with a rare earth permanent magnet is selected. A more thorough selection process would of course consider the design and measure the vibration power of the candidate motors. However, it is not attempted to design a DC motor or to modify the chosen motor.

The power requirement is determined to be approximately 9 W from the output torque and speed and allowing for a 100:1 transmission ratio with a 60% efficient reducer.

4.1.2 In-Line Spur Gear Actuator Design

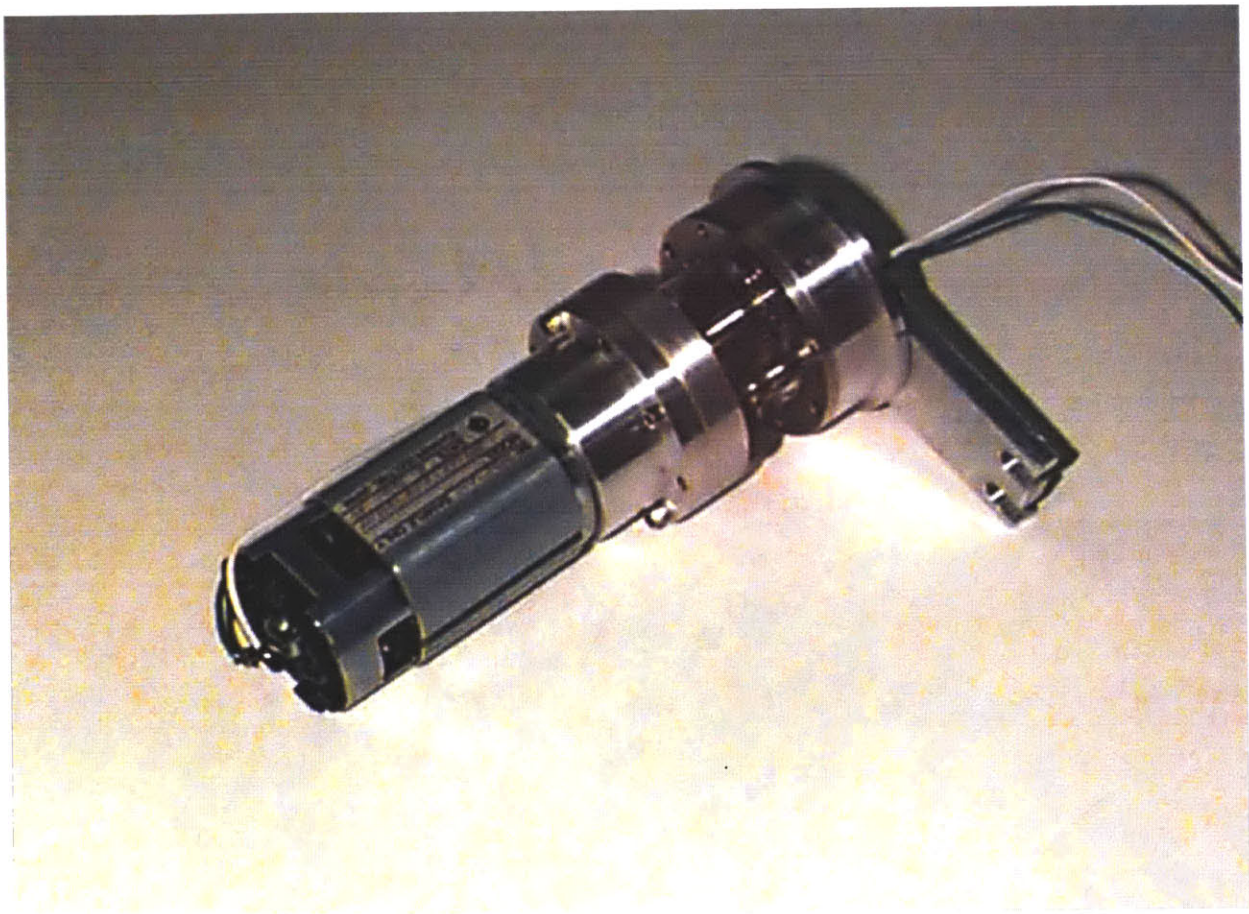

Figure 4.1 In Line Spur Gear Actuator Prototype

4.1.2.1 Architecture

The in-line concept provides a great degree of design freedom. Several configurations exist that fit inside the space envelope. A unique configuration is achieved by placing the motor in advance of the reducer. This minimizes the number of machine components needed (excepting lead wires to power the motor, which must be extended the length of the actuator). This arrangement uses the output element bearings to support the tube. The bearings are placed as close to the bracket mount as possible to minimize the moment and deflection, leaving the tube in a simply supported configuration. This architecture optimizes the use of

space. The only drawback is the need for the actuator mount to bear the entire moment, reducing the flexibility in mounting methods compared to the tube-supported actuator architecture.

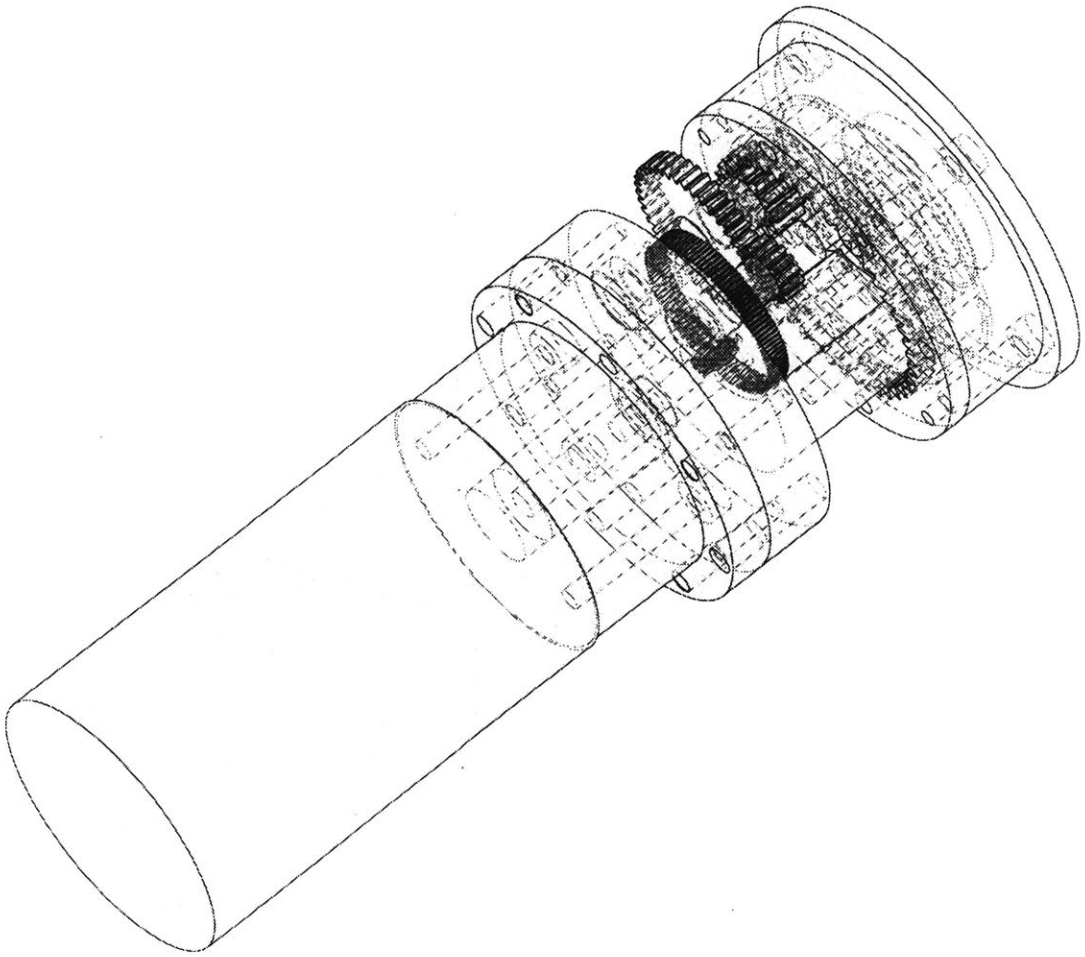

Figure 4.2 In-Line Spur Gear Actuator Prototype CAD

The assembly is shown in Figure 4.3. The motor is mounted to a coupling plate to allow room for the coupling between the motor shaft and pinion 1. In production, pinion 1 would be cut integral to the motor shaft, eliminating the need for such a large coupling plate. The coupling plate is mounted to the first bearing mount. This mount is cut to allow room for the gears yet supports the motor rigidly. The first bearing mount is screwed to the second. The

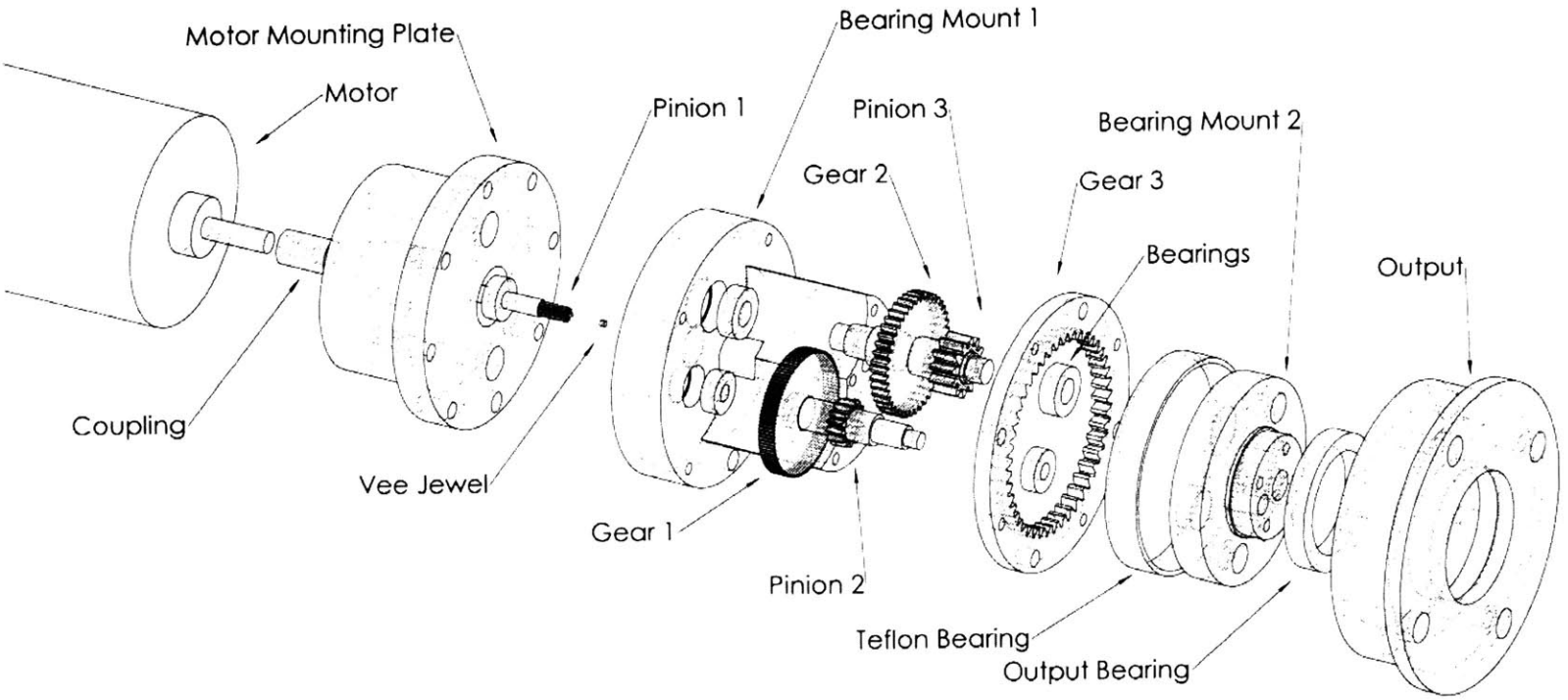

Figure 4.3 In-Line Spur Gear Actuator

Exploded View

output member is held concentric and axially constrained to the second bearing mount by two bearings. Gears and bearings are placed as shown. The second bearing mount is held fixed by a mounting bracket. The operation is straightforward: the motor turns pinion 1, and power transmission to the output member occurs through contact at the gears. It is helpful to refer to the figure during the following sections.

Note that for all prototypes, bearings, pins, and shoulders are used to locate parts at assembly. Most custom parts are machined from aluminum and all fasteners (not shown in assemblies for clarity) are stainless steel.

4.1.2.2 Speed Reduction

Ratio:

The speed ratio is calculated as:

$$Ratio_{EachStage} = D_{Gear} / D_{Pinion} \qquad (4.1)$$

for each reduction stage. The overall ratio is obtained by multiplying the ratios for each stage:

$$Ratio_{Overall} = R_1 \times R_2 \times R_3 \qquad (4.2)$$

Layout:

With the motor shaft concentric with the tube, the layout for a two-stage reducer does not give a high enough ratio. This is based purely on the geometry of packing pitch circles into the tube and maximizing ratio subject to minimum commercially available pinion sizes. The highest possible ratio is roughly 35:1.

Laying out a three-stage design gives a satisfactory ratio. Recall that center distance is defined as one-half the difference in pitch diameter for two mating gears. For the three-stage

layout in Figure 4.4, the center distances CD (and hence the ratio) are related to the angular separation of the first two stages θ according to:

$$\theta = \cos^{-1}\left[\frac{CD_2^2 - CD_1^2 - CD_3^2}{-2CD_1CD_3}\right] \qquad (4.3)$$

Several geometric rules must be followed in the layout (for example, the gear ODs must clear the tube and shafts).

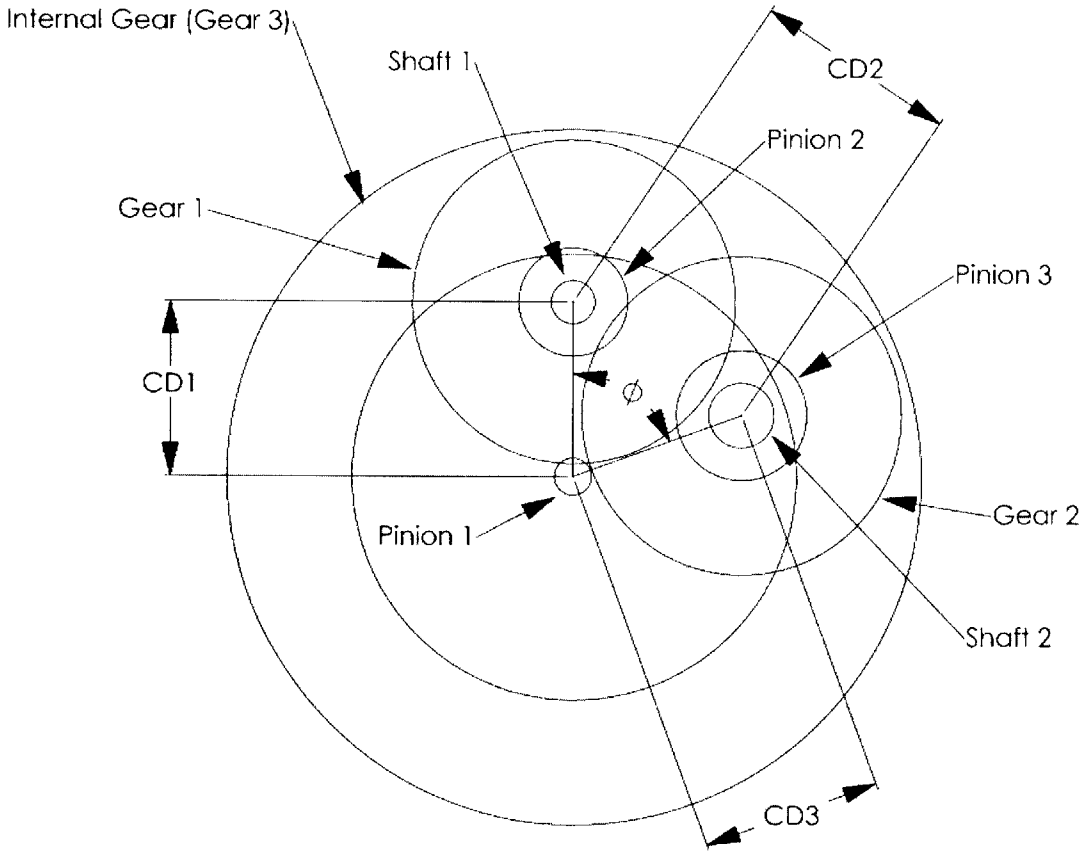

Figure 4.4 Three-Stage Spur Gear Reduction Layout

The maximum ratio for this layout is well over 200:1. The ratio is weighed against allowance for material to pass through the reduction stages to serve as the support structure for the motor, and standard sizes of gears are found to closely match the optimized pitch diameters.

A ratio of 120:1 is chosen, allowing freedom for later ratio refinements and plenty of material to support the motor.

4.1.2.3 Gears

Type:

Compare the use of spur vs. helical gears. Spur gears have the advantages of low cost, wide availability of sizes including internal spur gears, high efficiency, and no axial load. Helical gears have a larger pitch diameter for a given number of teeth at a given pitch and thus a higher load capacity, and produce axial bearing loads. Helical gears are generally considered quieter than spur gears due to their greater contact ratio and lesser variation in stiffness throughout the tooth mesh and therefore lesser transmission error. The lower efficiency of helical gears is due to the greater degree of sliding of the tooth surfaces. Internal helical gears are difficult and expensive to produce, and can not be found as a standard design item (the internal helical on the Bayside planetary is cut into the output member). However, helical gears can replace spur gears for almost any application, and the noise reduction, which must be determined by testing, could outweigh the increased cost and difficulty of design.

Spur gears are selected for the advantages described above. Helical gears can replace the spur gears and tested if noise is unacceptable.

Diameter, Pitch, and Pressure Angle:

Standard sizes of spur gears are selected for the prototype design, due to their low cost and high availability and ease of replacement. The smallest available pinion is chosen for pinion 1, consistent with ratio and load calculations. The pinion teeth are enlarged to avoid undercut (this allows some safety in the stress calculations as well). Ideally a finer pitch can be used, but the lead time for custom gears is discouraging. Similarly, the largest available internal gear is chosen for gear 3, based on pitch diameter and an outer diameter of 2". Pitch and pitch

diameter for pinions 2 and 3 are selected based on allowable stress, and gears 1 and 2 are selected to maximize the ratio within the space envelope. The selected pressure angle is 20°.

Material and Face Width:

Stainless steel 303 is the material of choice, for several reasons. The first is availability. Second, any corrosion will have a much larger effect on miniature gears because the surface damage is a greater percentage of the tooth thickness. Third, the standard face for 303 stainless steel gears is 1/8", a good size for a compact gear train. The only gear to exceed this is pinion 3, which sustains the highest contact and bending stresses of all the gears.

Plastic and carbon steel are also considered for materials. Carbon steel is much stronger than stainless (yield strength up to 100,000 psi as opposed to 30,000 psi for 303 stainless), and cheaper, but the strength is not necessary. Plastic gears are far cheaper and can be molded or cut. Molding is not a precise process for miniature gears, however (accuracy up to AGMA quality number 6 whereas steel can be hobbed to at least 14). Water absorption and its accompanying dimensional change is another issue. The main drawback is strength: a typical nylon gear needs at least 5 times the face width of a 303 stainless gear.

Tooth Load and Stress:

Tooth loads are given by

$$W_t = \frac{2\tau}{PD} \qquad (4.4)$$

$$W_n = W_t \tan\phi \qquad (4.5)$$

$$W_r = \frac{W_t}{\cos\phi} \qquad (4.6)$$

Subscripts t, n, and r denote tangential, normal, and resultant, τ is the torque on each gear, and ϕ is pressure angle.

Each gear must satisfy load rating requirements based on tooth contact stress and bending stress (AGMA Standard 420.04 pitch line velocities below 500 fpm and pinion speeds not exceeding 3600 RPM, and 421.06 for high speed gears). For spur gears, assuming unity contact ratio, bending stress rating is given by:

$$S_t = \frac{W_T K_a}{K_v} \frac{P_d}{F} \frac{K_s K_m}{J} \qquad (4.7)$$

S_t is stress in psi, and is compared with the allowable bending stress S_{at} of the gear material:

$$S_t \leq \frac{S_{at} K_l}{K_t K_r} \qquad (4.8)$$

W_t is tangential tooth load, P_d is diametral pitch, F is face width, and J is a geometry factor depending on the pressure angle and the number of teeth in the pinion and its mating gear. The K's are constants dependent on operating conditions for the gears. The subscripts a, s, t, r, m, l, and v denote, respectively, smoothness of operation considering overloads, size, temperature, reliability, load distribution, life, and dynamic load. All factors are chosen to exceed specifications. K_v is the only factor to be modified for high speed and only for pinion 1 (rated at over 4000 RPM). Compressive stress is given by:

$$S_c = C_P \sqrt{\frac{W_t C_a}{C_v} \frac{C_s}{PD \bullet F} \frac{C_m C_f}{I}} \qquad (4.9)$$

This is compared to the allowable compressive stress S_{ac}:

$$S_c \leq \frac{S_{ac} C_h}{C_t C_r} \qquad (4.10)$$

The C's in equations 4.9-10 correspond to the K's in equations 4.7-8, except C_h, the hardness ratio of the gear and pinion materials, and C_p, the elastic coefficient, given by:

$$C_p = \sqrt{\frac{1}{\pi\left[\left(\frac{1-\mu_p^2}{E_p}\right)+\left(\frac{1-\mu_g^2}{E_g}\right)\right]}} \qquad (4.11)$$

μ and E are Poisson's ratio and Young's modulus, and p and g denote pinion and gear. I is a geometry factor depending on the contact ratio and radius of curvature of each gear and pinion:

$$I = \frac{\frac{R_{lp}R_{hg}}{R_pR_g}\frac{\cos\phi}{2}\left(\frac{M_g}{M_g \pm 1}\right)}{M_n} \text{ (+ for external mesh, - for internal mesh)} \qquad (4.12)$$

M_g and M_n are the gear and contact ratios, and R is the radius of curvature at any point on the profile, given by:

$$R = \sqrt{\left(\frac{R_b}{\cos\phi}\right)^2 - R_b^{\,2}} \qquad (4.13)$$

Subscripts p, g, lp, and hp denote the pitch point on the gear, the pitch point on the pinion, the lowest point of single tooth contact on the pinion, and the highest point of single tooth contact on the gear. R_b is the base radius and ϕ is the pressure angle.

The stress calculation is checked by the allowable power for each gear. The formulas are:

$$P_{at} = \frac{\omega_p PDK_v}{126{,}000k_a}\frac{F}{K_m}\frac{J}{K_sP_d}\frac{S_{at}K_l}{K_rK_t} \qquad (4.14)$$

for allowable power (in hp) based on bending stress, and:

$$P_{at} = \frac{\omega_p F}{126{,}000} \frac{IC_v}{C_s C_m C_f C_a} \left(\frac{S_{ac} PD}{C_p} \frac{C_l C_h}{C_r C_t} \right) \qquad (4.15)$$

for allowable power based on compressive stress. ω_p is pinion speed in RPM.

Mounting:

Precision tolerances are held for dimensions affecting gear center distances (allowing for minimal backlash) and shaft alignment. The axial positions of the gears are matched by precision shims, and the gears mounted by Permabond adhesive, selected from a destructive test of several adhesives (press fit calculations show that press fits will not sustain the gear torques). The internal gear (gear 3) is pinned to the output member in four places and fixed by four cap screws. To further increase precision, the internal gear could be cut into the output member, but this is unnecessary since it is a very low speed mesh.

Lubrication:

The procedure for selecting the viscosity of a spur gear lubricant is given by Bartz [107]. The force/pitch-line-velocity factor, W_t/v, is determined by computing the Stribek contact pressure $p_{Stribek}$, based on the contact stress:

$$S_c = c\sqrt{p_{Stribek}} \qquad (4.16)$$

c is a constant that depends on the gear and pinion materials. The viscosity is read off a W_t/v - $p_{Stribek}$ chart. The results indicate that each gear needs different lubricant. This leads to a problem since only three total lubricants can be used. A versatile gear lubricant, Krytox GPL-263, is chosen for all meshes.

Thermal Effects:

The actuator never reaches a steady state temperature due to the variation in load and intermittent operation. Minimal clearance is allowed for backlash, the same clearance accounting for thermal expansion of the gears.

4.1.2.4 Bearings

Bearing loads are calculated from the tooth resultant loads and a layout for the gear train based on gear center distances and placement of the gears on their shafts, and bearing locations. Loads are applied at the gear teeth, at the axial midpoints of gears and bearings. The load imposed by the tube is included in the calculations.

Radial ball bearings are selected over roller and angular contact bearings for lower cost and availability in a wide range of sizes since no significant thrust loads arise. In addition, noise level increases parabolically with angle of contact for ball bearings [13].

Bearings are sized according to the ratings given them by the manufacturer. Conservative choices are made from available radial ball bearings. Unshielded bearings are selected for easy cleaning and re-lubrication, but shielded bearings would be better, considering that in practice they are replaced for every change and re-assembly. Lubrication and fit tolerances are provided by the manufacturer.

In the case of pinion 1, the shaft cannot be supported on one end by a ball bearing. A fitting sapphire vee-jewel bearing is selected. The end of the pinion shaft is modified to fit the vee-jewel. Note this bearing could be spring-loaded for easy assembly, but this is not done, to eliminate dynamic effects of imperfect pinion loading conditions.

In the case of the internal gear and output member, the bearing selection is more difficult. The largest low-cost precision radial ball bearing is 1" OD x 0.75" ID. This size determines the bolt pattern for the mounting bracket attachment. Rather than use two bearings in series to

obtain a fixed end condition, a custom Teflon bearing is made to fit snugly in the annular space between the output member and the second bearing mount. This gives stable output rotation.

4.1.2.5 Shafts and Couplings

Shafts are rated on bending, shear, and torsion stresses. Bearing and gear reactions are used with simply supported beam models of circular solid cross-sections to determine the necessary diameters. This is done in parallel with bearing selection.

A helical coupling, modified to fit the motor shaft, is selected to connect the pinion and motor shafts. It is easy to mount and provides the necessary amount of parallel and angular misalignment based on the tolerance stack-up.

The coupling between the output member and tube is by friction. Later, a thin layer of damping material is used as the coupling (section 4.3.3). For production, the output member should be keyed to fit the tube extrusion profile. The profile can be enlarged to allow for isolation material.

4.1.2.6 Design Notes

Ideally, the bearing mounts are combined in a monolithic piece to ensure parallel shafts. The assembly then becomes difficult. The two parallel shafts could be assembled, based on assembly geometry, but there is no way to assemble the internal gear without requiring one set of bearings to be under-rated and mounted from the opposite side of the bearing mount. This requires two bearing retainers that have to be removed every time the prototype is disassembled. Also, the output member OD could be smaller if the internal gear is cut integral to the output member, allowing for more isolation between the actuator and tube. Finally, the entire gear train could be enclosed to immerse the gears in lubricant.

4.1.3 Differential Cycloidal Cam Actuator Design

Figure 4.5 Differential Cycloidal Cam Actuator Prototype

Figure 4.6 Differential Cycloidal Cam - Output Gear Removed

4.1.3.1 Architecture

It is not possible to use the in-line actuator architecture for the cycloidal cam prototype. The architecture developed is shown in Figures 4.5-8. The motor is mounted to the mounting plate, in turn mounted to the housing, in turn mounted to the housing mount. An idler coupling to the tube is held concentric and axially coincident to this bearing mount by the idler bearing. A key is pressed into the face of the housing mount for insertion into a mounting bracket. The transmission is similar in architecture to the Mectrol, but features are designed to be lower in cost and easy to assemble. Just as for the gear prototype, the design is limited by the size of available low-cost precision bearings for the output. The Mectrol uses a high aspect ratio bearing to support the output member, allowing an axially compact arrangement, but increasing the diameter and cost. For the prototype, the 1" OD precision bearing is used in a similar arrangement as for the gear prototype. In this case the two output support bearings are stacked for ease of assembly and to eliminate the need for two types of bearing to support the output member. Since the tube supports the actuator, there is no moment loading to deflect the mount (the moment is taken up by the actuator). The fixed gear, comprising a roller or cam follower mount and a set of cam followers, is fixed to the motor mounting plate. The output gear is comprised of a moving roller mount to which is mounted a second set of cam followers. The output gear is attached concentric to the output member. The input member is an eccentric shaft, supported by bearings seated in the fixed and moving roller mounts, is coupled to the motor shaft by the same coupling used for the gear prototype. The compound planet is mounted to this shaft by two bearings stacked axially. The planet consists of two gear or cam sections of the appropriate outer profile, separated by a step to ease manufacture. As the input shaft turns, the planetary gear orbits the fixed gear, and turns the output gear in the opposite direction. Notice this is an inherently unbalanced configuration. A balancer is mounted to the eccentric shaft to bring the center of mass of the shaft/bearing/planetary gear assembly back to the center of the shaft. Coupling to the tube is by the same method as for the gear prototype.

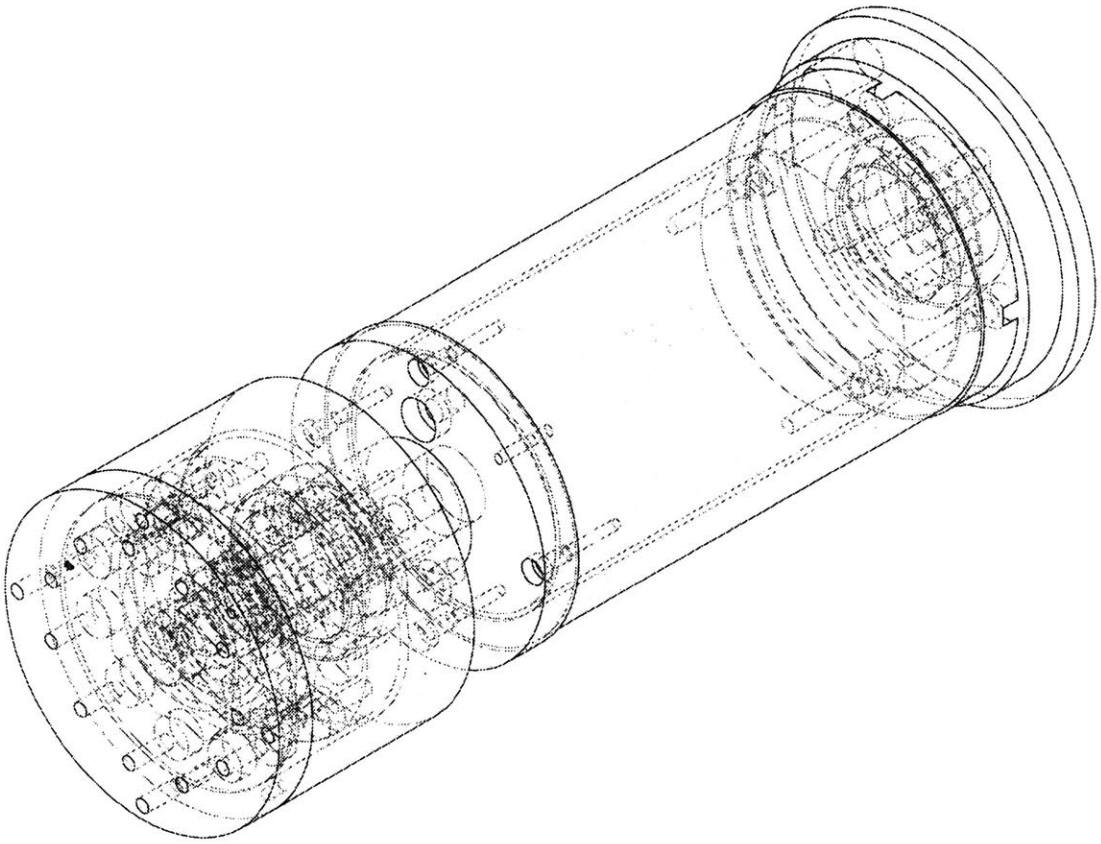

Figure 4.7 Differential Cycloidal Cam Actuator Prototype CAD

4.1.3.2 Ratio

The transmission ratio of the cycloidal cam is given in section 3.1.2.6. A ratio of -99: 1 can be obtained by using 9 lobes for the first planetary gear and 10 lobes for the second. This corresponds to 10 cam follower rollers for the fixed gear teeth and 11 for the moving output gear. The negative sign means that the output turns in the opposite direction to the input. This ratio is verified by simulation (section 4.1.3.9).

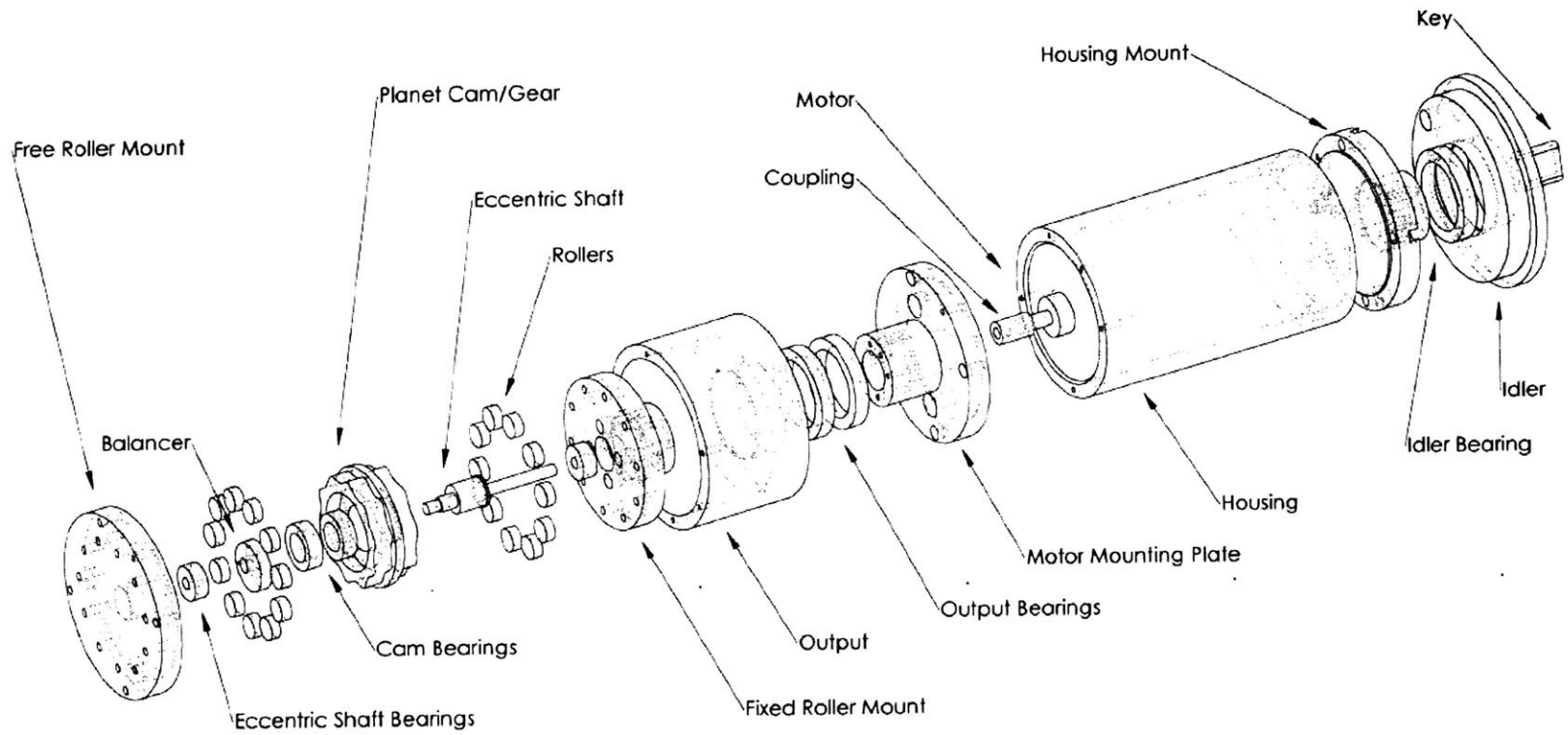

Figure 4.8 Differential Cycloidal Cam Actuator

Exploded View

4.1.3.3 Planet Gear or Cam Profiles

The planet gear tooth profiles are derived for the given number of teeth or lobes and rollers. The layout of Figure 4.9 is used to explain the derivation. A similar derivation is given by Braren [108].

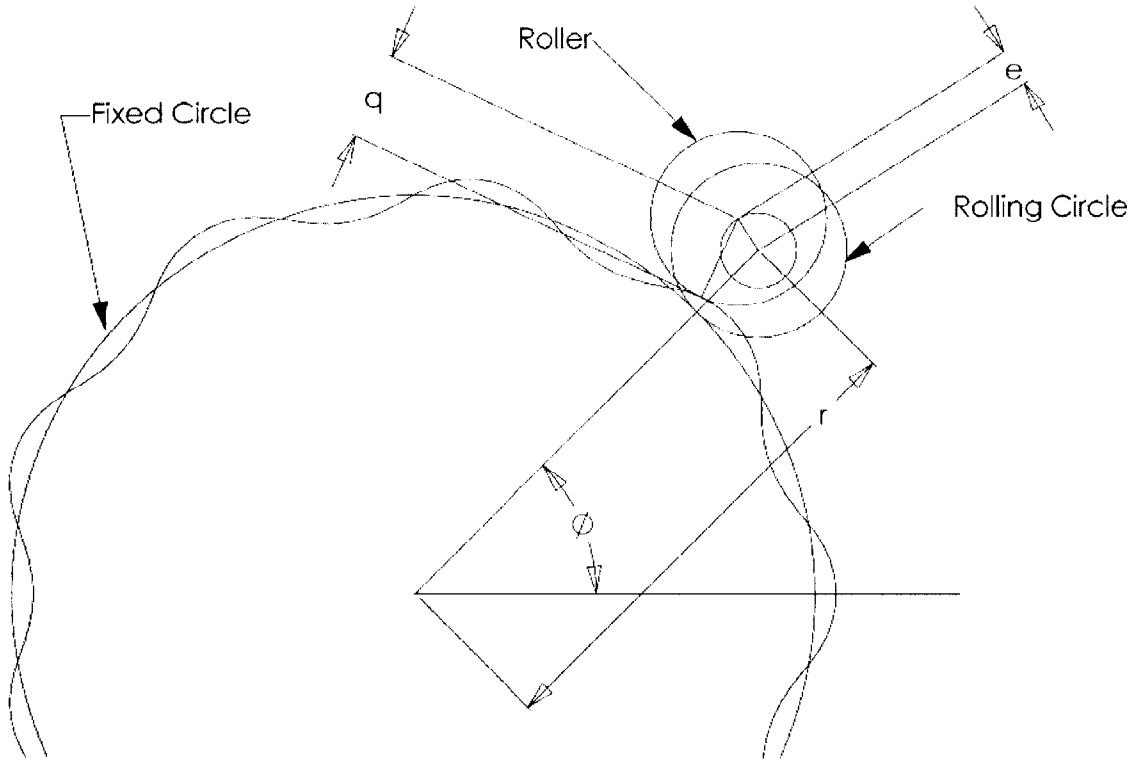

Figure 4.9 Roller/Planet Profile Layout for Profile Derivation

A point on the perimeter of a circle rolling around the outside of a larger circle traces an epitrochoid. A point at a radial distance e, some fraction c of the radius of the smaller circle, traces a shortened epitrochoid. This point is always in contact with the epitrochoid because it defines it. If the radius of the larger circle is some integer multiple n of the radius of the small circle (corresponding to n complete rotations of the smaller circle along the larger circle), then both the epitrochoid and shortened epitrochoid are closed curves. Suppose the point describing the shortened epitrochoid is marked at n+1 equally spaced intervals around the larger circle. The shortened epitrochoid necessarily touches all n+1 points. This locus of

points is offset from the center of the larger circle by a distance equal to e. Creating circles of radius q concentric to the n+1 points, the locus of points of constant contact with the circles is given by the following parametric equations (ϕ is the parameter, the angle of rotation of the center of the smaller circle about the center of the larger circle):

$$x = r\cos\phi + e\cos(\phi(1+n)) - q\cos\left(\phi + \arctan\left(\frac{\sin(n\phi)}{\left(\frac{1}{c} + \cos(n\phi)\right)}\right)\right) \qquad (4.17)$$

$$y = r\sin\phi + e\sin(\phi(1+n)) - q\sin\left(\phi + \arctan\left(\frac{\sin(n\phi)}{\left(\frac{1}{c} + \cos(n\phi)\right)}\right)\right) \qquad (4.18)$$

Again, the offset of the locus of centers is e. Here r is the sum of the radii of the larger and smaller circles describing the unshortened epitrochoid. Rolling the circles around the fixed shortened epitrochoid while maintaining their positions relative to each other is the inverse of orbiting the epitrochoid about the fixed (but free to rotate) circles. The above equations thus describe the planet profiles. Note that the same effect can be obtained by the use of cam followers rolling about the inside of a shortened hypotrochoid. In this case, the planet has the rollers and the gears have hypotrochoidal profiles.

For a given shaft eccentricity e, radius to the center of the rollers r, radius of the rollers q, and number of cam lobes or gear teeth n, c is determined by:

$$c = \frac{en}{r} \qquad (4.19)$$

and the x-y Cartesian coordinates are given by the parametric equations.

Profiles are generated based on standard cam follower selection (4.1.3.4) and space constraints. Profiles are cut into the single piece planet gear/cam as shown in Figure 4.8. The layout for the rollers and profiles is shown in Figure 4.10.

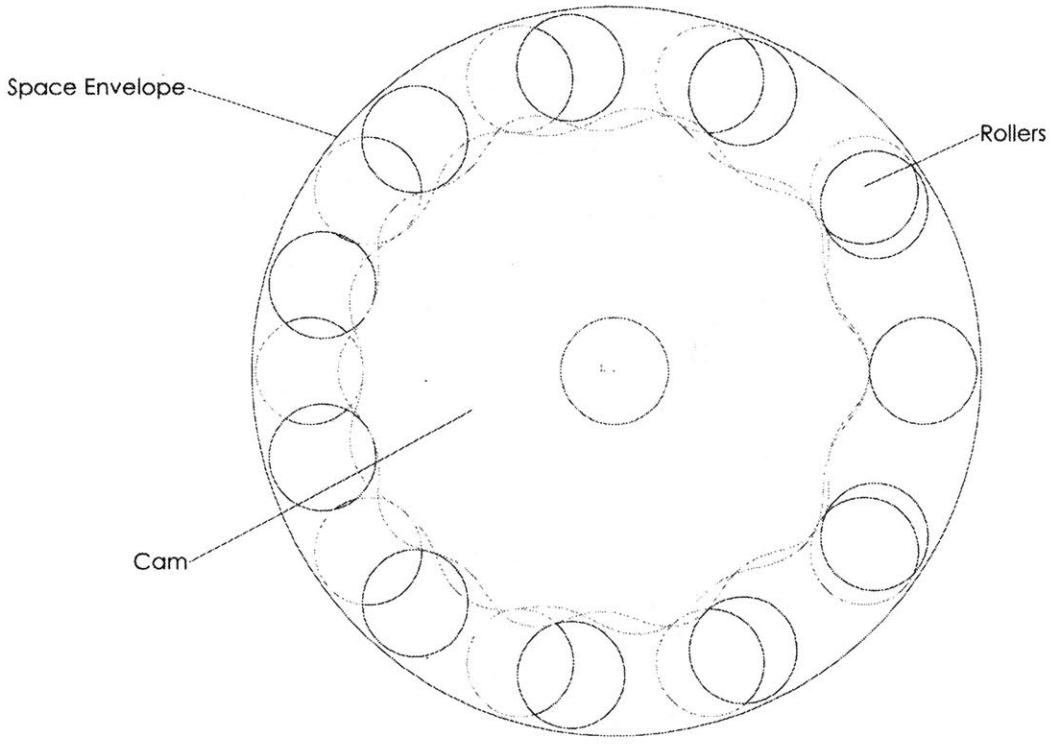

Figure 4.10 Differential Cycloidal Cam Planet – Roller Layout

Issues:

In reality, theoretical profiles will not work: some clearance is needed in the mechanism, just as backlash is needed for gears. Braren refers to this as rotation reversal tolerance, and gives a method of obtaining new, reduced profiles to minimize the deviation from theoretical operation. The method is similar to relieving gear tooth profiles. Here, the effect of varying r and q to obtain clearance is found by simulation, including those values close to Braren's minimum rotation reversal tolerance.

Another issue is measurement of profile accuracy. An optical comparator or coordinate-measuring machine could be used. In practice, the CNC machine is trusted to hold its tolerances. Unfortunately, it is practical to use only a finite number of points to define the profiles. The CAD software, SolidWorks 98Plus, generates splines to connect the points. In addition, bearings, although precisely machined and mounted, are subject to tolerances. Such errors will result in vibration as the rollers roll along the profiles.

4.1.3.4 Cam Followers

The cam followers used as rollers are selected according to load rating, diameter, and precision. Radial ball bearings are available down to 1/8" OD, but load capacity is low. On the other hand, bearings exceeding 1/4" OD result in gear profile shapes that do not fit well into the space envelope. Thus, 1/4" bearings are selected. Needle roller bearings are also available, and would add a certain amount of precision to the mechanism due to the smaller degree of play. They are axially longer than ball bearings, and are rated at much higher loads than are encountered. Ball bearings have the advantages of smaller size and play to allow easier assembly of planet to fixed and output gears. They can be mounted by pins or screws (screws are less accurate, but satisfactory with precise holes and cam followers). Thus, 1/4" radial ball bearing cam followers are selected. They are rated for well over the shock load based on a fixed beam-point load model.

Another option is to make custom cam followers. This is not attempted, but hybrid cam followers are made for lower noise. Smaller radial ball bearings are coated with a 1/16" layer of urethane to test the effects of a soft layer on fit of theoretical profiles and noise. Urethane tubes are purchased and measured for wall thickness uniformity. The most accurate is selected and cut to fit 3/16" OD stainless steel radial ball bearings. Loc-tite 495 is the adhesive used (determined from destructive testing).

Pierrat suggests designing for zero backlash by using adjustable position cam followers [109]. The cam followers are mounted on eccentric shafts that can be turned to bring each roller into contact with the planet gear.

4.1.3.5 Bearings and Shafts

Bearings and shafts are selected using a layout as for the gear prototype, but are over-rated due to relaxed space constraints. The moment imposed on the actuator by the tube is taken into account.

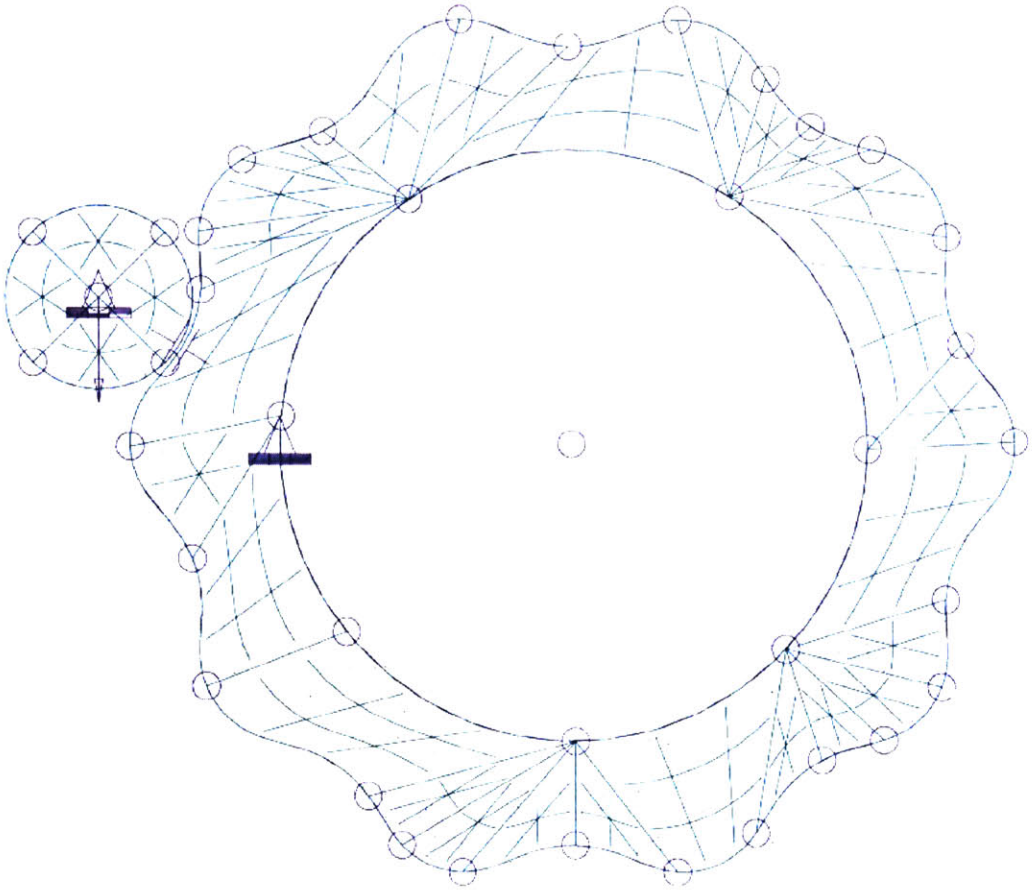

Figure 4.11 FEA Model for Cam Stress

4.1.3.6 Torque

The cam material is Delrin, a common gear plastic. A plane-strain finite element model is created in Mechanica to check the stress and deflection at the worst-case load condition

(single roller contact). The model is shown in Figure 4.11. The maximum computed stress is 3300 psi. This is well under the safe stress of Delrin for the required number of cycles, suggesting that load sharing is not necessary for successful operation.

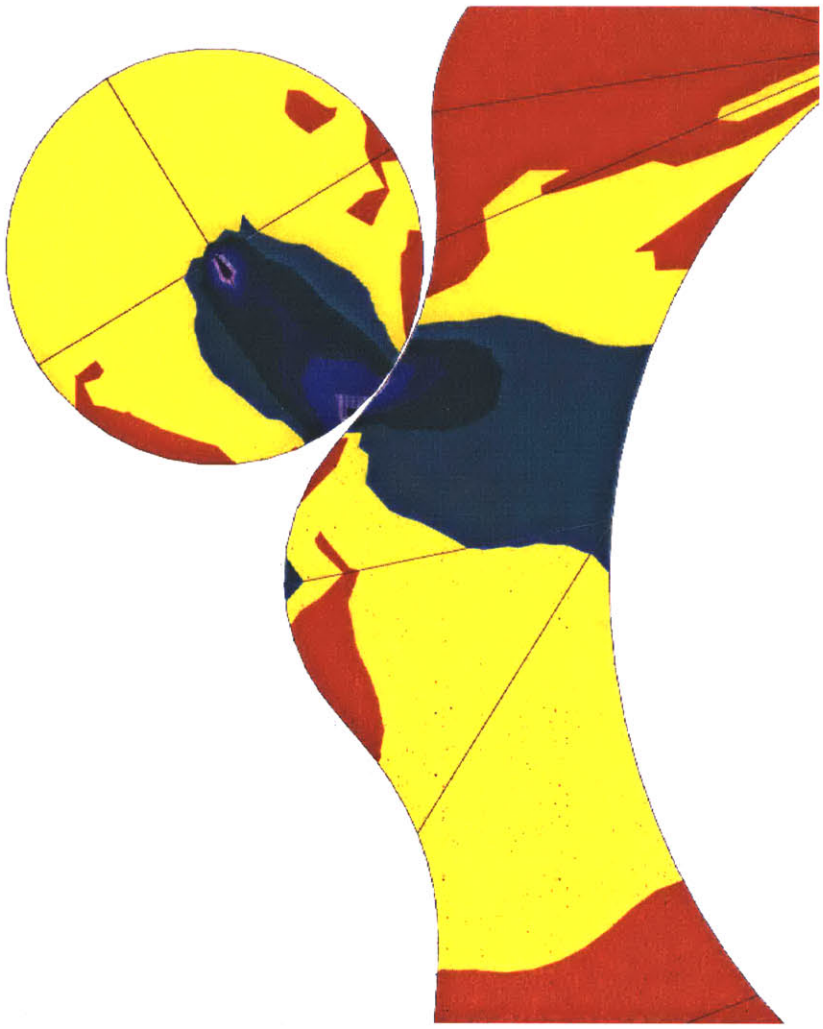

Figure 4.12 Delrin Cam Stress Distribution at Worst-Case Load

4.1.3.7 Balancing

The balancer is designed such that the center of mass of the input shaft/bearing/planet gear assembly lies on the shaft axis. The center of mass of each component is calculated based on the eccentricity and the total center of mass is calculated based on the center of mass and mass

of each component. Bearing mass is measured, balancer and shaft mass are assumed close to the CAD values, and planet mass is obtained by volume integration. The balancer introduces a couple to the shaft due to a slight difference in plane of mounting. The difference is considered negligible due to the short length of shaft and over-rated support bearings.

4.1.3.8 Lubrication

There are no standards for lubrication of cycloidal gears. The Mectrol units are submerged in oil for lifetime lubrication. Theoretically, no lubrication is needed except for the bearings. For the prototype, no lubricant is used. Delrin is commonly used with no lubrication in bearings and gears. Cams are also made of Teflon-impregnated Delrin for comparison.

4.1.3.9 Dynamic Simulation

A dynamic simulation is implemented for the cycloidal cam design. The CAD assembly is imported into Working Model 3D and appropriate constraints are applied (Figures 4.13 and 4.14). Orientation, Angular Velocity, and Angular Acceleration meters are created for the output gear to predict vibration and verify the transmission ratio.

The simulation does not run with the theoretically perfect profiles and roller parameters. The simulation works when at least 0.002" clearance is allowed between the planet cam and rollers. The radius to the roller and the diameter of the roller are varied in increments of 0.0005" to obtain this clearance and effects are observed for a range of values. The effect is positive when both parameters are reduced slightly. Decreasing the roller diameter for a given profile has the most dramatic effect. The cam follower diameter can not be reduced easily in practice. Thus, modified profiles defined using reduced q and r values are substituted for the perfect profiles. Varying the profile has a similar effect to varying both parameters at once, as expected. The meters for the best parameter values are shown in Figure 4.15, and are consistent with the simulated motion of the output gear. The simulation suggests that the transmission is not at constant velocity, giving rise to spikes in acceleration.

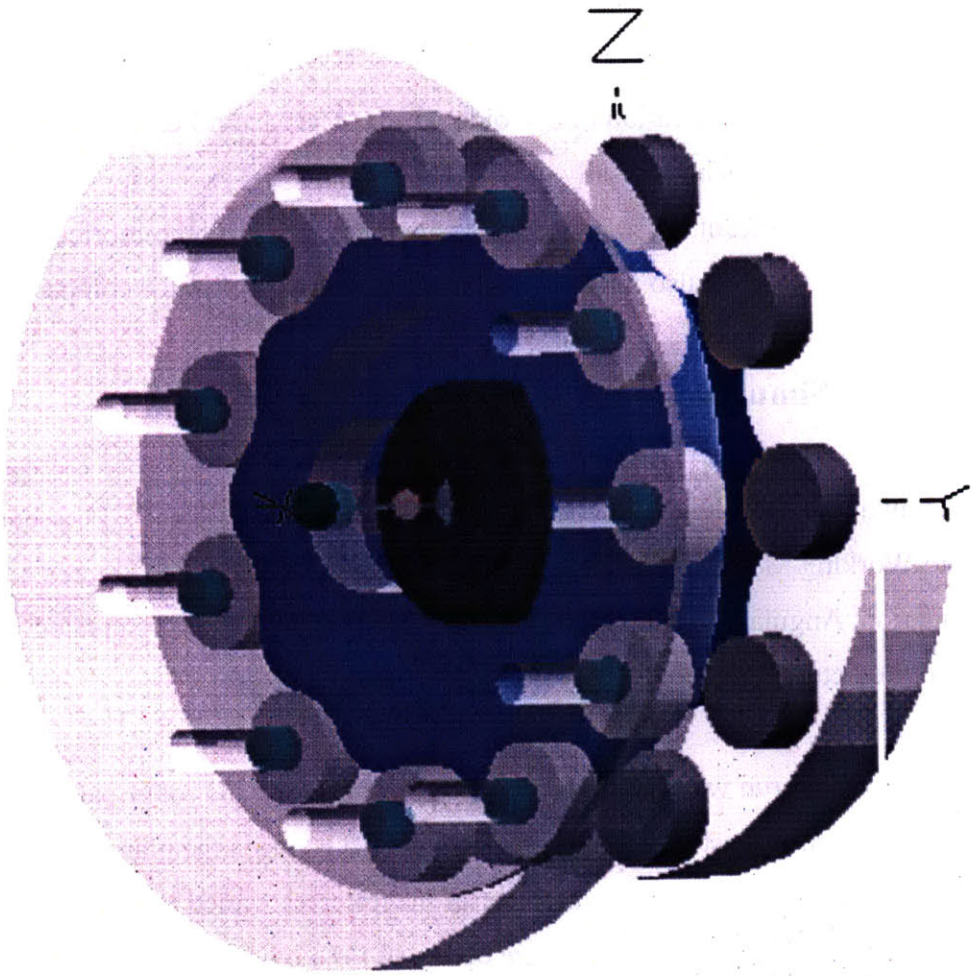

Figure 4.13 Differential Cycloidal Cam Dynamic Simulation

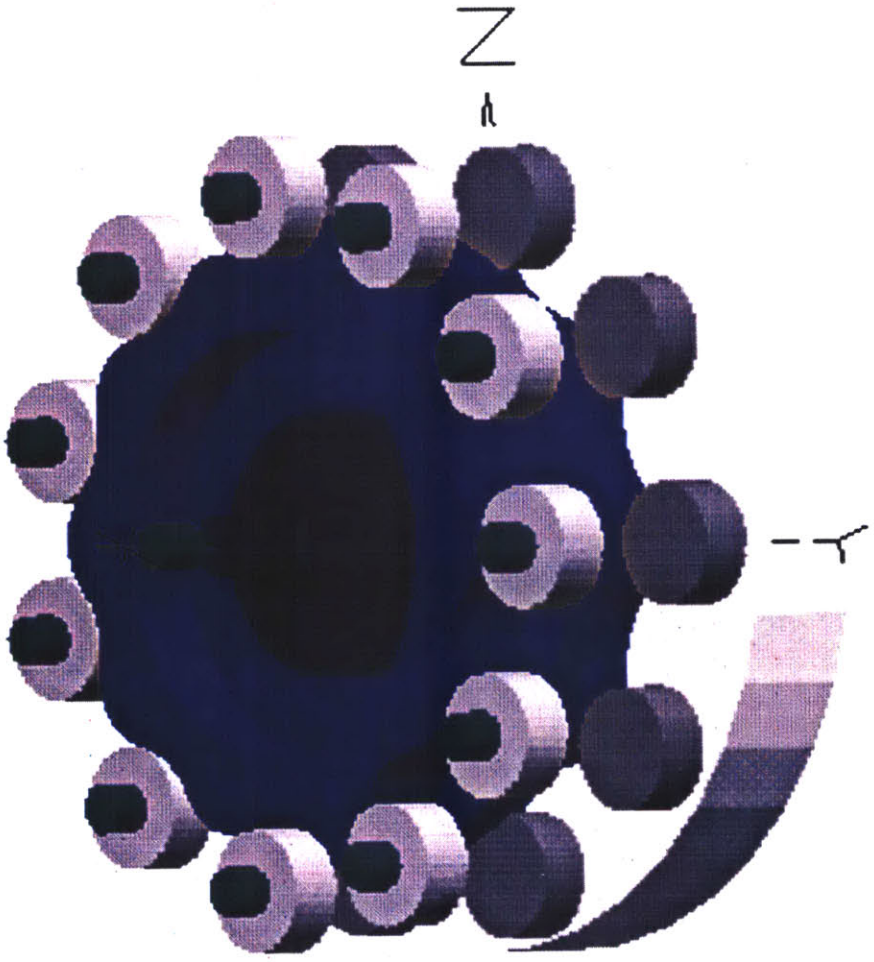

Figure 4.14 Differential Cycloidal Cam Dynamic Simulation – Moving Roller Mount Hidden

Rx Ry Rz (deg) vs. t (sec)

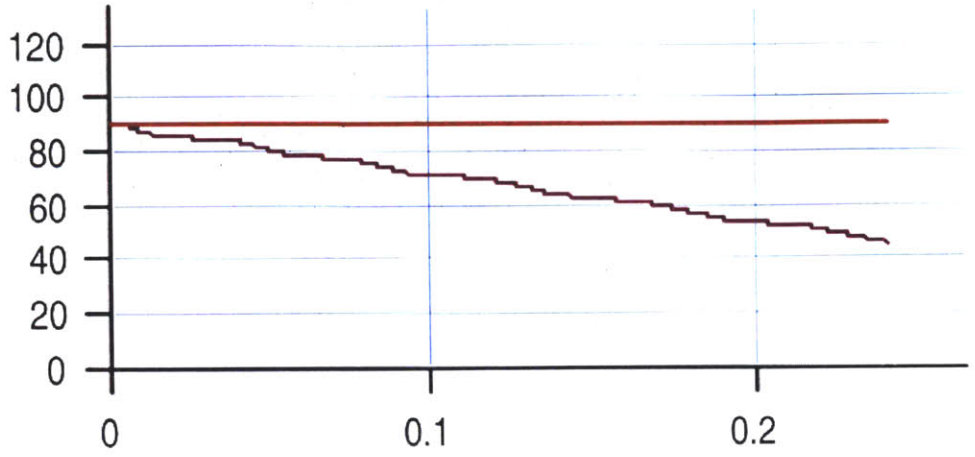

Wx Wy Wz (deg/sec) vs. t (sec)

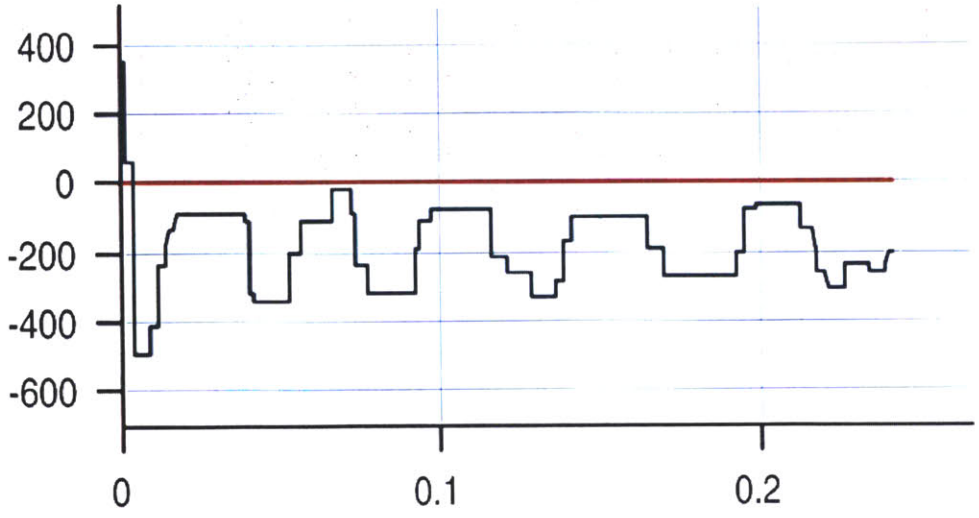

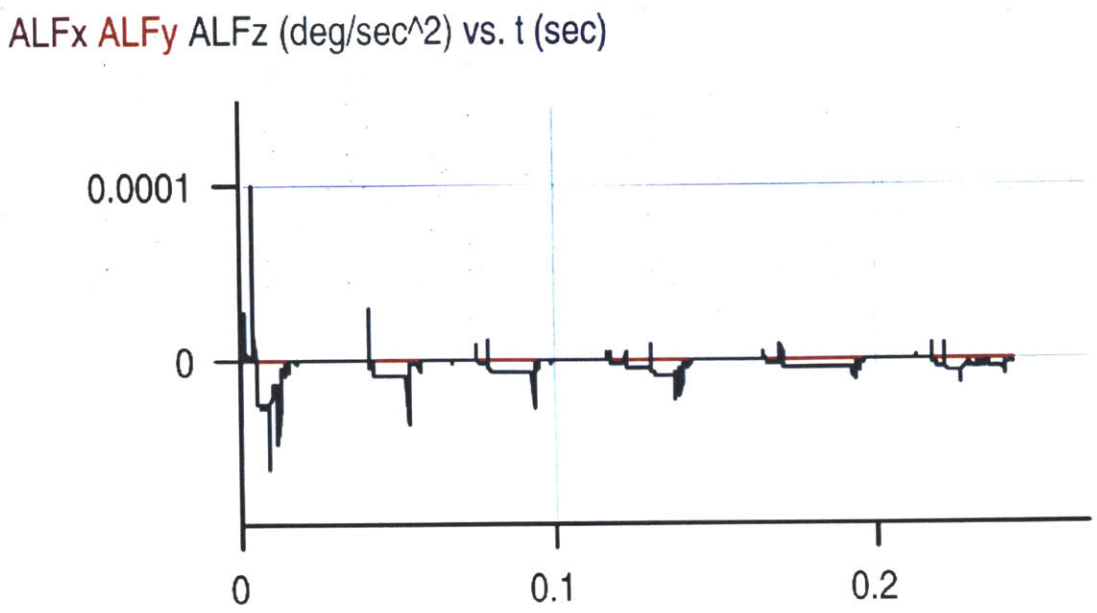

Figure 4.15 Moving Roller Mount Orientation (R), Velocity (W), and Acceleration (ALF) ($\Delta q = 0.0015"$, $\Delta r = 0.001"$).

The results of the simulation are captured as .AVI files and stored on the disk accompanying this thesis (Appendix A).

4.1.4 Flexural Wave Actuator Design

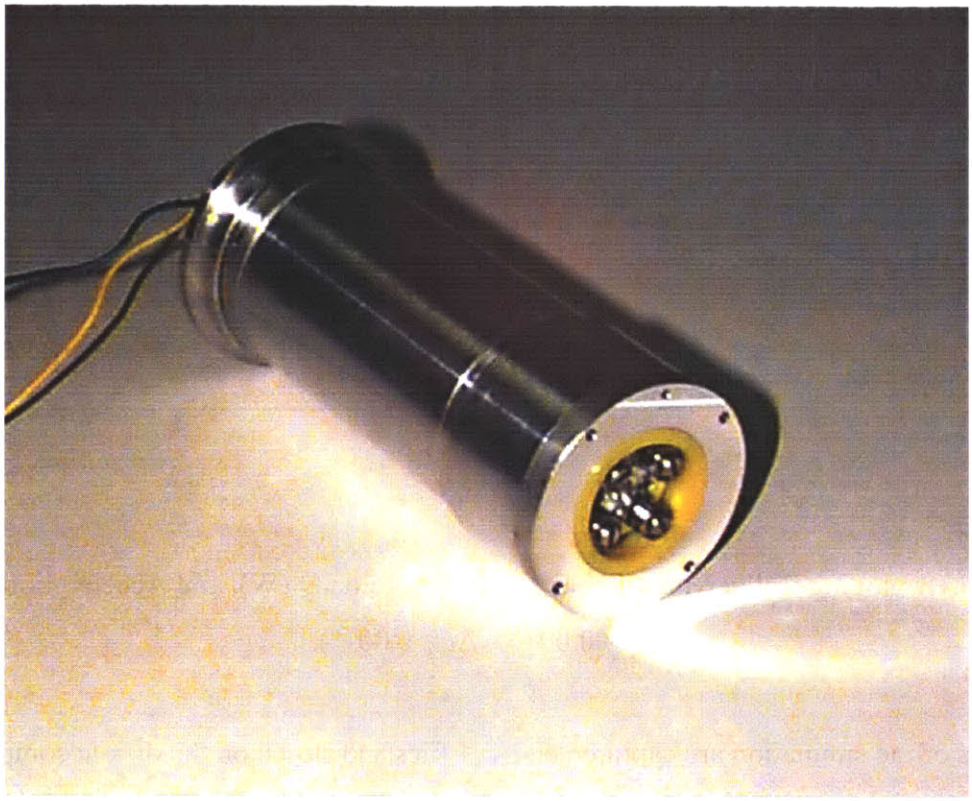

Figure 4.16 Flexural Wave Actuator Prototype

4.1.4.1 Architecture

The flexural wave actuator is subject to the same architecture constraints as the cycloidal cam (structural elements can't go through the transmission). The simplest configuration is almost identical to that of the cycloidal cam (Figures 4.16-18). The motor mounting is configured the same way. The flexible tube mount is mounted to the motor mounting plate. The output member is the same except for the axial length. The rollers are mounted to the roller mount, in turn mounted to a coupling attached directly to the motor shaft. The rotor is mounted concentric to the output. The flexible tube is mounted to the tube mount by interference fit, and is compressed between the rotor and cam follower rollers. When the motor turns the input shaft, the cam follower rollers roll around the ID of the flexible tube, inducing a

travelling wave in the tangential direction around the circumference. The resulting elliptical motion at the OD of the flexible tube drives the rotor by friction. Coupling to the tube is accomplished in the same way as for the cycloidal cam.

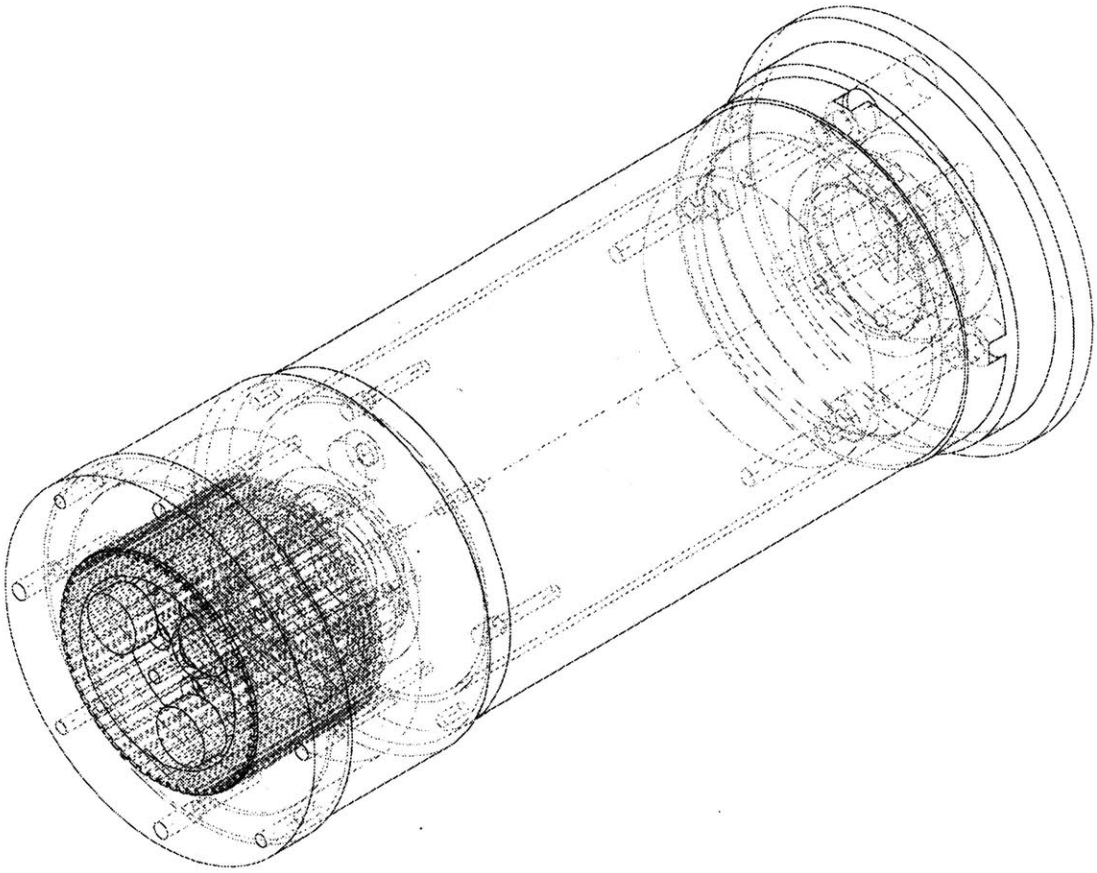

Figure 4.17 Flexural Wave Actuator Prototype CAD (Toothed Flexible Tube Shown)

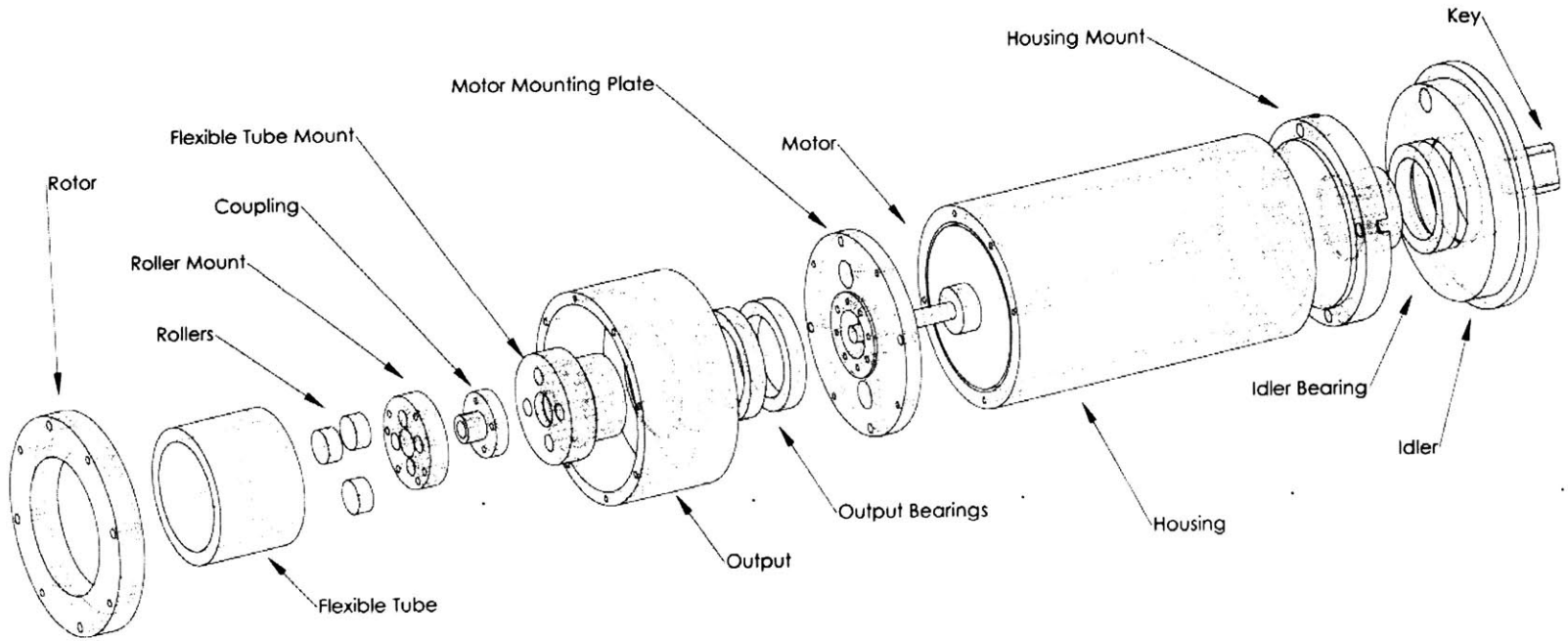

Figure 4.18 Flexural Wave Actuator

Exploded View

4.1.4.2 Layout Considerations

Tube Size:

It is not practical to machine flexible tubes. They are usually created by extrusion or molding. A limited number of extruded tube sizes is available. A variety of readily available elastomeric and plastic tubes is evaluated. The standard size chosen for the prototype is 1" ID by 1.25" OD. Smaller sizes are tested with poor results, and larger sizes vary so much in wall thickness that it is impractical to design with them. The length is chosen to minimize the axial length of the transmission while allowing simple assembly. Another consideration is torque. The maximum output torque is dependent on torsional buckling and shear strength of the tube.

Roller (Cam Follower) Size and Layout:

Cam follower size is important in determining the degree of elliptical motion. As diameter decreases, total angular excursion of the flexible tube cross section and hence tangential amplitude of the flexible tube surface increases, but required input torque increases. An acceptable diameter is obtained through trial and error in lieu of time for modeling.

The cam followers must be positioned symmetrically about the motor shaft for balanced operation and wave creation in the flexible tube. Hole patterns for two, three and four cam followers are cut into the roller mount for testing with various numbers of followers and points of contact between the input and output (one follower is not tried because it results in unbalanced force on the input shaft).

Compression:

The degree of compression of the flexible tube by the cam followers and rotor is critical to the operation of the flexural wave prototype. As compression increases, so does the output torque and required input torque. Also, only a certain amount of compression can be tolerated by the

material. The flexible tube, which is made from an elastomer or soft plastic, is susceptible to yield and compression set, or permanent distortion. Acceptable compressions are achieved for each material tested by trial and error, but this cannot be considered optimal.

4.1.4.3 Material and Surface Finish

Flexible Tube:

Material selection is important for the drive components (flexible tube and rotor): certain flexible tube materials, for example, result in very low torque or no torque at all. Flexible tube material selection is based on commercially available tubing and easily and cheaply molded materials. It is preferable to test a range of materials and a range of hardnesses and surface finishes for each material. The following properties are considered important:

- High friction: a friction drive requires a high coefficient of friction. Sometimes friction coefficient decreases with hardness.
- Abrasion resistance: the elliptical motion of the tube surface may abrade both the tube surface and the rotor inner surface.
- Resistance to compression set: when the drive is not activated, the rollers will compress local sections of the tube. Permanent set will result in a non-circular path for the cam follower, leading to vibration.
- Hardness: this should be varied to determine the best value for a given material.
- Surface finish: this should be varied also, and is dependent on manufacturing method. A smooth surface is produced by molding and extrusion, while a rough surface can be produced by grinding.

The following materials are tested:

- Polyurethane (both ester- and ether-based): this is the best material for compression set and abrasion resistance, and can be easily molded or extruded.

- Rubber (Natural Latex, SBR, Neoprene, Hypalon): natural rubber has good compression set and abrasion resistance properties also, and is cheaper than urethane.

- Thermoplastic Elastomers (Norprene and Santoprene).

- PVC.

- ML6 plastic [110]: this material has an unusually high friction coefficient at low durometers. Various hardnesses are tested. This material is also easily molded to high precision.

A wider range of materials, including Nitrile and EPDM, can also be tested.

Figure 4.19 Flexible Tube Materials (Left to Right: PVC, ether-based polyurethane, natural rubber, ML6 Plastic 30, 40, and 50 durometer. Center: ester-based polyurethane)

Rotor:

The rotor should be rigid so that there is a reaction to the friction force generated by the flexible tube. It should also have a high coefficient of friction with the flexible tube material.

Another desirable property is cooling capacity. Heat is generated at the friction contact, which may have adverse effects on the flexible tube material such as accelerated wear or softening and subsequent loss of force. Aluminum is chosen as the test material.

In practice, the ultrasonic motor uses a polymer layer bonded to the rotor to increase traction at the rotor-stator interface. The wear and life of this interface are critical to motor development [111]. The same approach can be taken for the flexural wave actuator.

A final consideration is surface topology. A smooth surface is used in the prototype to maximize friction contact area, but the effects of varying surface topology, i.e. roughness or teeth, should be tested.

4.1.4.4 Bearings and Shafts

Bearings and shafts are selected in the same way as for the gear prototype.

4.1.4.5 Noise

Any imperfection in the rotor ID or flexible tube surfaces, variation in flexible tube wall thickness, or eccentricity of any component with respect to the motor shaft will cause a vibration at a frequency equal to the motor shaft frequency times the number of rollers used. Rotor eccentricity will cause a vibration at rotor frequency.

4.2 Ultrasonic Motor

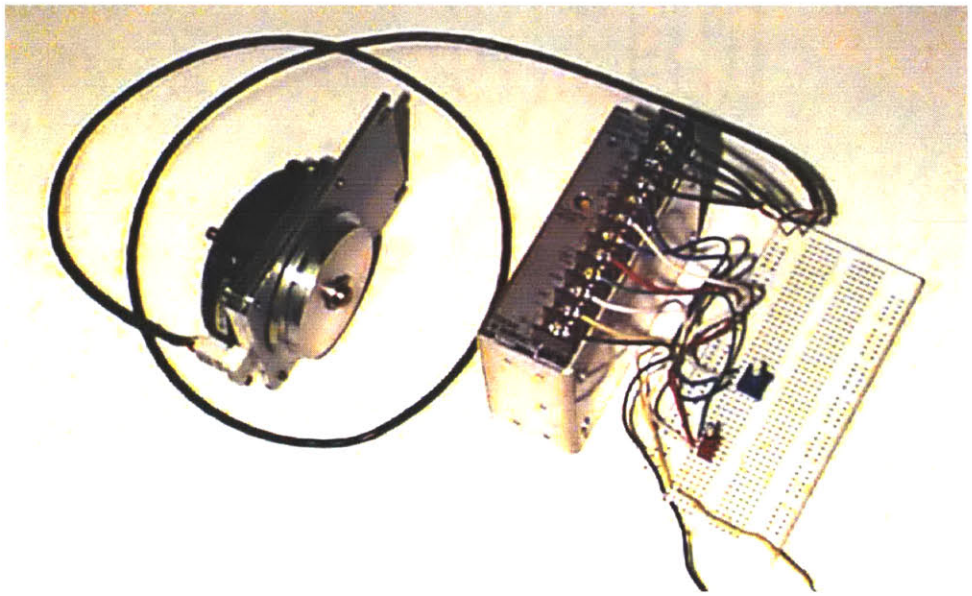

Figure 4.20 Travelling Wave Ultrasonic Motor and Driver

4.2.1 Selection

The highest torque commercially available motor is selected. Sizes are available to fit inside the tube, but torque increases with diameter, as discussed below. The motor comes with a driver and instructions to build a control circuit, consisting of a potentiometer and a switch. A small prototyping board is used with standard 22-gage wire for the connections. The potentiometer controls the frequency of the input signals, and therefore the speed of the motor. Theoretically, changing the frequency brings the stator disk away from resonance, decreasing the torque, but the effect is not great. The switch controls the direction of rotation.

The ultrasonic motor is mounted rigidly to a custom bracket as in Figure 4.20. Notice the motor must lie outside the tube because the motor OD is over 2". An output member is made to adapt the tube to the motor. The output member is keyed to the motor output shaft.

4.2.2 Travelling Wave Ring Motor Design

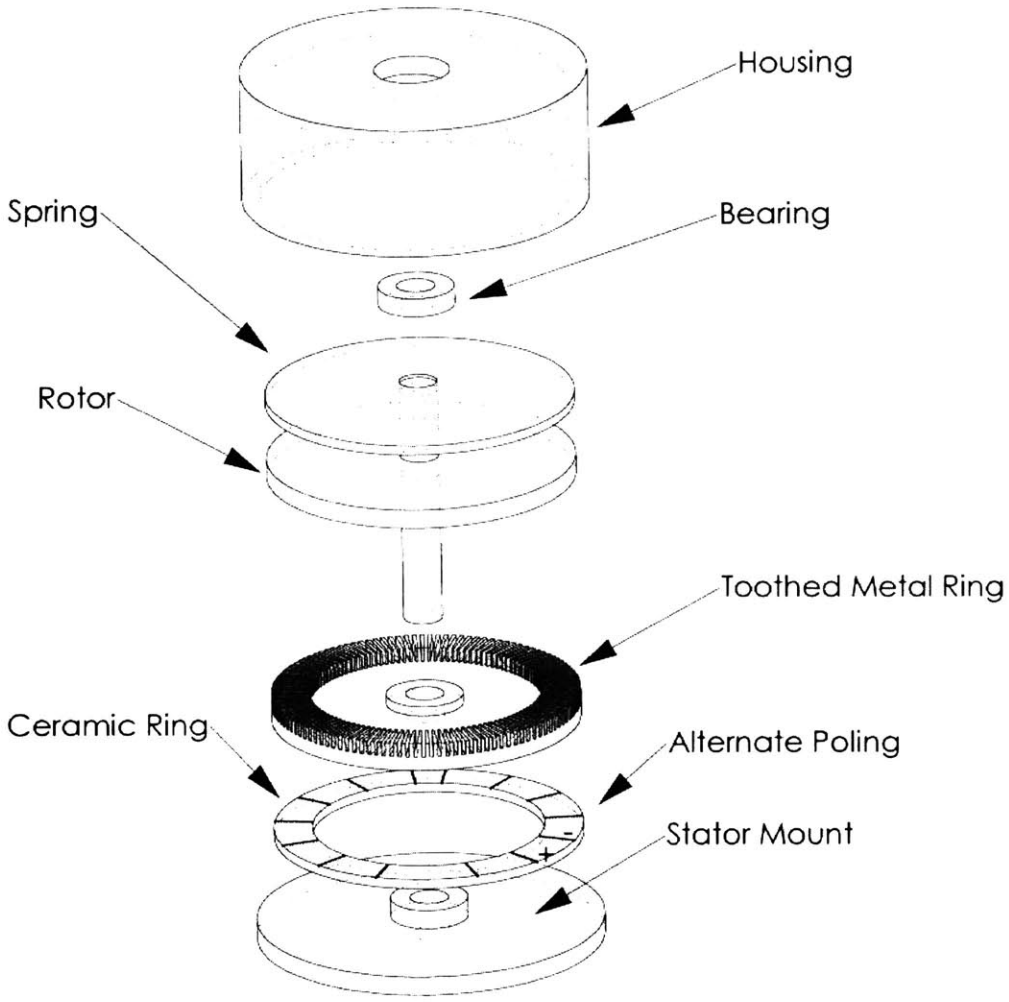

Figure 4.21 Travelling Wave Ring Ultrasonic Motor - Exploded View

The ultrasonic motor architecture is shown in Figure 4.21. A composite stator disk or ring is held fixed to a mount by means of a thin metal web. The rotor disk is mounted to a shaft and pressed against the stator at a controlled pressure by a Belleville spring. Bearings, seated in a two-piece housing, support the rotor shaft. The stator is constructed from a ceramic ring and a metal ring. Electrodes are placed on the ceramic ring. The ceramic is then polarized according to the desired mode of vibration. Note that the Curie Temperature of piezoelectric

ceramic is roughly 300°C. Operating the motor at higher temperatures, while unlikely, will de-pole the ceramic ring. The ceramic ring is bonded to the metal ring to create the composite stator beam. The metal ring is machined beforehand. Machining includes cutting radial slits in the surface to contact the rotor, forming teeth to amplify the elliptical motion of the surface by giving the surface less bending stiffness and bringing the neutral axis away from the rotor. The toothed surface of the composite ring is lapped for precision contact with the rotor (the amplitude of the surface motion is on the order of microns). The stator ring dimensions are designed for resonance at the desired drive frequency. This is accomplished by treating it as a composite beam and deriving the relationship between ID, OD, ceramic and metal thicknesses, and the natural frequency of vibration at the desired mode number. The interaction of the rotor with the stator undoubtedly affects the dynamic behavior. Thus, it is believed that the rotor parameters may be tuned to optimize performance.

Motor starting and rated torque is proportional to radius cubed, and is rated at 5 in.-lbs. at 100 RPM. The maximum efficiency is 50%. Life depends on operating conditions, and must be determined by testing. Spring load and operating speed are two parameters affecting life. The speed of the ring motor is inversely proportional to the diameter (the selected motor has an operating range from 0-200 RPM, desired operating point at 100 RPM). The maximum output power and efficiency are experimentally determined to be at about half of the no-load speed, which is dependent on the piezoelectric material properties, the diameter of the stator, and the starting current [90].

4.2.3 Travelling Wave Tube Motor Design

A concept for a high-torque, radially compact, tubular cylindrical ultrasonic motor is shown in Figures 4.22 and 4.23. This design is very similar to the disk design presented above. Instead of plane vibration modes of a ring or disk, the radial modes of a tube are exploited (Figure 3.17). A stator tube is formed by fitting and bonding a ceramic tube, poled circumferentially similarly to the ceramic ring in the ring motor, to the inside of an elastic metal tube. The rotor is also a tube, which is clamped around the stator. Static pre-load and thus holding torque are

achieved by adjusting the clamping force. Teeth are shown cut into the stator to achieve the same amplification effect as for the disk motor. The stator is mounted rigidly. It is shown open-ended here, but could be held at both ends if the ceramic tube were placed in the center between the supports. The rotor tube is supported by bearings at one end and by the stator at the other in the same way as the output member of the flexural wave actuator prototype.

It is expected that the output torque of this motor is higher than for the disk motor due to the dramatic increase in size. The torque is expected to increase with axial length of the composite section, maintaining the pressure between the rotor and stator. The tubular shape is ideal for the application.

A complete design study is not performed. The design is expected to be analogous to the ring motor and flexural wave actuator designs in most respects.

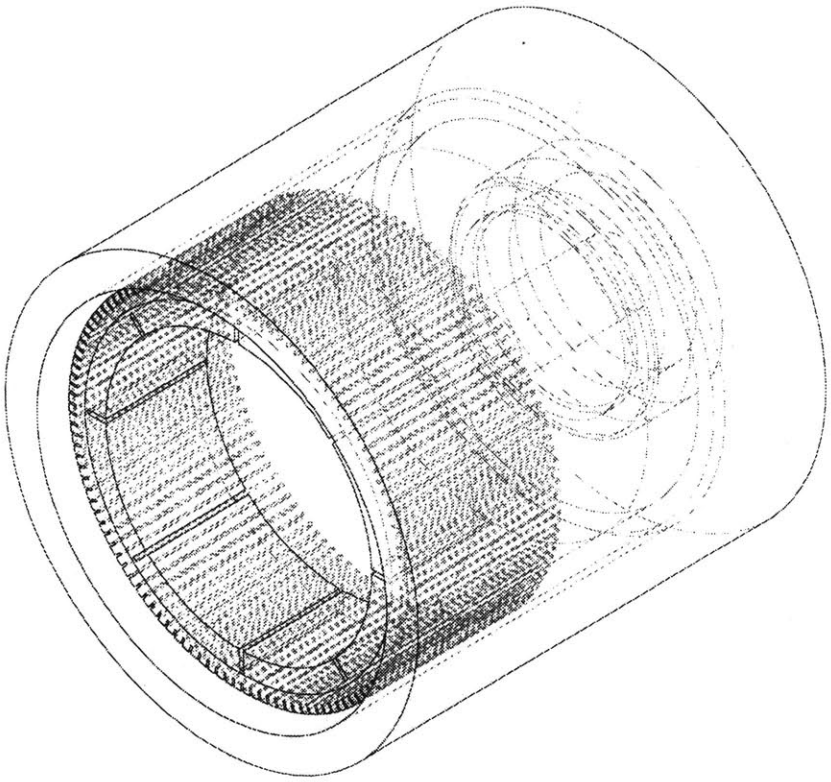

Figure 4.22 Travelling Wave Tube Ultrasonic Motor Design

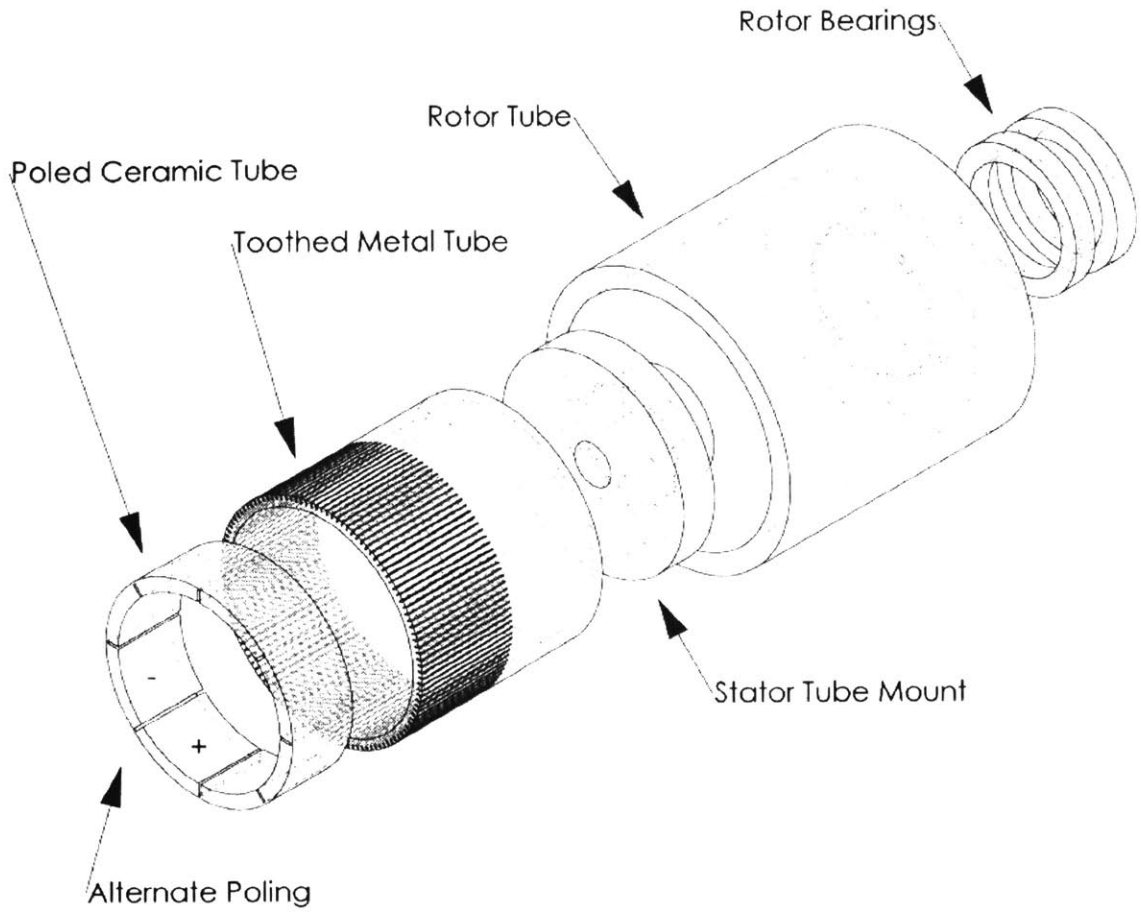

Figure 4.23 Travelling Wave Tube Ultrasonic Motor Design – Exploded View

4.3 System Design

4.3.1 Actuator and Mounts

For each prototype, excitations are designed away from resonances wherever possible, the mass of rotating parts is minimized, and tight tolerances are held to reduce the effects on noise performance.

In the case of unacceptable vibration transmission to the support structure, isolation can be used between actuator elements as discussed above, and between the actuator and the support. It is the purpose of this thesis to minimize the vibration at the source, but zero vibration at audible frequencies is difficult, so isolation is considered. A high degree of isolation can be achieved with simple elastomeric mounts [112]. For light loads and forces in the shear plane predominating, as in this application, shear loaded mounts can be selected or designed. This is reserved for future work.

4.3.2 Tube

4.3.2.1 Sound Radiation

Considering the tube as a sound radiator, it is best to minimize the diameter to minimize sound radiation capability. The radiation factor, a measure of ability to radiate sound, increases with diameter for a cylindrical tube [13]. The radiation factor is really a more complicated function of frequency and tube material and wall thickness. Also, at certain modes the radiation factor increases with the length to diameter ratio.

4.3.2.2 Natural Frequencies

A closed from solution for the natural frequencies and modes of a simply supported circular cylindrical shell is given by Soedel [113]. Simplified and extended solutions for simplifying assumptions, elastic supports, and acoustic radiation are also given. The solutions are sensitive to modeling, and take time to arrive at for any given set of constraints. The faster finite element method is used instead.

A simple finite element shell model (Figure 4.24) of a tube can be used to predict resonant frequencies within the range of human hearing (and thus to be avoided in actuator design). For any given length, diameter, and wall thickness within reasonable limits for the application, the analysis shows many mode shapes resonating within the range of hearing.

Some resonant frequencies for a 35" long, 2" diameter polycarbonate tube with 1/8" wall thickness is given in Table 4.1 (one end free to rotate about the longitudinal axis, the other end simply supported). The results are similar as constraints, loads, and material properties are varied. The frequencies can be controlled to some extent by varying parameters, but it is unlikely that all machine element frequencies can be avoided. For comparison, the excitation frequencies of the actuators are given in the table. In the future, when tube size and material are specified for a particular application, design away from the frequencies that radiate most powerfully could be attempted. The closed form solution should be used to check the finite element approach, and surface velocity measurement should be performed to check the accuracy of the models.

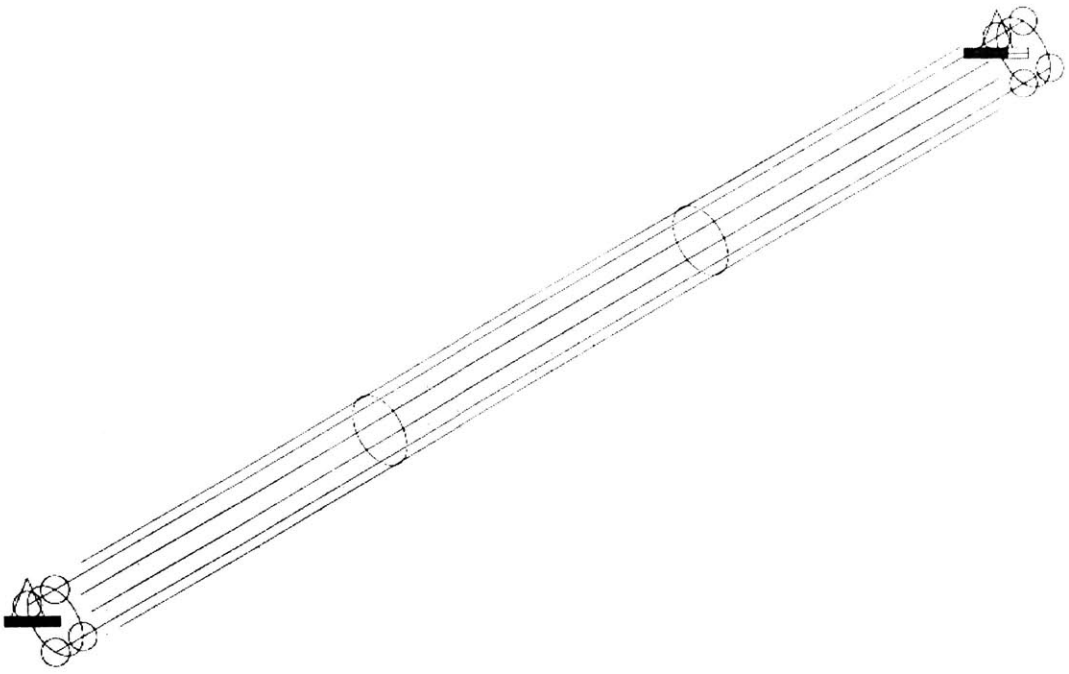

Figure 4.24 Shell Model of Tube

Table 4.1 Some Natural Frequencies of Polycarbonate Tube and Some Exciting Frequencies of Actuators

Tube	In-Line Spur Gear	Cycloidal Cam	Flexural Wave
	0.6 (output)	0.7 (Output)	0.4,0.7,0.9 (Output)
	2.4		
	7	6.1 (Orbit)	
24	29		
	57		
68	73 (Motor Shaft)	73	73
101	100		
236	200		234 (Roller)
300			292 (Roller Pass)
493	728	730	
1170	788	800	
1465	1455		
1605	1575		
2260			

In addition to the frequencies listed, each actuator will have some resonant frequencies due to the dynamic interaction of the machine elements. Many gear experts model the mechanics of gear drives using rigid shafts and housings and ideal and nonlinear elements to connect the gears to each other and the shafts to the bearing housings [114-116] [117]. The dynamics are complicated by contact mechanics (i.e. variable stiffness throughout gear tooth contact) and load varies with position for this application, thus the resonant frequencies are subject to continuous change.

4.3.2.3 Design

Another way to minimize housing radiation is to make more extensive changes to the design of the radiator. Adding ribs and other stiffeners can be effective. This can be done by trial and error, or by simulation and optimization. Inoue finds the optimal shape for a plate-shaped radiator under certain forcing conditions [118]. For a tube, the extrusion profile can be varied and stiffening inserts can be applied. An extreme measure is to use a solid tube, perhaps made of a damped material, with the end modified for the actuator and coupling. Other options include filling or coating the tube with a highly damped material. The drawback to relying on these approaches is that as more material and machining is added, cost increases.

4.3.3 Actuator-Tube Coupling Design

A properly designed coupling can be used to attenuate vibration transmission to the tube from the actuator. For each prototype, a thin layer of material is used as the coupling, and tube size is varied slightly to test the effect of different materials. In the final product, power transmission is most likely by keyed fit of the actuator and coupling into the tube, but for simplicity, the coupling is by friction fit between the actuator, coupling, and tube surfaces. In cases where the friction torque is not high enough to support the load, a layer of double-sided tape is used.

For worst case noise measurements, no coupling is used at all, and the actuator is simply snugly fit into the tube. Subsequently, 1/8" and 1/4" layers of Poron, Confor, and Isoloss polyurethane foams, Sorbothane damping material, and Buna-N rubber O-rings are used as couplings. The layers are 1/4" thick axially; two are needed for the cycloidal cam and flexural wave actuators (to sustain the moment) and one for the gear actuator (simple support).

Chapter 5

Results and Discussion

5.1 In-Line Spur Gear Actuator

5.1.1 Gear Design Modification

Mounting the gears to shafts with adhesive results in significant knocking sounds at gear 1 and 2 shaft frequencies, suggesting eccentric mounting. The next step is to replace the shafts with more costly but precise monolithic compound gears cut integral to their shafts. Knocking noise is thus eliminated, and the only noise left is a light scraping noise from the first mesh.

Note that for gears to be cut on the same shaft, a certain axial distance must be maintained between them. In this case some accuracy may be sacrificed because the hobs for the pinions interfere with the larger gears, thus the pinions are shaped, a process which cannot achieve the level of accuracy of a hob.

5.1.2 Disassembly

Disassembly is necessary several times. After the a few disassemblies, the noise emitted by the prototype increases. This could indicate a slight skewing of the gear shafts due to looseness in the bearing mount pins or damage to bearings due to disassembly forces.

5.2 Differential Cycloidal Cam Actuator

5.2.1 Operating Clearance

A cam with theoretical profiles will not fit into the follower pattern due to the lack of clearance. With a reduced profile, the cam orbits smoothly. The prototype performs as predicted by the dynamic simulation, with a rapidly varying transmission ratio. The effect of the variation decreases slightly with load.

5.2.2 Material

A Delrin cam orbits smoothly, but at high load binds. Teflon-impregnated Delrin is substituted, and a significantly higher torque is achieved before binding occurs.

5.2.3 Balancer

The effect of the balancer is uncertain. Performance is nearly the same whether or not it is present. The dynamic effect is very small for such a small mechanism.

5.3 Flexural Wave Actuator

5.3.1 Elliptical Motion

High-speed video (Appendix B) is taken for the flexural wave actuator using a Kodak Ekta Pro 1000 Imager and EM Processor. Video is taken of the motion of the stator and rotor for several materials and with and without the rotor attached. The frame rate is 1000 frames/sec. The rotation of the beam section about the neutral axis, as explained in section 3.5.2, can be seen clearly when the recording is played back at 30 frames/sec. The video is also used to

determine the speed ratio of the drive for different numbers of rollers, holding the input speed nearly constant.

5.3.2 Ratio

The ratio for the harmonic drive is given in section 3.1.2.12. The theoretical ratio for the flexural wave actuator prototype based on this equation is 126. This is a geometric theory and not a possibility. The wedging action of teeth is needed to bring about the operation of the harmonic drive and obtain the theoretical ratio. In reality, for the finite-thickness beam mechanism, the ratio depends on:

- Number of rollers and thus frequency, as for the ultrasonic motor.
- Excursion of the stator surface (which depends on the size and hardness of the roller, the thickness and hardness of the flexible tube and rotor, and the friction coefficient between the stator and rotor).
- Resonance of the stator tube.

The transmission ratios for different numbers of identical rollers are given in Table 5.1. These reflect the dependence of ratio on frequency. Note that the harmonic drive ratio formula would predict an increase in the ratio with the number of rollers, if any change, due to the increased radial stretching of the flexible tube.

Table 5.1 Dependence of Ratio on Number of Rollers for Flexural Wave Actuator

Number of Rollers	Ratio
2	200:1
3	112:1
4	80:1

5.3.3 Material and Surface Finish Variation

The ester-based polyurethane tube (durometer 85 A) provides the highest torque. Roughening the surface increases the torque even further. It is expected that cutting slits or teeth in the outer surface of the flexible tube has the same amplification effect as with the ultrasonic motor. It remains for future work to prove this.

5.3.4 Noise and Temperature Effects

The actuator is very quiet, but vibrates at roller pass frequency for the urethane. Because this vibration disappears for the precisely molded ML6 material, it is assumed that it is due to the variation in wall thickness of the tube. Measurement confirms a region of increased wall thickness on the order of 0.010".

The operation of the drive with the urethane tube becomes smoother as it heats up. This can be explained by the softening of the urethane. The rollers pass more easily past the region of increased wall thickness due to the warmer, more flexible material.

5.4 Ultrasonic Motor

The ultrasonic motor performs as specified in the product literature. There is no audible noise whether alone or coupled to the tube. The only minor problem is that the motor heats up during operation, and a thermal safety circuit in the driver sometimes shuts the driver off at startup.

5.5 Comparative Measurements

Table 5.2 presents noise, torque, and efficiency measurement results.

Table 5.2 Actuator Noise, Torque, and Efficiency Measurements

Actuator	Noise (dB) (Alone)	Noise (dB) (Worst-Case)	Maximum Torque (in.-lbs.)	Efficiency (%)
In-Line Spur Gear Actuator	8 Light Scraping	10 Twanging	20	80
Differential Cycloidal Cam Actuator	18 Damped Rattling	21 Rattling	10	30
Flexural Wave Actuator	5 Fan-Like	8 Twanging	6	20
Ultrasonic Motor	0	0	7	20

5.5.1 Noise

Noise measurements for each prototype under identical ambient conditions are presented in the first three columns of Table 5.2. The first column of the table gives the level increment over background sound pressure level of the actuator by itself and the second column the worst case noise (no isolation, simplest mounts possible). Qualitative descriptions of the

noise follow the level increments. The sound level meter measures levels down to 30 dB with an accuracy of ± 1 dB. The background sound pressure level for all measurements is 32 dB. Note that the resonance of the tube appears to have nearly the same effect for the DC motor actuators, suggesting that the motor frequency may be the dominant tube excitation.

With the flexible coupling and mounting the system to a damped structure, noise performance is greatly improved over the worst case, suggesting that the simple support mounts transmit vibration to the structure and reflect it back to the actuator, and also radiate noise to some extent.

The noise for each test is captured on 8mm tape for subjective and quantitative analysis (Appendix B).

5.5.2 Torque

The third column of Table 5.2 presents the maximum torque for each actuator. The drive torque shown is for four input rollers. The ultrasonic motor stall torque is slightly lower than expected. Both values represent the highest load borne before slipping occurs. For the cycloidal cam, the torque shown is the binding torque. For the gear actuator, the maximum torque applied is arbitrarily chosen as 20 in.-lbs. to avoid damage.

5.5.3 Efficiency

The fifth column of Table 5.2 presents the experimental efficiency of the actuators, based on input power at maximum load at 35 RPM. Note that the flexural wave drive compares to the ultrasonic motor in both torque and efficiency. Note also that efficiency may not be optimal for any of the actuators at 35 RPM.

5.5.4 Cost

Comparative cost estimates are given in Table 5.3. Price quotes are for quantities of 10,000/year. The most expensive items (parts and process) are listed. Gear actuator cost is dominated by gear cost. Ultrasonic motor cost is dominated by ceramic and stator finishing costs. The driver cost is estimated at 30-50% of total cost. Cycloidal cam cost is dominated by cam follower cost (21 are required). Flexural wave actuator cost is dominated by bearing cost, and is therefore much lower than for the other drives. Note that much cheaper gears and bearings can be purchased, at the cost of precision.

Table 5.3 Comparative Expected Production Cost

In-Line Spur Gear Actuator		**Differential Cycloidal Cam Actuator**		**Ultrasonic Motor**		**Flexural Wave Actuator**	
Item	Cost	Item	Cost	Item	Cost	Item	Cost
Motor + Gear 1	$10	Motor + Cam	$10	Ceramic Ring	$25	Motor	$5
Compound Gears (2)	$10			Stator Lapping	$5		
Gear 6	$10			Driver	$20		
Bearings (8)	$5	Bearings (27)	$5	Bearings (2)	$5	Bearings (8)	$5
Base Total	$70		$145		$60		$45

5.5.4.1 Commercial Actuator Cost

The ultrasonic motor costs $900 off the shelf. The cycloidal cam and helical planetary transmissions discussed above cost $1600 and $700 respectively. A precision off the shelf in-line spur gear reducer costs $700. High end DC motors cost about $200. The roller shade actuators discussed in section 3.4 are priced roughly as follows:

- Cheapest Somfy: $170 (small AC actuator) from Rollease.
- Cheapest Elero: $214 (AC actuator), $145 (smaller DC actuator) from BTX.

5.6 Summary of Actuator Advantages and Disadvantages

Table 5.4 Summary of Actuator Advantages and Disadvantages

Actuator	Advantages	Disadvantages
In-Line Spur Gear Actuator	• Highest Torque • Highest Efficiency • Noise Reduction Possible	• Vibration and Noise • Precision Gears Expensive
Differential Cycloidal Cam Actuator	• Large Industrial Unit Quiet • Profile Development Possible	• Vibration • Binding • Sensitive to Planet Profiles • Precision Rollers Expensive
Flexural Wave Actuator	• Cheapest • Quiet • Torque and Efficiency Increase Possible	• Low Torque • Low Efficiency
Ultrasonic Motor	• Truly Silent • Tubular or Double Sided Motor Development Possible	• Wrong Shape • Low Efficiency • Low Torque

5.7 Conclusion

Four actuators are designed, built, and tested. The readiness for market for each depends on development time and/or which specification(s) can be relaxed. This work provides a baseline for further investigations and comparative studies (e.g. noise, configuration, life, isolatability, torque). It is hoped that all important design issues have been treated.

Chapter 6

Suggestions for Future Work

There are two approaches to future work: eliminate the selected designs and find a better one, or pick one concept and eliminate its weaknesses. Following are suggestions for the latter approach.

6.1 In-Line Spur Gear Actuator

Vibration and noise can be reduced in several ways:

- Helical gears can be substituted: For helical gears, several characteristics must be determined, including helix angle and the use of standard or non-standard normal pitches. Helical gear profiles can be modified as well. The newly introduced thrust loads are not necessarily a problem: since the load is always in the same direction, an angular contact bearing needs to replace only one radial bearing for each shaft, and the compound gears can be designed to partially cancel each other's loads.

- The spur gear profile can be modified: tip and root relief can be tested if impact noise is the problem. Due to the variation in load, the only modification that should be attempted is articulated differential crowning. If this works, the cost must be evaluated.

- A different gear material can be substituted: for smaller loads, plastic or bronze gears of roughly the same dimensions can be substituted.

- Different lubricants can be applied to test the effect.

Note that for each remedy application to have meaningful results, a means of measuring gear tooth and assembly geometry must be decided upon. First, the current design should be measured. The results may indicate that some feature of the unmodified spur gears is the source of noise. Blindly applying remedies will only waste time and money.

6.2 Differential Cycloidal Cam Actuator

Planet profiles can be optimized. First, the theoretical instantaneous velocity ratio must be calculated to see if constant velocity is possible kinematically. Tsay presents a method for deriving the profiles based on rigid body transformations [119]. Second, modifications can be made to these profiles as for spur gears, for example:

- Reduce the material on one side of each lobe to create the necessary clearance, while maintaining the theoretically correct profile on the contact side (this takes advantage of the single direction loading).

- Find the best profile shape by using the simulation with variation of eccentricity, shortening ratio, and diameters.

Hashimoto presents a profile modification claimed to improve performance [120]. It is also probable that a certain aspect ratio is needed between the lobes and cam followers is needed. Using more lobes of a given size may require a larger radius to the rollers. Needle cam followers can be substituted, and the custom urethane cam followers can be tested. Finally, planet lubricants can be tested.

6.3 Flexural Wave Actuator

Torque and efficiency can be improved. Modeling and experimental approaches should be taken to optimize the torque and efficiency by choice of materials, surface finishes, and dimensions for the rotor and flexible tube, tube compression, and input roller dimensions and operating speeds.

6.3.1 Modeling

The output torque is proportional to normal force and hence compression, the size and number of rollers, and the hardness of the flexible tube, roller, and rotor materials. Torque is also proportional to friction coefficient and hence the finish of the contact surfaces. The input torque depends on cam follower bearing friction, and viscoelastic drag and deformation loss in the flexible tube. The losses are dependent on the tube wall thickness uniformity and material properties. There is also the possibility that resonance of the flexible tube can be excited to increase efficiency and output torque. The torque dependence on roller diameter should also be determined.

A simple viscoelastic model can be applied. Sashida and Ueha use equivalent circuits to model the ultrasonic motor. Friction contact presents the primary modeling difficulty.

6.3.2 Experiment

Optical measurements can characterize the flexible tube OD profile as function of time for use in correlating with models. The contact area can be measured, and friction coefficients tested for various pairs of materials can guide material selection. A layer of high-friction material can be placed between the stator and rotor as for the ultrasonic motor. Teeth or slits of various proportions can be cut into the flexible tube OD and tested.

6.4 Ultrasonic Motor

Torque and shape improvement can be achieved by development of tubular or double-sided designs. It is predicted that ultrasonic motors will continue to be improved, and once a major production facility opens, electromagnetic motors and transmissions will be replaced on a large scale. The shades in Tokyo City Hall and the Lexus steering column motors are the first of such large-scale applications of high-torque ultrasonic motors.

6.5 General Suggestions

For any actuator, a thorough noise analysis can be performed to diagnose and solve problems. An isolation approach may also be taken. Any component of the system can be redesigned. Actuator mount and coupling design is critical if the actuator vibrates. Ideally, the radiator is completely isolated from the actuator. One way this can be accomplished is by fixing the actuator and its rigid output shaft supports to a large, immovable mass (i.e. a wall), and by coupling the output shaft to the tube by means of a carefully designed flexible coupling and/or viscous damper. This is at the expense of increased cost and mounting difficulty, and nearly eliminates the possibility of placing the actuator in the tube for the power pack concept. An axially and diametrically compact actuator could be mounted rigidly to the wall with little vibration amplitude and fit into the tube with allowance for space for a flexible, damped coupling. Another alternative is to add a coupling protrusion to the end of the actuator to fit into a large coupling deeper inside the tube. Clearance would have to be maintained between the tube and actuator, and the increased bending moment accounted for.

Simulation can be applied at any stage, but it must be realistic and may require further experiment to obtain relations between parameters.

The controller must be applied and the control response and positioning accuracy of each actuator determined.

As a final note, as size decreases, precise machining and assembly becomes more difficult and the effects of inaccuracy are amplified. The relation between precision, noise, and cost needs to be more fully explored for each actuator.

References

1. Schempf, H., Comparative Design, Modeling, and Control Analysis of Robotic Transmissions, Ph.D., Woods Hole Oceanographic Institution, 1990, Massachusetts Institute of Technology.

2. AGMA 299.01 Sound Manual, 1989, American Gear Manufacturers Association, Alexandria.

3. Warring, R., Handbook of Noise and Vibration Control, 1983, Trade & Technical Press, Surrey.

4. Sabot, J. and Perret-Liaudet, J., *Computation of the Noise Radiated by a Simplified Gearbox*, 1994 International Gearing Conference, University of Newcastle upon Tyne, UK, September 1994, 1994, Mechanical Engineering Publications, p. 63-74.

5. Kato, M., *Evaluation of Sound Power Radiated by a Gearbox*, 1994 International Gearing Conference, University of Newcastle upon Tyne, UK, September 1994, 1994, Mechanical Engineering Publications, p. 69-73.

6. Oswald, F., *Comparison of Analysis and Experiment for Gearbox Noise*, Proceedings of the 6th International Power Transmission and Gearing Conference, Scottsdale, AZ, Sept. 13-16, 1992, ASME, v. 2, p. 675-679.

7. Nurhadi, I., Investigation of the Influence of Gear System Parameters on Noise Generation, Ph.D., Mechanical Engineering, 1985, University of Wisconsin-Madison.

8. Zhang, T. and Kohler, H., *A Gearbox Structural Optimization Procedure for Minimizing Noise Radiation*, 1994 International Gearing Conference, University of Newcastle upon Tyne, UK, Sept. 1994, 1994, Mechanical Engineering Publications, p. 87-91.

9. Rook, T. and Singh, R., *Mobility Analysis of Structure-Borne Noise Power Flow Through Bearings in Gearbox-Like Structures*, Noise Control Engineering Journal, 1996, **44**(2): p. 69-78.

10. Blanchard, D., GM Develops Intelligent Gear Design System, *http://lionhrtpub.com/orms/10-95text/edge.html*, 1995, Institute for Operations Research and the Management Sciences.

11. Steyer, G. and Lim, T., System Simulation Methods for Solving Noise and Vibration Problems, *http://www.sdrc.com/ref/papers/1995/steyer_lim/*, 1999, Structural Dynamics Research Corporation.

12. Standards Handbooks and Compendia, *http://www.iso.ch/infoe/handbooks.html*, 1999, International Standards Organization.

13. Timar, P., Noise and Vibration of Electrical Machines, 1989, Elsevier, New York.

14. Adachi, E. and Taninaga, S., *Experimental Analysis and Reduction of High-Frequency Noise of an Automotive Direct-Current Motor*, Transactions of the Japan Society of Mechanical Engineers, Part C, 1993, **59**(567): p. 3469-3473.

15. Harris, C., Handbook of Acoustical Measurements and Noise Control, 1991, McGraw-Hill, New York.

16. Dudley, D., Gear Handbook, 1962, McGraw-Hill, New York.

17. Lynwander, P., Gear Drive Systems Design and Application, 1983, Marcel Dekker, New York.

18. Handbook of Gears, Stock Drive Products, Sterling Instrument / Division of Designatronics, Inc. Catalog D190-5, 1997.

19. Staab, W. and Henning, R., Gear Noise, M.E., Mechanical Engineering, 1950, University of Cincinnati.

20. Aitchison, T., Correlation of Gear Noise with Manufacturing Process, National Engineering Laboratory, Report 507, 1972.

21. Greeves, C., Correlation of Gear Noise with Material - Cast Iron, National Engineering Laboratory, Report 521, 1972.

22. WenBeen, L., Finite Element Analysis for an Involute Spur Gear Noise Excitation by Impact Effects, M.S., Mechanical Engineering, 1993, Pittsburg State University.

23. Rouverol, W., *Zero Transmission Error Gearing*, US, 5083474, 1992.

24. M. Nielsen, W.P., and W. Rouverol, Minimizing Gear Noise Excitation, AGMA Technical Report 85FTM12, 1985.

25. Cai, Y. and Hayashi, T., *The Optimum Modification of Tooth Profile for a Pair of Spur Gears to Make its Rotational Vibration Equal Zero*, Proceedings of the 6th International Power Transmission and Gearing Conference, Scottsdale, AZ, Sept. 13-15, 1992, ASME, v. 2, p. 453-460.

26. Tavakoli, M., Optimization of Spur Gear Transmission Error Using Profile Modifications, M.S., Mechanical Engineering, 1983, Ohio State University.

27. Yoon, K., Analysis of Gear Noise and Design for Gear Noise Reduction, Ph.D., Mechanical Engineering, 1993, Purdue University.

28. Attia, A., *Noises of Gears: A Comparative Study*, Proceedings of the 1989 International Power Transmission and Gearing Conference, Chicago, IL, Apr. 25-28, 1989, ASME, p. 773-779.

29. Hardy, A., *Gearing*, US, 3881365, 1975.

30. Rouverol, W., *New Modifications Eradicate Gear Noise and Dynamic Increment at All Loads*, Proceedings of the 7th International Power Transmission and Gearing Conference, San Diego, CA, Oct. 6-9, 1996, ASME, p. 17-21.

31. Rouverol, W., *Articulated Differential Crowning*, US, 5485761, 1996.

32. Rouverol, W., *Zero Dynamic Incerement Gearing*, US, 5341699, 1994.

33. Rouverol, W., *Low-Excitation Gearing*, US, 4651588, 1987.

34. Wyeth, M., Differential Crowning: A New Weapon Against Gear Noise & Vibration, 1996, AGMA, Alexandria.

35. Nonaka, T., *Silent Gear Design for Mass-Produced Gears with Scatters in Tooth Form Accuracy*, Proceedings of the 6th International Power Transmission and Gearing Conference, Scottsdale, AZ, Sept. 13-15, 1992, ASME, v. 2, p. 589-595.

36. Michalec, G., Precision Gearing: Theory and Practice, 1966, John Wiley & Sons, New York.

37. Mori, R., *Small-Sized Reduction Gear with Radial Beam Between Axially Extending Columns of a Carrier*, US, 5366423, 1994.

38. Hambric, J., *Rotational Power Transmission Apparatus*, US, 4590820, 1986.

39. Yamamori, T., *Gear Noise Suppressing Type Final Gear Train of Transaxle*, US, 4480500, 1984.

40. Mochizuki, M., *Planetary Reduction Gear*, US, 5240462, 1993.

41. Maier, K., *Device for the Manufacture of Gear Wheels for Low Noise Gearings*, US, 4449869, 1984.

42. Tsuda, A., *Transmission Mechanism Capable of Suppressing Vibrational Noise*, US, 5657666, 1997.

43. Tsunoda, K., *Vibration-Damped Rotatable Drive Member*, US, 3857296, 1974.

44. Hansen, C., *Noisless Stepper Motor*, US, 4655099, 1987.

45. Tsukamoto, K., *Silent Gear Wheel*, US, 4174643, 1979.

46. Rivin, E., *Conjugate Gear System*, US, 4944196, 1990.

47. Bowers, G., *Gearing with Vibration Damping Means*, US, 3808906, 1974.

48. Mizuno, K., *Gears with Damped Vibration*, US, 4635501, 1987.

49. Nilsson, S., *Planetary Gear System*, US, 4095488, 1978.

50. Igaku, S., *Unified Asymmetric Planetary Gear Assembly*, US, 5098358, 1992.

51. Yi, J., The Study of the Damping Characteristics of a Bimetallic Structure for the Design of Silent High-Performance Gears, M.S., Mechanical Engineering, 1998, MIT.

52. Seragnoli, E., *Device for Reducing Noise in Gear Wheel Couplings, with a High Safety Degree*, US, 4033198, 1977.

53. Imazaike, M., *Gear*, US, 4437356, 1984.

54. Neimann, G., Machine Element Design and Calculation in Mechanical Engineering, 1978, Springer-Verlag, Berlin.

55. Ce, Z. and Zhong, L., *Modification of the Noise Calculating Formula of the Involute Gear*, Proceedings of the 3rd International Modal Analysis Conference & Exhibit, Orlando, FL, 1985, Union College, v. 1, p. 668-671.

56. Hirt, M., *Gearing Assembly*, US, 4513637, 1985.

57. Hayduk, M. and Jacobs, E., *Helicopter Noise Reduction Through Gearing Modifications*, US, 5271288, 1993.

58. Oswald, F., Influence of Gear Design Parameters on Gearbox Radiated Noise, NASA Technical Memorandum 106511, 1994.

59. Furukawa, T., Influence of Gear Mating Contact Ratio on Vibration and noise of Cylindrical Gear System, 1991, Mitsubishi Heavy Industries Ltd., Tokyo.

60. Heidrich, G., *Noise Muffling Assembly*, US, 5125289, 1992.

61. Pekar, F., *Noise Attenuating Transmission Casing*, US, 3902567, 1975.

62. Kurre, M. and Faulkner, L., *Noise Reduction of a Synchronous Motor Gearbox Mechanical Drive*, Proceedings of the 1980 International Conference on Noise Control Engineering, Miami, FL, Dec. 8-10, 1980, Noise Control Foundation, v. 1, p. 161-164.

63. Bouthors, P., *Electric Motor and Reduction Gearing Unit*, US, 3741024, 1973.

64. Stealth Planetary Gearheads, Bayside Controls Inc. Product Literature 1998.

65. Lagarde, E., *Planetary Reduction Gear for Use with Tubular Motors*, US, 5429558, 1995.

66. Elder, I., *Speed Reducer*, US, 2528470, 1946.

67. Andantex-Corbac Reducers and for Robotics and Servo-Drives, Andantex Inc., Product Brochure, 1997.

68. SM-Cyclo Speed Reducers and Gearmotors, Sumitomo Machinery Corporation of America, Product Literature, 1997.

69. Gyromax Speed Reducers, Shimpo Drives Inc., Product Brochure, 1998.

70. Romiti, A., *Kinematic Analysis of a Gearless Articulated Speed Reducer*, Mechanics Research Communications, 1995, **22**(5): p. 415-429.

71. Pierrat, M., *Mechanical Drives*, US, 3998112, 1976.

72. Mectrol Precision Speed Reducers, Mectrol Corporation, Product Literature, 1998.

73. Three-Gear Differential Planetary Gear Drives, Trogetec, Inc., Product Literature.

74. Kedrowski, D., *Wobbling Gear Drive Train for Cordless Screwdriver*, Proceedings of the ASME Winter Conference, New Orleans, LA, 1993, v. p. 1-8.

75. Sanden, *http://www.sanden.com/sanden/index.html*, 1998, Sanden International (USA) Inc.

76. Distin, R., *Nutating Drive Mechanism Having Spherical Ball Driving Elements*, US, 4620456, 1986.

77. Q-Ten Zero Backlash Ball Speed Reducer, Lansea Systems Inc., Product Literature.

78. Chironis, N., Mechanisms and Mechanical Devices Sourcebook, 1991, McGraw-Hill, New York.

79. Harmonic Drive Precision Gearing and Motion Control Components, HD Systems, Product Literature.

80. Jensen, P., Classical and Modern Mechanisms for Engineers and Inventors, 1991, Marcel Dekker, New York.

81. Small Parts Catalog No. 18W, Small Parts Inc., Catalog.

82. Lead Screws International, Inc., *http://www.lsitvc.com/design.htm*, 1998, Lead Screws International, Inc.

83. Sato, K., *Dynamic Behavior of Lead Screw Mechanism with Backlash*, Transactions of the Japan Society of Mechanical Engineers, Part C, 1995, **61**(584): p. 1423-1430.

84. PIC Catalog 44, Precision Industrial Components Corporation, Catalog, 1997.

85. Green, R., Machinery's Handbook, 1996, Industrial Press, New York.

86. HSI Linear Actuator Stepper Motors, Hayden Switch and Instrument Inc., Product Literature.

87. Handbook of Timing Belts, Chains & Friction Drives, Stock Drive Products, Sterling Instrument / Division of Designatronics, Inc. Catalog D210-3, 1997.

88. Slocum, A., Precision Machine Design, 1992, Prentice-Hall, Engelwood Cliffs.

89. Uchino, K., Piezoelectric Actuators and Ultrasonic Motors, 1997, Kluwer Academic Publishers.

90. Sashida, T. and Kenjo, T., An Introduction to Ultrasonic Motors, 1993, Oxford University Press, Oxford.

91. Ueha, S. and Tomikawa, Y., Ultrasonic Motors Theory and Application, 1993, Oxford University Press, Oxford.

92. Glenn, T., Ultrasonic Motor Development, *http://web.mit.edu/amsl/research/motor/motor.html*, 1999, MIT Active Materials and Structures Laboratory.

93. Stover, D., Wireless Motor Tilts Wheel, *http://www.verge.com/content/automotive/news/990220.a.html*, 1998, Popular Science.

94. Ashley, S., *Magnetostrictive Actuators*, Mechanical Engineering, 1998, **120**(6): p. 68-70.

95. Tadokoro, S., *Elliptic Friction Drive Element Using ICPF Actuator*, IEEE International Conference on Robotics and Automation, Apr. 22-28, 1996, v. 1, p. 205-212.

96. York, M., *Electronically-operated, Linear, Variable-reluctance, Integrating, Reversible Actuator*, IEE Proceedings - Electric Power Applications, 1998, **145**(1): p. 11-16.

97. Xu, H., *Motion Conversion by Means of Perturbation of Elastic Field*, Journal of Mechanical Design, 1994, **116**(1): p. 232-237.

98. Contract Series Motorized Roller Shade Specifications, Rollease Inc., Product Literature, 1997.

99. The Motor Book, BTX Window Automation, Product Literature, 1998.

100. Window Treatments, *http://www.sdbinc.com/window.html*, 1998, Shaffer DeSouza Brown, Inc.

101. The ElectroShade© System, *http://www.mechoshade.com/m2.htm*, 1999, MechoShade Systems.

102. Musser, C., *Strain Wave Gearing*, US, 2906143, 1955.

103. Gosling, A., *Mechanical Gearing*, US, 4059030, 1977.

104. Fahey, T., *High Ratio Drive Mechanism*, US, 3668946, 1972.

105. Hellen, J., *Torque Transmission Device*, US, 3304809, 1964.

106. Prior, W., *Variable Speed Drive Mechanism*, US, 3199370, 1962.

107. Bartz, W., Lubrication of Gearing, 1993, Mechanical Engineering Publications, London.

108. Braren, R., *Cycloidal Gears*, US, 4050331, 1977.

109. Pierrat, M., *Speed Reducer and Method for Eliminating Backlash*, European, 0086393, 1983.

110. Material ML6 High Friction Precision Molded Parts, Meridian Laboratory, Product Literature.

111. Ishii, T., *Wear and Life Prediction of Frictional Materials for Ultrasonic Motors*, Japanese Journal of Applied Physics, 1995, **34**(5B): p. 2765-2770.

112. Handbook of Design Components, Stock Drive Products, Sterling Instrument / Division of Designatronics, Inc. Catalog D220-4, 1997.

113. Soedel, W., Vibrations of Shells and Plates, 1993, Marcel Dekker, New York.

114. Nevzat, H. and Houser, D., *Gear Dynamic Models Used in Noise Analysis*, Noise-Con 87, State College, PA, June 8-10, 1987, Noise Control Foundation, p. 47-52.

115. Smith, J., Gears and Their Vibration, 1983, Marcel Dekker, New York.

116. Bolze, V., Static and Dynamic Transmission Error Measurements and Predictions and Their Relation to Measured Noise For Several Gear Sets, M.S., Mechanical Engineering, 1996, Ohio State University.

117. Blankenship, G. and Kahraman, A., *Gear Dynamics Experiments, Part 1: Characterization of Forced Response*, Proceedings of the 7th International Power Transmission and Gearing Conference, San Diego, CA, Oct. 6-9, 1996, ASME, p. 373-380.

118. Inoue, K., *Optimum Design of a Gearbox for Low Vibration*, Proceedings of the 6th International Power Transmission and Gearing Conference, Scottsdale, AZ, Sept. 13-16, 1992, ASME, v. 2, p. 497-504.

119. Tsay, D., *Geometric Design of Roller Gear Cam Reducers*, Proceedings of the 7th International Power Transmission and Gearing Conference, San Diego, CA, Oct. 6-9 1996, 1996, ASME, v. 88, p. 153-160.

120. Hashimoto, M., *Outer Tooth Profile of Planetary Gear Apparatus*, US, 5695425, 1995.

Appendices

Appendix A: Differential Cycloidal Cam Dynamic Simulation

A1: Differential Cycloidal Cam Dynamic Simulation Front View

File Name: CycloSim.AVI

Format: 100M IBM Zip Disk

A2: Differential Cycloidal Cam Dynamic Simulation Isometric View

File Name: CycloSimUL.AVI

Format: 100M IBM Zip Disk

Appendix B: Actuator Videos

B1: Prototype Videos w/ Audio

Running Time: 2 Minutes

Format: 8mm, Color, Sound

Table B.1 Prototype Video

Count	Subject	Notes
00:00	In-Line Spur Gear Actuator – Alone	Rigid Mount to Wall (Magnetic)
00:18	In-Line Spur Gear Actuator – Worst Case Mount	Tube Resonates
00:34	Differential Cycloidal Cam Actuator – Alone	Rattling Noise
00:41	Power Pack	10 Seconds to Install
00:45	Installation Procedure	
00:52	Differential Cycloidal Cam Actuator – Worst Case Mount	Rattling Noise Amplified but Changed by Tube
01:13	Flexural Wave Actuator – Alone	See Operation
01:21	Flexural Wave Actuator – Worst Case Mount	Tube Resonates

B2: Flexural Wave Actuator Video

Running Time: 14 Minutes

Format: VHS, Black & White, Silent

Table B.2 Flexural Wave Actuator Video

Count	Subject	Notes
00.00	Flexural Wave Actuator	
00.10	Actuator Operated 0-10V	Observe Wave
01.31	Front View	
01.43	Actuator Operated 0-10V Front View	
02.50	Slow Motion (30 frames/sec)	
03.30	Actuator Without Rotor	
03.41	Motion Without Rotor	
03.59	Slow Motion Without Rotor	
04.29	Actuator With Rotor	
04.39	Actuator Operated 0-10V With Rotor	
05.35	Slow Motion With Rotor (30 frames/sec)	
06.20	Close Up Wave Action Urethane	
07.06	Close Up Wave Action Yellow ML6	
07.41	Close Up Wave Action Orange ML6	
08.15	Close Up Wave Action Natural Rubber	
08.38	Close Up Wave Action Yellow ML6 (again)	
09.30	Slow Motion With 2 Cam Followers	Check Ratio
10.03	Slow Motion With 3 Cam Followers	Check Ratio
10.22	Slow Motion With 4 Cam Followers	Check Ratio
10.43	Wave, Gear, Cycloidal Drive Action	Neat